α2β1 integrin in Retinopathy and Sprouting Angiogenesis

By

Aasakiran Madamanchi

Dissertation

Submitted to the Faculty of the

Graduate School of Vanderbilt University

in partial fulfillment of the requirements

for the degree of

DOCTOR OF PHILOSOPHY

in

Cancer Biology

May, 2016

Nashville, Tennessee

Approved:

Mary Zutter, M.D.

John M. Stafford, M.D., Ph.D.

Jin Chen, M.D., Ph.D.

Volker H. Haase, M.D.

John S. Penn, Ph.D.

ABSTRACT

Angiogenesis expands the vascular network during normal development and in response to angiogenic stress. Dysregulation of this dynamic process contributes to the pathogenesis of many diseases including retinopathies. The α2β1 integrin, a collagen and laminin receptor which is linked to risk of vascular retinopathy, plays an important yet incompletely understood role in angiogenesis. In this dissertation, I employ multidisciplinary approaches to examine the function of this integrin during both pathological and developmental angiogenesis in the retina.

The major goal is to contribute clinically relevant knowledge through mechanistic investigation of the link between α2β1 integrin in vascular retinopathies and careful exploration of this integrin's role in angiogenesis. The central questions addressed in this thesis are, 1) does the α2β1 integrin contribute to the progression of retinopathies, and through what mechanism? And, 2) how does α2β1 integrin interface with the major angiogenesis pathways, and does that explain the divergent effects of α2-integrin deletion in different vascular beds?

Using the oxygen-induced retinopathy (OIR) model for retinopathy of prematurity (ROP) on wild type and α2-null mice, I elucidated the role of α2β1 integrin in both endothelial cells as well as in the retinal microenvironment. I uncover a novel, potentially mechanistically important role for the integrin in regulating retinal Müller cell function.

To clarify the role of α2β1 integrin in angiogenesis, I use in vitro, in vivo and in silico methods to characterize wild type and α2-null mice during postnatal development of the retinal vasculature. I develop a hybrid mathematical model to simulate cell signaling and vascular morphology in the developing postnatal murine retina. Using this

model, I study how the VEGF-notch signaling system directs the development of morphological features including, retinal vascularization, plexus density, and plexus irregularity. I also use the model to predict how crosstalk to the VEGF-Notch axis from other angiogenic signals affects vascular phenotypes. Finally, I use the computational model as a platform for evaluating proposed signaling relationships between α2β1 integrin and the VEGF-Notch axis and present a molecular model which may explain how α2-integrin deletion causes disparate vascular phenotypes in different vascular microenvironments.

ACKNOWLEDGEMENTS

There are so many people that made this work possible.

I have the deepest graditude to my advisor, Dr. Mary Zutter. I have had the amazing good fortune to have an advisor who gave me the freedom to explore on my own, and at the same time the guidance to turn my wanderings into productive research. Mary taught me how to question thoughts and express ideas. Her patience and support helped me overcome many crisis situations and finish this dissertation.

In addition to my advisor, I would like to thank the rest of my thesis committee: Dr. John M. Stafford, Dr. Jin Chen, Dr. Volker H. Haase, and Dr. John S. Penn. I am also forever indebted to the wonderful members of the Zutter lab who have helped me with countless experiments. Without the help of Brenda Jaris, S. Kent Dickeson, Zhenghzhi Li and in particular Dr. Ling Geng I could not have graduated.

My years at Vanderbilt have been better than I have ever hoped for. Many friends have brightened my time here. In particular Roman Covarrubias, Tony Chen, Adam Bissonnette, Clint Hasenour, and David Cappel have become treasured friends. The highlight of my time at Vanderbilt has been meeting the person I am spending the rest of my life with, Jennfer DeBoer. The friendship and support of these people has shaped me forever.

Finally, none of this would have been possible without the love and patience of my family. My brother Chaitu, and my parents to whom this dissertation is dedicated to, have been a constant source of love, concern, motivation and strength.

TABLE OF CONTENTS

LIST OF FIGURES

LIST OF TABLES

Chapter 1

INTRODUCTION

This chapter reprints sections of:

Madamanchi A, Santoro SA, Zutter MM. alpha2beta1 Integrin. Adv Exp Med Biol 2014; 819: 41–60.

Vascular retinopathies, such as retinopathy of prematurity (ROP) and proliferative diabetic retinopathy (PDR), are among the leading causes of vision complications globally. These disorders are marked by aberrant growth of fragile, leaky blood vessels in the preretina which can cause vision-impairing hemorrhage and retinal detachment. The α2β1 integrin is associated with risk for vascular retinopathy and is known as an important, if incompletely understood, actor in angiogenesis. The major goal of this dissertation is to provide mechanistic insight into the link between α2β1 integrin in vascular retinopathies and enhance our understanding of the integrins role in angiogenesis in order to contribute clinically relevant knowledge. In this introduction, I will survey existing knowledge on (1) α2β1 integrin, (2) angiogenesis, (3) modeling of biological networks, and (4) the retina and retinopathies.

1.1 α2β1 integrin in health and disease

The α2β1 integrin, also known as VLA-2, GPIa-IIa, and CD49b, was first identified as an extracellular matrix receptor for collagens and/or laminins.[1,2] It is now recognized that the α2β1 integrin serves as a receptor for many matrix and nonmatrix molecules.[3–5] Extensive analyses have clearly elucidated the α2 I domain structural motifs required for ligand binding and also defined distinct conformations that lead to inactive, partially active, or highly active ligand binding.[6–12] The mechanisms by which the α2β1 integrin plays a critical role in platelet function and homeostasis have been

carefully defined via *in vitro* and *in vivo* experiments.[13–16] Genetic and epidemiologic studies have confirmed human physiology nd disease states mediated by this receptor in immunity, cancer, and development.[17–22]

1.1.1 The α2β1 integrin: Expression and Function

Expression of the integrin is primarily dependent on cell type and stage of differentiation. The α2β1 integrin is primarily expressed *in vivo* by epithelial cells, platelets/megakaryocytes, and fibroblasts.[23] In addition, α2β1 integrin expression on T-cells and endothelial cells varies depending on differentiation and the state of activation.[1,2,24,25] The roles and functions of the integrin are therefore highly dependent not only on cell type but on signals from other cells and the associated microenvironment.

The majority of earlier work defined the role and function of the α2β1 integrin by studies of human platelets and *in vitro* models. These early studies implicated the α2β1 integrin in a wide range of biologic and pathobiologic functions including platelet adhesion required for hemostasis and thrombosis, epithelial differentiation and branching morphogenesis, tumor biology, wound healing, angiogenesis, and inflammation and immunity. Much has been learned over the last 10 years since development of state of the art inhibitory antibodies and gene silencing approaches, novel *in vitro* culture systems, and new animal models including the global α2 integrin-subunit deficient and the more recent tissue-specific α2 integrin-subunit deficient mouse. These studies and their impact on our understanding of the integrin in human biology and disease will be reviewed.

1.1.2 Platelet α2β1 integrin in ligand binding

Patient studies first established the link between α2β1 integrin and platelet function. In 1985, Nieuwenhuis identified a deficiency of platelet glycoprotein 1a (α2 subunit) in a patient with abnormal bleeding.[26,27] Later, other patients with either reduced levels of platelet expression of the α2β1 integrin or the presence of autoantibodies to the integrin were also described to exhibit impaired platelet activation by collagen but not by other agonists.

Studies using purified human platelets established the α2β1 integrin-dependent adhesion to collagens I-VIII in an Mg2+-dependent manner. Although the α2β1 integrin is expressed at relatively low copy number on platelets (2000 to 4000 copies per platelet), the integrin is required for firm attachment of platelets to collagen in the subendothelium after vascular injury.[2,28,29] Experiments with purified platelets from genetically modified α2-deficient mice confirmed these results. Platelets from α2-deficient animals fail to adhere to type I collagen under both static and flow conditions.[30] Platelets from animals heterozygous for the α2-null allele adhere to type I collagen to a lesser degree than platelets from wild type animals, consistent with a gene dosage effect.

Platelets, however, have not one, but two major collagen receptors: the high affinity α2β1 integrin and the lower affinity glycoprotein VI (GPVI)/Fc receptor γ-chain (FcRγ) complex.[31–33] Despite the significant evidence supporting the role of α2β1 integrin in platelet adhesion to collagen, the relative contribution and precise roles of α2β1 integrin and GPVI/FcRγ in collagen-induced platelet adhesion and activation are still focus areas of experimental inquiry. The Santoro group originally proposed a two-step, two-site model of platelet adhesion and activation to collagen in which the higher

affinity α2β1 integrin supports the initial rapid platelet-collagen interaction that mediates platelet adhesion to vessel wall under conditions of flow.[5,29,34–36] This allowed the subsequent engagement of a lower affinity, signal-transducing co-receptor GPVI to bind collagen and mediate collagen-induced platelet activation and aggregation. GPVI, a member of the immunoglobulin superfamily noncovalently and constitutively associates with the Fc receptor y (FcRγ) chain to form a multimeric signaling complex. In this model, the α2β1 integrin mediates strong adhesion but does not contribute to platelet activation.

Other work raised question about the two-step, two-site model. Studies using a variety of agonists and inhibitors defined the contributions and mechanisms leading to conformational changes resulting from integrin activation and provided evidence that the α2β1 integrin can mediate GPVI-independent, collagen-induced platelet activation.[37–41] Collagen-induced phosphorylation of PLCγ2 and Syk was inhibited by antibodies that block α2β1 integrin adhesion to collagen or by selective proteases that cleave the β1 integrin subunit of the α2β1 integrin. In other studies, collagen-induced phosphorylation of c-Src was mediated by the α2β1 integrin.[41] Platelet adhesion to intact collagen stimulated a different response than adhesion to GPVI-mimetics, further supporting distinct signaling from the α2β1 integrin and GPVI/FcRγ.[38,42]

New work attempted to reconcile these conflicting stories. Auger et al. used flourescence video microscopy to monitor increase in intracellular free Ca^{2+} concentration ($[Ca^{2+}]_i$), an early stage in GPVI/FcRγ-mediated platelet activation, upon platelet adhesion to collagen under flow conditions.[43] In both human and mouse platelets under flow conditions, they identified a population of platelets that displayed an immediate increase in $[Ca^{2+}]_i$ upon collagen contact, as well as a second population of

platelets that exhibited a delayed increase in $[Ca^{2+}]_i$ (1-30 s after adhering to collagen). The first population was unaffected by anti-α2β1 integrin antibody blockade suggesting a GPVI/FcRγ-centric mechanism for both adhesion and activation as suggested by Nieswandt et al. The second population conformed to the traditional two-step model. The authors speculated that the apparently heterogeneous mechanism would allow for optimal response to different types of vascular injury. A similar study by Mazzucato et al. used inhibitory antibody-treated human platelets as well as mouse platelets from null animals to link short-lasting α-like and long-lasting γ-like $[Ca^{2+}]_i$ oscillation peaks to α2β1 integrin and GPVI signaling, respectively.[44] Interestingly, they found that α2β1 integrin-mediated α-like calcium oscillations occur even in GPVI-null backgrounds indicating that inside-out priming of the integrin may also come from non-GPVI sources. Indeed, Majoram et al. reported a role for platelet GPCRs, including protease activated receptor 1 and 4 (PAR1 and PAR4), in PLC-mediated α2β1 integrin activation.[45]

Together, these studies demonstrated greater synergy between α2β1 integrin and GPVI/FcRγ in mediating these processes than was previously understood. Resting platelets express the integrin in a low-affinity conformation. Activation, downstream of activation of GPVI, PAR1 or PAR4, or another pathway, leads to a conformational change to a high-affinity state which enhances adhesion to Type I collagen and promotes a more permissive binding to other ligands including Type IV collagen and laminin.

1.1.3 Collagen Receptors-Structure and Ligand binding

The structure of the α2β1 integrin consists of an obligate heterodimer formed from the α2 integrin subunit non-covalently associated with the β1 subunit. It is one of

four ‘I domain’ integrins, named for the presence of a highly conserved, extracellular, (inserted) I domain, which mediates specific binding of ligands including, most prominently, collagen. The α2 subunit I domain is an autonomously folding domain of approximately 220 amino acids.[46] The I domain found in the collagen receptors is shared with the alpha subunits of the leukocyte β2 integrins and is highly homologous to the A domain found in Von Willebrand factor, in cartilage matrix protein, in some collagen subtypes, and in components of the complement system. The crystal structure of the α2 integrin I domain was first defined in 1997.[47] The α2 subunit shares many similarities in structure and ligand binding with the other I domain integrins, including the Mg^{2+} dependence for binding and enhancement of integrin function by Mn^{2+}.[29,35,48,49] The I domain contains a conserved cation binding site, the metal ion-dependent adhesion site (MIDAS) with clear preference for Mg^{2+}/Mn^{2+}. The MIDAS motif is critical for collagen recognition.[50]

Structural studies of the α2 I domain have identified an inactive or closed conformation, an intermediate or low-affinity conformation, and an active or high-affinity conformation.[6–12] Experimental approaches have characterized the role that distinct I domain residues play in receptor conformation and ligand binding capability. Mutation of the Mg2+ binding site at T221 disrupts the MIDAS site and inactivates I domain function.[51,52] Insertion of a disulfide bridge between helices locks the I domain into a low affinity conformation.[53] Within the α2 integrin I domain, amino acid E318 forms a salt bridge with amino acid R288, thereby maintaining the α2 integrin I domain in a closed conformation. Recent reports by Carafoli et al. indicate that mutation of E318 to alanine causes disruption of this salt bridge and promotes the transition to the open, high affinity conformation, which enhances α2 integrin I domain binding to low-affinity ligands.

Crystal structures of the I domain complexed with the GFOGER peptides revealed two domains bound to a single triple helix, suggesting that a single GxOGER motif in the heterotrimeric collagen V or the FACIT forming collagen IX may support binding of the activated integrin. Similarly, crystal structure of the analogous E317A mutant also resulted in an opening of the helices, and modelling of a similar peptide, GLOGEN, onto E317A allows similar conclusions to be drawn for α1β1 integrin [54].

The α2β1 integrin has high affinity for collagen Type I. Evaluation of the role of the α2β1 integrin structure and function has led to the identification of a number of novel ligands. The other ligands can be subdivided into other collagens, non-collagenous molecules with collagen-like triple helical structures, laminin and molecules with laminin domains, and proteoglycans, as well as infectious organisms, primarily viruses, and other potential non-matrix ligands.

Among collagens, the α2β1 integrin preferentially binds fibrillar isoforms (I-III, V and XI), but also recognizes the network forming collagen IV, the beaded-filament forming collagen VI, and the transmembrane collagen XIII when in an active, high-affinity conformation.[12,55,56] Modulation of integrin conformation by cytoplasmic signals provides an integrin-specific mechanism for adjusting ligand affinity known as 'inside-out' signaling. However, the binding of purified recombinant α2 integrin I domain to collagen type I or IV reflects the same relative affinity for this ligand as does the parent integrin, indicating that differences in the integrin-binding motifs of these isoforms most likely account for the differential recognition by the integrin.[57] The development of overlapping sets of collagen-derived peptides, termed Toolkits, facilitates systematic mapping of motifs for integrin binding and identifies the collagen sequence GFOGER as the major high-affinity binding motif for the α2β1 integrin.[51,58,59] The GFOGER motif,

found in Type I, II and IV, is uniquely able to bind platelet integrin α2β1 without prior activation [60], suggesting the ability to induce the active conformation without the inside-out signals needed for lower-affinity motifs.

More recently, other collagens were defined as α2β1 ligands. Collagen XVI, a member of the fibril-associated collagens with interrupted triple helices (FACITs), binds to the α2β1 integrin, as well as to the α1β1 integrin.[61] The α2β1 integrin ligand, collagen XXIII, a transmembrane collagen, has been reported as the primary apical binding partner for the integrin in keratinocyte adhesion in the epidermis.[62–64]

Many molecules of the immune system contain segments of a collagen triple helix, including C1q. As discussed below, our laboratory showed that α2β1 integrin-mediated stimulation of an innate immune response required α2β1 integrin dependent-adhesion to C1q in an immune complex.[65] The full length α2β1 integrin and the α2 integrin I domain adhere to C1q as well as to members of the collectin family of proteins, including surfactant protein A and mannose binding lectin. The α2 integrin I domain adheres to C1q in the absence of activation. However, the activated E318A mutant of α2 I domain bound to C1q with higher affinity than wild type α2 integrin I domain.

As with collagens, adhesion to laminin isoforms is mediated by the α2 integrin I domain; however laminin binding only occurs in the active, high-affinity conformation.[48,57,66] Isolated full-length α2 integrin subunit has been shown to bind to laminin-111 (previously laminin-1) and laminin -332 (previously laminin-5). Netrin-4, a member of the netrin family of guidance signals, demonstrates high homology to the beta 1 chain of laminins, binds to the α2β1 integrin and to the α3β1 integrin.[67] To date, an extensive and detailed molecular analysis to identify the recognition site/s on laminin

has not been performed. Laminin-binding has proven to occur constitutively in some cell types, and inducibly in others. However, the role of these adhesive events is not well understood.

Perlecan, a heparin sulfate proteoglycan, and its C-terminal fragment, endorepellin, bind the α2β1 integrin.[68,69] The terminal globular domain of endorepellin, lG3, interacts directly with the α2 I domain. This interaction has been studied in the context of angiogenesis and shown to be important α2β1 integrin dependent angiogenesis. Decorin, another small leucine-rich proteoglycan modulates α2β1 integrin matrix interactions by playing an important role in regulating extracellular matrix assembly as well as directly interacting with the integrin.[70–73] Decorin binding to collagen has been shown to affect fibril formation by initially delaying lateral fibril growth and reducing average fibril diameter.[74] Additionally, decorin interacts with α2β1, but not α1β1 integrin, at a site distinct from the collagen-binding domain. Adhesive interaction between decorin and the α2β1 integrin was first identified in platelets and later discovered be important in angiogenesis.

Single nucleotide polymorphisms in the integrin α2 gene, as discussed later in more detail, have an important role in the predisposition of patients to cardiovascular disease. One such minor allele difference (rs1801106; G1600A) has now been shown to attenuate adhesion of platelets to decorin but not to collagen and is associated with increased risk for recurrence of stroke.[75] The non-conservative amino acid substitution E534K is the basis of the human platelet alloantigen system HPA-5, providing the first evidence of a functional effect of HPA-5 alleles.

The α2β1 integrin serves as a receptor for many different infectious organisms. In many cases, the organisms usurp α2β1 integrin's routine biology for attachment, cell

entry, and transmission throughout the body. The best studied interaction of α2β1 integrin is with echovirus (EV1).[76–79] EV1 is a human RNA virus which binds directly to the I domain of human α2β1 integrin. Unlike most viruses that exploit integrin receptors, EV1 does not undergo clathrin-mediated endocytosis, but instead clusters on caveosomes and is internalized via a clathrin- and caveolin-independent macropinocytosis-like mechanism.[80,81] Additionally, EV1 binding has been demonstrated to activate PKCα, while inhibition of PKCα signaling blocks EV1 internalization.[82] Interestingly, EV1, unlike other α2β1 integrin ligands, preferentially binds the inactive, closed conformation of the integrin over the active, high affinity conformation.[83]

Not only do infectious organisms utilize the integrin as a receptor, lectins that recognize high mannose glycans on viruses that are produced from bacteria, algae, plants and animals also bind the α2β1 integrin. A recently characterized anti-HIV lectin from *Pseudomonas fluorescens* Pf0-1 exhibited potent antiviral activity against influenza.[84] The lectin induced loss of cell adhesion and viral death that was dependent on binding to the α2β1 integrin. Following lectin binding to the α2β1 integrin, the complex was internalized to the perinuclear region and not recycled. The process resembled that described for echovirus mediated cell entry and death.

1.1.4 The α2β1 Integrin during Wound Healing and Fibrosis

Early *in vitro* studies suggested that the α2β1 integrin was required for wound healing. Studies using skin explants *ex vivo* showed that keratinocyte-specific α2β1 integrin expression was re-oriented from the basal cell area to the forward-basal aspect of migrating keratinocytes where the integrin is in contact with type I collagen.[85]

Keratinocyte migration into the wound was inhibited by antibodies against the α2β1 integrin.[86]

In the late phase of wound healing after reepithelialization, tissue contraction of collagen fibers results in a strengthened scar. The scar is the result of extensive fibrosis, a process of tissue replacement by dense extracellular matrix composed of abundant collagen I. The α2β1 and the α1β1 integrins, both expressed by fibroblasts, are key regulators or collagen turnover in the skin, and other organs including the kidney.[87,88] After binding to collagen, the α1β1 integrin activates a pathway that down-regulates collagen synthesis. In contrast, activation of the α2β1 integrin promotes collagen synthesis.[89] The alignment of the collagen fibers that occurs in healing wounds is recapitulated in three-dimensional collagen gels. The *in vitro* models provided evidence supporting critical roles for the α2β1 integrin wound healing and fibrosis.

Surprisingly, despite the results of *in vitro* and explant studies of wound healing, α2-deficient mice demonstrated no defect or delay in wound repair compared to wild-type animals.[62,90] The morphology of the wounds also failed to demonstrate any difference in keratinocyte migration over exposed dermis at the wound site, suggesting that α2β1 integrin does not play an obligatory role in wound healing. No differences in scar formation or strength were noted.

Differences between the *in vitro* experiments and α2-null mouse model systems have several possible explanations. First, human and genetically altered mouse models may not be mechanistically equivalent. Acute loss-of-function as observed with use of inhibitory antibodies may have different effects than the germ-line deletion of α2β1. In addition, antibodies that inhibit integrin binding may produce ‘negative signaling’ which is distinct from the absence of integrin signaling in the null context.

Interestingly, Zweers et al. and Grenache et al. both reported increased neoangiogenesis in the wound microenvironment in α2-null mice, providing *in vivo* evidence for an anti-angiogenic role for α2β1 integrin.[62,90] The increased angiogenesis in the wound healing model was quite surprising. Many studies have focused on understanding the role of the integrin in vascular development and angiogenesis, as discussed below.

Fibrosis also occurs in other tissues; the involvement of α2β1 integrin is particularly well studied in the kidney.[91] Glomerulosclerosis, characterized by excessive collagen deposition in the glomerulus is the most common cause of end stage kidney disease. The specific role of α2β1 integrin in regulating glomerulosclerosis is somewhat controversial. Mesangial cells and podocytes express the α2β1 integrin. One report studying α2-null mice on the C57Bl/6 background suggested that the integrin protected from glomerular injury.[92] In contrast, a study in which α2-null mice were crossed with the COL4A3-null mice, a model of Alport disease demonstrated that α2β1 integrin expression exacerbates glomerular injury, decreased survival, and reduced glomerular matrix deposition and scarring.[93]

Consistent with a role for the integrin in promoting collagen synthesis, Miller et al. show that inhibition of integrin α2β1, using a high-affinity small-molecular weight inhibitor, protects mice from glomerular injury.[94] The anti-α2β1 inhibitor also reduced collagen synthesis in wild type but not α2-null mesangial cells, consistent with the α2β1 integrin-dependence of its anti-fibrotic effect.

In contrast to the kidney, the α2β1 integrin appears to have an anti-fibrotic role in the lung. Xia et al. reported that in idiopathic pulmonary fibrosis (IPF), reduced fibroblast α2β1 integrin levels allowed escape from anti-proliferative signals that normally limit

fibroproliferation after tissue injury.[95] Fibroblastic foci in IPF patients were shown to be characterized by low fibroblast α2β1 integrin expression. IPF fibroblasts demonstrated decreased α2β1 integrin-mediated PP2A phosphatase activity. Downstream increases in activity of GSK-3β and β-catenin provided the proliferative signals that mark the pathological IPF fibroblast phenotype. Although this work provided an elegant model for how α2β1 integrin downregulation may contribute to the pathogenesis of IPF, the relevant mechanisms for α2β1 integrin loss remain uninvestigated. Additionally, it is unclear how the established role for α2β1 integrin in promoting collagen biosynthesis and ROS production may be involved. Are the disparate elements of α2β1 integrin function somehow context- or tissue-specific? Reconciliation of the pro-fibrotic and anti-fibrotic properties of the α2β1 integrin demands further study in light of its potential clinical relevance.

1.1.5 The α2β1 Integrin in the Innate and Acquired Immune Response

The α2β1 integrin was initially identified as an integrin expressed at very late stages of T cell activation, thus the designation very late activation antigen-2 (VLA-2) (CD49b).[1,2] The α2β1 integrin was then noted on a variety of cells of the inflammatory and hematopoietic system, including activated T cells, but not naïve T cells in chronic inflammatory settings. Early studies showed that α2β1-dependent adhesion to collagen enhanced T cell receptor mediated T cell proliferation and cytokine secretion.[96] Boisvert et al. defined one possible mechanism; they reported that collagen I stimulated α2β1 mediated both activation-independent and T cell receptor-dependent interferon γ expression via the ERK and JNK MAPKs and PI3K/AKT signaling pathways.[97]

The α2β1 integrin also influenced T cell activation by inhibiting fas ligand expression and apoptosis in effector T cells in a collagen I dependent manner.[98,99] In animals, inhibitory monoclonal antibodies directed against the α2β1 integrin significantly inhibited the effector phase of both contact and delayed type hypersensitivity. These early results established a role for the α2β1 integrin in T cell mediated function. The role of the α2β1 integrin in the innate and acquired immune response has been an area of active investigation.

To better the define the role of the α2β1 integrin in T cell function, expression of the α2β1 integrin on T cell subsets and in response to antigenic challenges was investigated. Kassiotis et al. reported that expression of α2β1 integrin defined two functionally distinct subsets of memory T cells that played a role in the response to infection and immunization.[100] α2β1 integrin expression was stably induced by antigen on approximately 50% of memory T cells with helper function and stimulated production of tumor necrosis factor-α. The α2β1 integrin expressing, CD49b+, and memory Th cells demonstrated enhanced ability to mediate macrophage activation and to kill of intracellular bacteria.

Sasaki et al. demonstrated that mature Th1 and Th2 cells exhibited distinct α2β1 integrin expression profiles.[96] Although naive Th cells did not express α2β1 integrin, Th1 cells acquired high levels of α2β1 integrin expression during maturation in an interferon-γ (IFN- γ) and interleukin (IL)-12-independent manner. This study suggested that high level α2β1 integrin expression on Th1, but not Th2, cells was functionally important, because stimulation of Th1 or Th2 cells with α2β1 integrin ligands caused selective activation of Th1 cells to produce interferon-γ after long-term culture.

Richter et al. studied α2β1 integrin expression during influenza infection in the lung.[101] During the acute phase of infection, the α2β1 integrin was expressed by a significant proportion of both CD4+ and CD8+ T cells in the lung; however, the integrin was expressed less frequently on memory cells, particularly CD8+ T cells. A similar expression pattern for the α2β1 integrin in the spleen was found in a model of lymphocytic choriomeningitis viral infection.[102] The data suggested that α2β1 integrin expression directed localization of CD4+ and CD8+ T cell subsets within the lung and promoted T cell migration within extralymphoid spaces, particularly during the acute phase of infection.

A role for α2β1 integrin expression by Th17 cells has been described. Boisvert et al.showed that human naïve CD4+ T cells stimulated toward Th17 polarization preferentially upregulate α2β1 integrin.[97] Th17 cells adhered to collagens I and II, but not IV in an α2β1 integrin-dependent manner. α2β1 integrin-dependent adhesion combined with anti-CD3 antibody co-stimulated the production of IL-17A, IL-17F and IFN-γ by human Th17 cells.

The importance of α2β1 integrin to T cell memory has remained controversial. Work by several groups suggested that professional memory CD4 cells reside and rest in the bone marrow. Recently, Hanazawa et al. demonstrated that memory CD4 cells expressed high levels of α2β1 integrin and that antibody-mediated inhibition of α2β1 integrin of memory CD4 cell precursors caused failure to transmigrate from blood through sinusoidal endothelial cells into the bone marrow.[103] These results suggested that the α2β1 integrin was required for the migration of memory CD4 cell precursors into their survival niches of the bone marrow.

In addition to its expression on activated T cells, the α2β1 integrin is expressed at high levels on almost all NK cells and mast cells and on subpopulations of monocytes and neutrophils.[104,105] Arase et al. identified the NK cell recognition epitope of the widely used DX5 pan-NK cell monoclonal antibody as CD49b or the α2β1 integrin. These investigators demonstrated that α2β1-expressing and non-expressing subsets of NK cells are present in the mouse spleen and raised the possibility that α2β1 integrin expression is important in NK cell function. The role of the α2β1 integrin on subsets of neutrophils and monocytes has also been studied. One study found expression of the α2β1 integrin on extravasated neutrophils in human skin blister chambers and in the rat peritoneal cavity following chemotactic stimulation.[24] These studies, as well as others, suggested that the α2β1 integrin on neutrophils is involved in neutrophil migration from the vasculature into extravascular tissue in response to cytokine induction.

Work from our lab has clarified the function of the α2β1 integrin in mast call activation. We initially observed decreased inflammatory responses to Listeria monocytogenes in α2-null mice.[65] This innate immunity defect was determined to arise from a requirement for α2β1 integrin activation on peritoneal mast cells (PMCs) for mast-cell activation and cytokine release *in vivo*. We also identified C1q complement protein and collectin family members, including mannose binding lectin and surfactant protein A, as novel ligands for the integrin in mast cell activation in vitro in response to Listeria. Since ligation of the α2β1 integrin alone was insufficient to activate cytokine secretion, we hypothesized that an additional signal emanating from a co-receptor was required to activate mast-cell cytokine secretion. We identified the required co-receptor as hepatocyte growth factor (HGF-R)/c-met.[106] We demonstrated that Listeria induced mast cell activation and cytokine secretion requires costimulatory signals from α2β1

integrin ligation to either type I collagen or C1q as well as c-met activation. The synergistic signal from the two coreceptors resulted in mast cell release of the proinflammatory cytokine IL-6 to trigger the early innate immune response.

1.1.6 α2β1 in Epithelial Biology

The α2β1 integrin is expressed at high levels on numerous epithelial cells, including not only the squamous epithelium, but also ciliated columnar epithelium of the respiratory tract, the epithelial cells of the gastrointestinal tract and urinary tract, and the glandular epithelium of the breast [30]. In contrast to the high α2β1 integrin expression in the normal breast epithelium, markedly reduced or undetectable levels of α2β1 integrin were seen in poorly-differentiated carcinomas. Expression of α2β1-integrin was diminished or lost in a manner that correlated with a loss of epithelial differentiation and tumor progression in mammary carcinoma as well as other adenocarcinomas, including those of the prostate, lung, pancreas, and skin.

Our group's early studies focused on understanding the correlation between α2β1 integrin expression and a differentiated epithelial phenotype and, conversely, whether dysregulated α2β1 integrin expression contributed to the malignant behavior of cancer cells. Gain of function and loss of function models *in vitro* suggested that α2β1 integrin expression contributed to the differentiated epithelial phenotype and branching morphogenesis of mammary and other epithelial cells.[107–109] These observations were supported by findings from other laboratories. Using an immortalized primary human nonmalignant mammary epithelial cell line, Berdichevsky et al. and D'Souza et al. demonstrated that branching morphogenesis can be blocked by inhibitory monoclonal

antibodies directed against the α2 integrin subunit or by altered α2β1-integrin expression mediated by expression of the c-erbB2 proto-oncogene, respectively.[110–112]

The development of genetically engineered mice with global deletion of *ITGA2* permitted further analysis of the role for α2β1 integrin *in vivo*. The major changes in branching morphogenesis in vitro were not fully recapitulated *in vivo*. The α2-null mice have only modest defects in mammary morphology. The *in vitro* experiments were designed to study a single integrin interaction on epithelial cells with only a small number of matrix molecules. Mammary gland *in vivo* consists of epithelial cells, fibroblasts, endothelial cells, and immune cells embedded in a complex matrix. The complexity in *in vivo* systems and compensatory mechanisms may both mitigate the consequences of α2β1 integrin-deficiency.

1.1.7 The α2β1 integrin plays a role in cancer progression

Interest in α2β1 integrin in breast cancer began with the observation of a strong correlation between diminished α2β1 integrin expression and a less differentiated phenotype. The α2β1 integrin–deficient mouse model provided our laboratory the opportunity to investigate a role for integrin in the development and progression of breast cancer *in vivo*. Our group demonstrated that in the spontaneous MMTV-neu mouse model of breast cancer, α2β1 integrin-deletion did not significantly alter the incidence of tumor development or tumor growth, but markedly increased hematogenous metastasis.[113] Increased metastasis in this model resulted in part from increased capacity for cancer cell intravasation.

I performed detailed *in silico* examination of publicly available data from breast cancer patients to establish the clinical relevance of this finding; expression of the α2

integrin subunit, but not α1 or β1 integrin subunits, was a prognostic indicator of decreased metastasis and better patient outcomes. Similarly, retrospective analysis of lymph node-negative patients from the Wang cohort who relapsed with metastatic disease, revealed an inverse correlation between α2β1 integrin expression and the occurrence of brain lesions; patients with greater than twice the average α2β1 integrin expression suffered no brain metastasis whereas all nearly one third of all other patients suffered brain metastasis (P=0.0049).

Expression of the α2β1 integrin in prostate cancer was also predictive of metastasis and survival. The mouse and human studies supported the *in vitro* experimental analyses and the reported epidemiologic linkage between the single nucleotide polymorphisms regulating α2β1 integrin expression and poor prognosis in patients with breast cancer.[22] Together these data suggested that α2β1 integrin as a valuable biomarker for risk of metastasis in breast cancer. The success of wedding *in silico* data-mining with *in vivo* mechanistic exploration using the transgenic α2-null mouse has served as a template for planning both the pathological and developmental angiogenesis studies in this dissertation.

1.1.8 ITGA2 SNPs and α2β1 integrin expression

In addition to microarray studies, analysis of genetic polymorphisms has provided valuable information for the study of α2β1 integrin**.** There is substantial variation in the baseline expression of α2β1 integrin in the population; quantitative measurements of platelet surface membrane α2β1 integrin expression indicate as much as a 10-fold difference among normal patients.[114] The mechanism of genetic regulation of the gene encoding the α2 integrin subunit has been best delineated. The variation is genetically

determined and associated with three alleles of the α2 integrin subunit gene, *ITGA2.*[28,115] The three alleles have been defined by 8 nucleotide polymorphisms in the coding region of *ITGA2* gene at nucleotide 807(C or T) and 873(G or A). Individuals carrying the 807T/873A allele express high levels of platelet α2β1 integrin, whereas individuals carrying the 807C/873G allele exhibit low levels of α2β1 integrin expression. Cheli et al. described another variant in CA repeat length in the *ITGA2* gene promoter that demonstrated linkage disequilibrium with variants in the coding region.[116] It is presumed that the genetic regulation of α2β1 integrin expression is similar across many cell types.

Genetic regulation of α2β1 integrin expression has meaningful biological implications, which have been most widely appreciated in the area of hemostasis and thrombosis. Kunicki et al. reported functional significance of α2β1 integrin expression levels by demonstrating that the number of α2β1 integrin molecules per platelet correlated with the ability of platelets to adhere to Type I collagen.[28] Clinical and epidemiologic studies based on genetic polymorphism analysis demonstrated direct clinical significance of allelic differences in levels of α2β1 integrin expression. The alleles associated with high levels of α2β1 integrin expression were associated with nonfatal myocardial infarction in individuals less than a mean age of 62 years, with an increased risk of developing diabetic retinopathy in patients with Type II diabetes mellitus and with an increased risk of stroke.[117,118].

The original assumption was that increased integrin expression led to increased platelet adhesion to collagen and subsequent risk of thrombosis. Recently, an alternative mechanism for the association was suggested. The level of α2β1 integrin expression correlated with mean platelet volume in humans and during megakaryocyte

differentiation and proplatelet formation in mice.[119,120] Surprisingly, platelet specific deletion of the integrin using the platelet factor 4 promoter-Cre construct and mice with a floxed *ITGA2* gene demonstrated that mice lacking platelet-specific α2β1 integrin showed decreased megakaryocyte differentiation, diminished proplatelet formation and decreased mean platelet volume.[121] Since mice with global deletion of *ITGA2* failed to show altered megakaryocytic/platelet differentiation, compensation by alternative integrins, cell types, or pathways was sufficient to prevent this additional phenotype. Epidemiologic data linking levels of the α2β1 integrin expression with risk of pathologic thrombosis and other cardiovascular complications underscore the importance of further clarifying the role for α2β1 in platelet function.

1.2 The Vascular System

In embryogenesis, blood vessels form *de novo* from mesoderm-derived endothelial precursor cells known as angioblasts. These precursor cells form multicellular aggregates called blood islands in the visceral yolk sac.[122] In a process termed ‘vasculogenesis’ the blood islands differentiate into endothelial cells and form a simple tube-network that defines the primary vascular plexus. The major arteries and veins of the body which arise during embryogenesis are formed through this process. Extension of these major arteries into the surrounding tissue occurs through a process known as angiogenesis. The specific role of the α2β1 integrin in sprouting angiogenesis is the central focus of Chapter 3 in this dissertation, and is reviewed at length in this part of the introduction.

Mechanical and signaling cues organize developing blood vessels into a ‘hierarchical system’ consisting of arteries, veins and capillaries. Arteries act to carry

oxygenated blood from the heart to higher tissue and are characterized by thick muscular walls with relatively small lumens. Veins function to bring deoxygenated blood from the body back to the tissue and are typically large-bored low pressure vessels. Capillaries are minimalist vessels that connect the arteries and veins and their characteristic thin walls, which can be as small as a single endothelial cell in depth, providing the medium for exchange of nutrients and waste with the surrounding tissue. In each of these vessel types, form and function are mutually reinforcing; altered flow within vessels can drive vessel remodeling and changes in blood vessel size cause changes in flow. This is a dynamic that is involved in the pathogeneiss of many vascular diseases.

The primary building block of the blood vessel is the endothelial cell. Endothelial cells line the vessel lumen and are the minimal requirement for capillary formation. In larger vessels, capillaries are stabilized and supported by mural cells. Mural cells include pericytes which stabilize capillaries and vascular smooth muscle cells which cover veins and arteries. Compared to veins, arteries require larger, more complex networks of elastic fibers and vSMCs to accommodate high blood flow and pressure. In contrast, veins have valves and other structures to maintain uni-directional flow in a low pressure environment.

1.2.1 Angiogenesis

Angiogenesis, the growth and extension of the vascular network from existing blood vessels, is a highly complex process and includes a series of detailed morphogenic and cellular processes. Angiogenesis can occur in two distinct ways, intussceptive or sprouting angiogenesis. Intussceptive angiogenesis comes from the

splitting of two existing vessels. Initial steps in intussceptive growth come from the extension of an endothelial cell structure, called a ‘vascular pillar,’ through the center of a vessel. The pillar widens and recruits mural cells and deposits extracellular matrix until the vessel is completely split. After they are split, remodeling and response to growth factor gradients causes the paths of the two new vessels to evolve in different directions.[123]

Sprouting angiogenesis, the subject of my studies in Chapter 3, is reviewed in this section. I describe the various stages of sprouting angiogenesis including: the initial phase of neovessel formation, tube formation, vessel stabilization, and then finally vessel regression.

1.2.2 Vascular Sprouting and Patterning

Vessel patterning of the vascular network is highly organized. Each tissue or organ system is characterized by a uniquely adapted pattern or superstructure for the vascular network. These patterns arise from a guided process in which sprouting angiogenesis is carefully coordinated by gradients of attractive and repulsive cues. Vessel regression also plays a role by pruning unnecessary or unwanted vessels that arise.

Sprouting angiogenesis appears to be driven at the endothelial cell level. Endothelial cells are a highly plastic cell type. *In vitro* experiments have found relatively minor differences between primary endothelial cells from different contexts; however, within the specific *in vivo* context of the angiogenic sprout, endothelial cells sort themselves into distinct subpopulations characterized by unique morphologies.[124] The tips of angiogenic sprouts are characterized by an isolated endothelial cell with

extended filopodia directed towards an angiogenic cytokine gradient. This morphology was initially identified by Marin-Padilla in 1985.[125] The endothelial cells in the angiogenic sprout behind the leading Tip cell are called Stalk cells and are marked by limited filopodia. The differences in cell morphology and gene expression indicate a functional 'division-of-labor' between endothelial tip and stalk cells. Tip cells function as migratory leader cells which guide blood vessels towards attracting cues defined by a cytokine gradient secreted by cells of an avascular area. In contrast, the stalk cell phenotype is highly proliferative; stalk cells must divide fast enough to fill the voids left by migrating tip cells.

Interestingly, recent work from Jakobsson et al. has determined that the Tip and Stalk populations are in flux through a process termed 'shuffling' once again highlighting the dynamic and plastic quality of endothelial cells.[126] Stalk cells undergo lumen formation and create the interior lining of the new vessel. Gene expression studies using laser microdissection have determined that tip and stalk cells within the same vascular beds have radically different gene expression profiles; in fact, it appears that expression profiles from tip and stalk cells within a vascular bed are more different than the endothelial profiles of any two vascular beds. A specific marker of Tip-Cells has not been identified but a constellation of markers are enriched in tip cells compared to stalk cells. Tip cell express Pdgfb, Dll4, Unc5b, Kdr and Flt4 at dramatically higher levels than stalk cells.[124,127–130]

Vessel patterning is regulated, in part, by the distribution of cytokine gradients which act as attractive cues. Vascular endothelial growth factor-A (VEGF-A) is one of six members of the VEGF family, which includes VEGF-B, VEGF-C, VEGF-D, viral VEGF-Es encoded by the parapoxvirus Orf, and placental growth factor (PLGF).[131]

VEGF-A is comprised of two monomers arranged head-to-tail in a homodimer with two interchain disulfide bridges. Each VEGF-A monomer has a cystine knot motif, which consists of eight highly conserved cysteine residues bound by three intrachain disulfide bonds.[132] The expression and function of VEGF-A is critically important for haematopoiesis and cardiovascular development. In vascular development, VEGF-A is required for angioblast chemotaxis and differentiation, endothelial cell proliferation, vasculogenesis and angiogenic remodelling. Inactivation of a single Vegfa allele in mice is embryonic lethal at the E11 stage due to impaired endothelial cell development and vessel formation.[133,134]

The extracellular VEGF-A gradient is the primary gradient responsible for guided angiogenesis during initial vessel patterning, although there are subtler roles for other VEGF family members. Although VEGF-A is soluble, in *in vivo* settings VEGF-A gradients are laid in the extracellular matrix by heparin/heparan sulphate binding. In the postnatal development of the mouse retina VEGF-A164 and VEGF-A188 have been demonstrated to be required for generation of a steep extracellular VEGF-A gradient.[124,135] The VEGF-A gradient in the postnatal mouse retina arises from astrocyte secretion of VEGF-A in the avascular area ahead of the migrating vascular front. The highest VEGF-A concentration is found just beyond the periphery of vascular plexus and the lowest is found in the vascularized region near the optic nerve. Disruption of this VEGF-A gradient causes defective tip cell filopodia formation as manifested by shorter, aberrantly oriented filopodia.[124] Disruption of the VEGF-A gradient also impairs directed endothelial tip cell migration. These disruptions are phenocopied by activation of the major endothelial cell receptor for VEGF-A, VEGFR2. Together these findings demonstrate that guided sprouting angiogenesis requires the directed tip-cell migration

through a gradient of VEGFR2 agonists. Localization of VEGFR2 at high levels on the filopodia of endothelial tip cells has highlighted the importance of filopodia extension in migration during postnatal retinal development.[124]

Interestingly, endothelial cell in the stalk conformation are not responsive to the VEGF-A gradients. Presumably, this is because of decreased VEGFR2 containing filopodia on stalk cells. VEGFR2 activating mutations causes increased proliferation in stalk cells resulting in increased endothelial cell density and greater vessel diameter but does not affect branching frequency or vessel length.[136] Together, these results underscore the complex coordination of angiogenic functions by the tip and stalk cell phenotypes.

1.2.3 Vessel Morphogenesis and Stability: cues from the ECM and integrins.

Another consequence of their high plasticity is the ability for endothelial cells to adopt a wide range of morphologies. In the normal biological context, this is seen most radically in the course of lumen formation. In both vasculogenesis and angiogenesis, tube formation is carefully orchestrated; endothelial cells migrate and orient themselves to form solid cords in a polygonal conformation that ultimately matures to form tubes with hollow lumen.[137] Time-lapse imaging of developing blood vessels in the zebrafish embryo model system has beautifully captured dynamic changes in endothelial polarization and shape during sprouting, migration, and tube morphogenesis.

After the formation of a functional vascular network, the endothelial cells adopt a quiescent phenotype that maintains the integrity of the blood vessel until angiogenic cues indicate a need for remodeling of the vasculature. Interestingly, throughout vessel assembly and sprouting angiogenesis, endothelial cells maintain intercellular adhesions.

This ability allows for dramatic vessel remodeling and vascular expansion without compromising the tubular structure of blood vessels during sprouting. Understanding the external signals that direct and coordinate endothelial cells into a wide range of phenotypes is of significant scientific and clinical interest.

Increasingly, studies suggest that ECM interactions influence sprouting angiogenesis. Components of the ECM surrounding endothelial cells have been demonstrated to orchestrate specific signaling and morphology changes. For example, on Type I Collagen, endothelial cells adopt a spindle-shaped morphology. It has been demonstrated that in endothelial cells binding of Type I Collagen to α1β1 and α2β1 integrins suppresses cAMP and consequently cAMP-dependent protein kinase A (PKA) activity. Downregulation of PKA activity induces actin polymerization and contributes to prominent stress fiber formation and endothelial cell contractility, which accounts for the observed morphological changes.[138] These cellular changes recapitulate the remodeling that occurs during cord formation.[138] In addition to PKA-mediated changes, Collagen I binding also triggers activation of Src and Rho, which induce actin stress fiber formation and mediate cell retraction and vessel morphogenesis.[139] RhoA has also been demonstrated to play a regulatory role in endothelial cell assembly in the formation of new blood vessels *in vivo.*[140] In contrast, exposure to laminin-1 does not induce changes in cAMP or actin polymerization and consequently induces a different morphology along with its unique signaling.[138]

Integrin and ECM-interactions have a critical role in lumen formation. The formation of coherent, function endothelial tubes is indispensable for the development of a functional circulatory system. In 3D endothelial cell culture systems, lumen formation has been demonstrated to happen through an integrin-dependent pinocytic

process.[141,142] Initially, extensive vacuoles are formed through pinocytosis. This is followed by fusion of these vacuoles with basolateral membrane at sites of endothelial junctions to form a continuous luminal structure that extends through a number of endothelial cells.[142] A similar process of lumen formation and extension was observed *in vivo* in the zebrafish model system. Kamei et al. describe intracellular vesicle formation, vesicle fusion, and vacuolar merging during the formation of intersegmental vessels using high-resolution time-lapse imaging of transgenic zebrafish.[143]

The molecular signaling that underlies this process has been carefully characterized. Rho GTPases Cdc42 and Rac1 have been demonstrated to be required for formation of the vacuoles. Both *in vivo* and *ex vivo* experiments show strong staining of both Rac1 and Cdc42 on vacuole membranes.[142,143] In 3D cell culture systems it has been demonstrated that dominant negative Cdc42 and Rac1 proteins inhibit vacuole formation and lumenization.[142] Lumen formation also requires significant endothelial cytoskeletal remodeling. Cytoskeletal regulatory proteins such as myosin IC and myosin VI are up-regulated during endothelial cell vacuole and lumen formation.[142] Additionally, treatment with cytochalasin B or nocodazole, agents that inhibit cytoskeletal network formation, completely inhibit endothelial cell vacuole formation and lumenization.[144]

After formation of the vascular network, the endothelial cells of the blood vessels enter into a quiescent state. This is accomplished both by decreased exposure to ‘angiogenic stimuli’ and increased production of stabilization factors that promote vessel homeostasis. During this process junctions between endothelial cells tighten, and there is increased recruitment of mural cell populations. Additionally, vessel stabilization is reinforced through the deposition of a vascular basement membrane which in turn provides the vessel with both structural and signaling organizational cues.

The ECM components of the vascular basement membrane consist of laminins (predominantly laminin α4β1γ1 and laminin α5β1γ1), Type IV Collagens, perlecan, nidogens, collagen XVIII and von Willebrand factor.[145] Data from transgenic mouse models demonstrate that the structural support provided by the basement membrane helps to regulate mechanical signals for vessel remodeling; mice homozygous for deletion of collagen IV, perlecan and laminin α5 chain exhibit blood vessel dilation.[146–148] Basement membrane formation still occurs, in mice with deletion of collagen IV, perlecan or laminin α4, but the resulting basement membrane is fragile and breaks down over time in areas of high mechanical stress.[146,148,149] In addition to its indirect signaling role via modulation of mechanotransductive signals, the basement membrane also has a direct signaling role with endothelial cells. These signaling pathways are still being untangled. Laminin binding with integrins α3β1 and α6β1 are thought to stabilize vessels by promoting quiescent signaling. Specifically, laminin signaling through these molecules has been shown to suppress proliferative signaling through regulation of Ras-MAPK and NF-κB pathways.[150,151] Laminin-1 has also been shown to induce activation of Rac1 and PKA and suppress Rho activity, which has the effect of promoting endothelial cell quiescence.[137] Together these findings suggest that laminins act simply to maintain vessel homeostasis and turn off the angiogenic potential of the cell. However, more recent work has indicated that laminin-411 plays a critical role in inducing tip cell activation.[152] A possible explanation for this discrepancy is that the signals from matrix components are interpreted by endothelial cells differently depending on the degree of growth factor present in the microenvironment.

As a sidenote, in this section we have focused heavily on the role of laminins in the basement membrane. For historic reasons, the role of laminins in basement

membrane assembly has been emphasized, while the other components have been viewed as dispensable.[137] However, emerging knowledge about the organizing bonds within Type IV Collagen promise a greater appreciation for its role in coordinating the vascular basement membrane in the future.

In addition to directly signaling to integrins, the basement membrane also provides a barrier for neoangiogenesis through the presence of embedded substrates for the production of anti-angiogenesis molecules. For example, endostatin, a well-known negative regulator of angiogenesis from tumor studies, is a c-terminal proteolytic fragment of Collagen XVIII.[153] Endostatin's signaling partners are unclear, but it is suggested that it acts by inducing RhoA downregulation and interrupts focal adhesion and stress fiber formation upon binding to the α5β1 integrin.[145,154] Similarly, Tumstatin, another endogenouse anti-angiogenesis molecule is also a byproduct of ECM degradataion.[155] Tumstatin is thought to be a degron of Type IV collagen and appears to function through the αvβ3 integrin. Finally, Endorepellin, a degron of perlecan which acts via inhibition of α2β1 has broad anti-angiogenic activities. It has been shown to inhibit endothelial cell migration and tube formation *in vitro* and also impair growth factor-induced angiogenesis in the CAM assay and in 3D matrigel plugs.[156]

1.2.4 Notch Signaling

As we have discussed, guided angiogenic sprouting is an *emergent phenomenon* that arises from the specialization of ECs within the growing vessels into migratory 'tip' and proliferative 'stalk' cell phenotypes with differential response to a gradient of external stimuli and a patterned environment.[124,157,158] This specialization is the result of

the careful spatial localization of VEGFR1 and VEGFR2 levels via a complex schema of ‘lateral inhibition’ carried out by the Notch signaling system.

The notch signaling pathway is named for the ‘notched’ wing phenotype observed in drosophila when it was first characterized. The notch pathway is highly evolutionarily conserved, reflecting the depth of its involvement in primordial processes regulating body plan organization and embryonic development. It also acts in critical ways to regulate adult tissue homeostasis, and is an important mediator of stem cell maintenance.[159,160] Additionally, notch signaling has been found to be involved in basic cell biology processes including differentiation, proliferation, survival, and apoptosis.[161,162] It is increasingly obvious that the notch signaling system integrates with many other ancient signaling networks including the transforming growth factor β (TGFβ), Wnt, and ERBB signaling systems to provide the complex crosstalk necessary to provide robustness to cellular organisms. Untangling the specific conduits of crosstalk between the notch signaling system and other important signaling pathways has incredible potential for the treatment of human disease.

A number of diseases are characterized by aberrant notch signaling. Most prominently, cancers including T-cell acute lymphoblastic leukemia and head and neck squamous cell carcinoma have been linked to notch mutations.[163,164] Additionally, congenital diseases such as the Alagille syndrome, and Cerebral Autosomal Dominant Arteriopathy with Subcortical Infarcts and Leukoencephalopathy (CADASIL), underscore the critical importance of the notch pathway in development and maintenance of functional vasculature.

Mammals have five canonical Notch ligands, Delta-like 1 (Dll1), Delta-like 3 (Dll3), Delta-like 4 (Dll4), Jagged1 (Jag1) and Jagged 2 (Jag2), classified as DSL

(Delta, Serrate, LAG-2) ligands. DSL ligands are type 1 cell-surface proteins with extracellular domains consisting of multiple tandem epidermal growth factor (EGF) repeats. Mammals also have four Notch receptors, Notch1, Notch2, Notch3 and Notch4, which are large single-pass type I transmembrane receptors.

Notch receptor binding to a DSL ligand through its extracelluar domain initiates a series of proteolytic cleavages that release the Notch intracellular domain (NICD). The first receptor cleavage occurs by a member of the disintegrin and metalloproteases (ADAM) within the juxtamembrane regions (known as S2), followed by cleavage of the transmembrane domain by γ-secretase. Inhibitors of γ-secretase, are popular options for inhibiting notch signaling. Our studies in chapter 3 of this dissertation rely heavily on the use of the γ-secretase-inhibitor, DAPT.

Cleaved NICD is released into the cytoplasm and then translocated to the nucleus where it enacts several transcriptional programs. NICD directly interacts with the CSL (CBF1, Su(H), LAG1) transcription factor. Without NICD binding, CSL acts as a transcriptional repressor.[165] However, binding of NICD to CSL causes the formation of a transcriptional activator complex that include Mastermind-like 1 and histone acetyltransferases such as p300 to activate the expression of Notch target genes such as the basic helix-loop-helix (bHLH) proteins Hairy/Enhancer of Split (Hes), Hes-related proteins (Hey/HRT/HERP). Hes, Hey and other immediate notch targets, in turn mediate their own transcriptional programs to further propagate downstream notch signaling effects. The specific gene expression pattern of notch signaling appears to be very cell-type specific

In the vasculature, Notch signaling has important roles in vascular smooth muscle cells and endothelial cells. Chapter 3 of this dissertation focuses on notch

regulation within endothelial cells, so we will describe that signaling in detail here. In endothelial cells Notch receptors, Notch1 and Notch4 are expressed. Endothelial cells also express the DSL ligands, Dll1, Jag1 and Dll4.[127,166] Genetic deletion studies in transgenic mouse and zebrafish have identified Dll4 as the most prominent notch ligand in the blood vessel development and angiogenesis. Genetic deletion of Dll4 is embryonic lethal in mice, heterozygous Dll4+/- mice have a pronounced hypersprouting phenotype which reveals the importance of Dll4 in regulating tip and stalk specification. Experimental analysis of zebrafish intersegmental vessels (ISV) and tumour angiogenesis models also highlight the importance of Dll4/Notch signaling in regulating angiogenesis. Tip cells are marked by high levels of Dll4 while Notch signaling is characteristically high in stalk cells.[127,158] Endothelial specific deletion of Notch1, or Notch signaling inhibition by chemical γ-secretase inhibitors replicates the increased vascular plexus density and hypersprouting phenotype of the Dll4+/- mutants. All of these mutants exhibit aberrant overexpression of tip cell marker such as expression of Pdgfb. Additionally, in these cells, stalk cells have uncharacteristic filopodia induction.[158,167]

In summary, Dll4-expression in tip cells prevents tip cell fate in neighboring cells exposed to relatively similar VEGF-A gradients by inducing Notch signaling in the neighboring cell and conferring stalk cell status (Figure 1.1). Inhibition of Notch signaling results in upregulated vascular endothelial growth factor receptor (VEGFR) VEGFR2 expression in all endothelial cells, suggesting that Dll4 signals through Notch1 in adjacent cells to initiate negative feedback regulation of VEGFR2 levels in neighboring cells.[167,168] It is thought that this occurs directly through notch-stimulated Hey1 binding to the VEGFR2 promoter.[169] The tip cell phenotype is the default setting under

Figure 1.1 Notch-mediated Lateral Inhibition

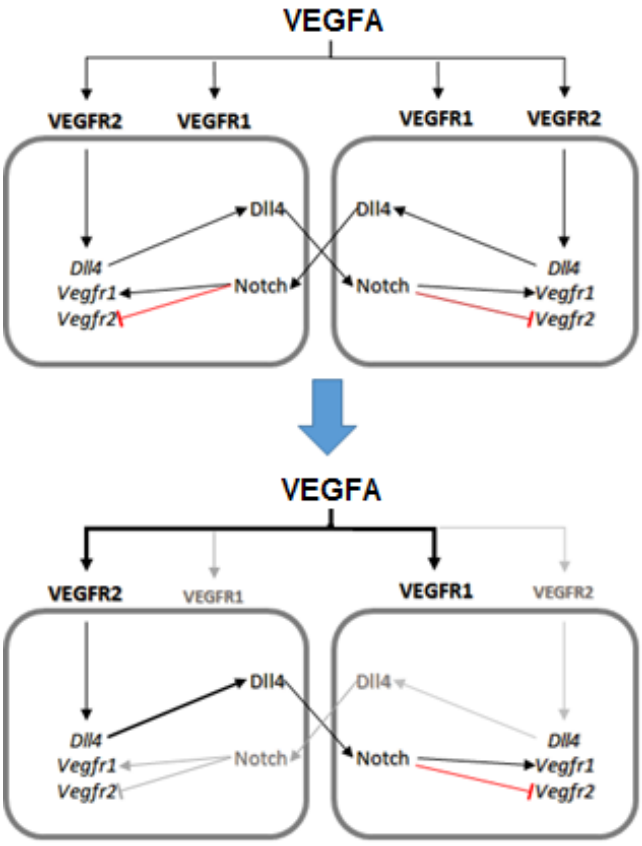

conditions of growth factor stimulation, whereas the stalk cell phenotype is only acquired by induction of Notch signaling.[158] Consequently, Dll4 functions to restrict tip cell formation and excessive sprouting and therefore, has what can be broadly defined as anti-angiogenic signaling.[170] The lateral inhibition system initiated by DLL4 is comprised of two interlocking negative feedback loops that combine to create a positive feed forward loop that provides powerful signal sensitivity and elegant control over the angiogenic response.

1.2.8 The α2β1 Integrin and Angiogenesis/Vasculogenesis

During VEGF-induced angiogenesis, *in vivo* expression of α2β1 integrin is up-regulated and α2β1 integrin expression has been observed on the sprouting tips of neonatal blood vessels.[171,172] Together these results suggested an important function for α2β1 in angiogenesis, however the precise nature of the integrin's role is still incompletely understood

The earliest investigations into the functional role of α2β1 in angiogenesis employed inhibitory antibodies during *in vitro* studies. Early reports from Gamble et al. indicated that anti-α2β1 antibodies inhibited endothelial cell proliferation on collagen[173]

Soon after, Davis reported that anti-α2 inhibited lumen and tube formation by HUVECs in a 3D collagen matrix.[174] Later studies using planar type I collagen gel angiogenesis assays, confirmed that inhibition of α2β1 integrins with function blocking antibodies disrupted tube formation.[175] Senger et al. demonstrated in vivo using subcutaneous matrigel plug angiogenesis assays in mice, that inhibition of α2β1 and α1β1 in combination decreased new vessel growth in the implanted plugs. Together these results suggested a pro-angiogenic function for the α2β1 integrin.[172]

Studies from α2-deficient mice have yielded contradictory results. Several labs, including our own, reported not only normal developmental angiogenesis, but also increased neoangiogenesis during wound healing in genetically-altered α2β1 integrin-null mice.[62,90] Similarly, our lab demonstrated that α2β1 integrin-deletion increased tumor angiogenesis in a growth factor-dependent manner via modulation of VEGFR-1 signaling.[176] Additionally studies in the diet-induced obesity model also showed increased angiogenesis in α2-null mice compared to wild type mice.[177] The contradiction between the evidence for pro and anti-angiogenic functions for α2β1 integrin are not totally based off of differences in mouse and human endothelial cells or in vivo compared to in vitro models. Cailleteau et al. used an α2 siRNA approach to alter integrin expression in HUVECs. These studies showed that α2β1 integrin engagement by laminin promoted endothelial cell cycle arrest and quiescence.[178] Additionally, α2β1 integrin binding to endorepellin in both human and mouse endothelial cells mediated the angiostatic effects.[68,69,156,179]

Based on these inhibitory studies pharmacological inhibitors of α2β1 may have potential anti-angiogenic drugs effects (see therapy section). Small molecule inhibitors (SMI) of α2β1 blocked both endothelial tube-formation *in vitro* and sprouting

angiogenesis in zebrafish.[180] A more thorough understanding of the role for α2β1 in angiogenesis promises novel insight into clinical application of α2β1 integrin targeting compounds. Recent studies implicating the α2β1 integrin in notch signaling offer an alternative paradigm for understanding α2β1 integrin in angiogenesis.[152,178,181] Estrach et al. reported that α2β1-mediated laminin signaling is necessary but not sufficient for induction of the tip cell determinant, Dll4.[181] Clarifying the functional relationship between α2β1 and notch signaling in the endothelium is a promising avenue of future study and a major component of our developmental angiogenesis investigations in Chapter 3.

1.3 Modeling of Biological Networks

In the 1990s, before the human genome project, it was widely estimated that humans had over 100,000 protein-coding genes. It turns out that there are actually only a fraction of that number. Current estimates indicate approximately 25,000 protein-coding genes, despite over 100,000 proteins. This example illustrates the complex regulatory schema that are at play in living organisms. Cellular systems are able to process complex environmental stimuli and use a limited number of genetic tools to craft nuanced responses.

It is increasingly clear that the ‘information-processing’ capacity of cellular systems has fundamental rules that govern its ‘logic’. Understanding how complex networks of interacting proteins and genes respond to different signals and how those responses are perturbed in disease states can be surprisingly informative. In the last several decades, researchers in diverse fields including economics, sociology, ecology, and engineering have discovered recurring principles governing interactions within the

systems they study. Recently, biologists have begun to use the same approaches to tease apart the simple regulatory principles that govern complex cellular control networks.[182]

1.3.1 Network Robustness

Robustness is the ability of network systems to preserve structure and function in response to internal or external variation. Biological networks have evolved to have strong robustness in order to preserve biological functions in extreme circumstances. One illustration of the high degree of biological robustness is the surprising rarity of embryonic lethality in genetic deletion mouse models.

There are several mechanisms that provide robustness to a biological network. Redundancy or functional duplication in the form of parallel network motifs can provide strong stimulus response while enhancing self-correcting resistance to environmental insults. Gaining additional negative feedback enhances robustness, while addition of positive feedforward stimuli increase signal sensitivity. An alternative approach is coupling feedback loops (FBL) or feedforward loops (FFL), to allow complex outputs with a limited number of components. Lateral inhibition in the notch signaling system is an example of a regulatory phenomenon which can be evaluated in terms of robustness. Kim et al, showed that interlinked negative feedback loops add robustness to a system.[183] In the context of the notch signaling system, pairing the VEGFA-VEGFR2-DLL4 negative FBL to the VEGFA-VEGFR2-VEGFR1 negative FBL allows for more rapid tip-stalk fate assignment and enhanced resistance to local variations in VEGFA abundance.[184] Identifying further coupled negative FBL and positive FFL may lead to the identification of novel adjuvant therapies for emerging VEGF and DLL4

targeting anti-angiogenic drugs. Understanding how deletion of components of the notch network affect robustness or signal sensitivity can point to previously undiscovered sources of positive or negative feedback.

1.3.2 α2β1 integrin signaling

Despite extensive experimental evidence that the α2β1 integrin plays a unique contribution in regulating cell migration, proliferation, and survival, we have relatively little information about the specific signaling initiated by the integrin. In this section, I will quickly summarize what is currently known. The α2, but not the α1, integrin cytoplasmic domain mediates p38 MAP kinase pathway activation and a migratory phenotype.[185,186] Expression of the constitutively active small G protein Rac1 augmented p38 MAP kinase phosphorylation and migration in mammary epithelial cell expressing full length α2 subunit. The role of the α2-cytoplasmic domain in activation of the p38 MAP kinase pathway was also established in fibroblasts. Fibroblasts grown in three-dimensional collagen gels require the α2-cytoplasmic domain for p38 MAP kinase activation that leads to α2β1 integrin-mediated up-regulation of collagen gene expression.[88] Together, these results support an important and specific role for the α2-cytoplasmic domain in mediating p38 MAP kinase activation. Similarly, the cytoplasmic domain of the α2 integrin subunit specifically supports insulin-mediated S-phase entry.[185] The α2, but not the α1, cytoplasmic domain mediated activation of the cyclin E/cdk2 complex, which allows entry into S-phase in the absence of growth factors other than insulin. These results suggest that the α2 integrin cytoplasmic domain and the insulin receptor synergize to regulate cell cycle progression.

More recently, Ivaska et al. suggested that the α2β1 integrin induced protein serine/threonine phosphatase 2A (PP2A) activity in a collagen-specific manner.[187] In their studies, collagen-induced PP2A activation and resulting dephosphorylation of Akt and glycogen synthase kinase 3β (GSK3β) in Saos-2 cells was α2β1 integrin-dependent. PP2A is a master regulator of a diverse set of cellular signaling pathways, so its interaction with α2β1 integrin has the potential to dramatically increase the scope of the signaling activities of the integrin. Careful investigation of these putative signaling mechanisms is necessary for a clearer understanding of the role for the integrin in various cell types. The relative dearth of signaling information that has been produced from extensive *in vivo* and *in vitro* studies, suggests that employing multidisciplinary, informatics and modeling based approaches to identify the network motif nodes occupied by the integrin may be a valuable alternative strategy for gaining information about the integrin's function and signaling.

1.3.3 Continuous models of Angiogenesis

Simply speaking, continuous models are a type of computational model that handles variables in a spectrum, rather than as individual values. In other words, they treat the tissue as a whole, rather than evaluating any particular cell. The advantage of continuous modeling is that one can relatively easily compute complex phenomena.

Continuous mathematical models of angiogenesis first emerged in the late 1970's and focused on tumor angiogenesis.[188] These models applied fundamental principles of mass conservation and chemical kinetics to predict the behavior of blood vessels using averaged quantitative metrics such as vessel and tip densities and capillary extension speeds. One of the seminal models of this sort was Balding and McElwain's work on

tumor-induced capillary growth from 1985.[189] They used three relatively simple equations in one dimension to account for the sprout tip density, capillary density, and angiogenic growth factor concentration. This model was novel at the time for the idea that the tips of angiogenic sprouts guide capillary formation. Their model was the first to explain the experimental data indicating proliferation of endothelial cells lagged behind tip cells growing towards tumors. It was also innovative in that it explained the bush-border effect - the increase in branching frequency as the vascular network approached the tumor.[190] With minimal parameterization, they were able to reproduce observed differences in vessel lengths and tip speeds. Later Byrne and Chaplain modified this basic approach and incorporated explicitly branching and tip-sprout anastomoses.[191] They concluded that this phenomena occurred only above a certain threshold of angiogenic growth factor concentration. They also modeled, for the first time, uptake of angiogenic growth factor by the endothelium. Many of the predictions from these early models presaged the experimental discoveries in the notch field.

This approach was extended into two dimensional fields in the 1990s. In 1997, Orme and Chaplain developed a two-dimensional model for tumor angiogenesis, that for the first time, attempted to incorporate cell-matrix interactions.[192] They incorporated endothelial cell haptotaxis along gradients of fibronectin. The addition of haptotaxis allowed for more accurate modeling of changes endothelial cell density as the vascular network migrated towards the tumor. Previous models that did not account for haptotaxis predicted anastomoses too early in the migration towards the tumor. This model was built upon the next year by changing the assumptions about growth factor concentrations; previously, models had assumed steady state growth factor gradients, but now Chaplain and Anderson used a quasi-steady state for growth factor

concentrations and a maximal limit on endothelial growth factor receptor sensitivity [193]. These changes allowed for differences in branching behaviors to emerge based on the layout of the tumors.

These early models were remarkably powerful given the lack of signaling information available at the time. However, these models had several flaws that prevented ready application to modeling of retinal development, the most important of which is use of steady state profiles to model growth factor concentration. In tumor models, this is justified, as the diffusion of growth factors happens relatively quickly compared to the migration of the endothelial cells. In developmental contexts such as the retina, most growth factors, including VEGF, are sequestered by the ECM and biologically unavailable except to specific cells. Consequently, the ability to incorporate differential interaction with steep local growth factor gradients by neighboring cells is essential for productively modeling developmental angiogenesis.

1.3.4 Discrete models of Retinal Angiogenesis

Discrete or hybrid models calculate the actions of individual cells separately over time. Continuous models were able to recapitulate basic angiogenic phenomena and accurately model sprout density, rates of vascular expansion, and the distribution of capillary sprouting. However, detailed structural analysis was impossible to model and had to be explicitly coded. Discrete or hybrid modeling approaches allow modelers to ask questions about issues such as plexus irregularity, and branching complexity of individual sprouts or endothelial cells must be tracked. Discrete or hybrid modeling approaches allow for this innovation.

In 1991, Stokes and Lauffenburger published one of the earliest discrete models for angiogenesis [194]. They used stochastic differential equations to govern the velocity of individual vessel tips, and, as a result, were able to model the growth of individual sprouts within the capillary network. This adjustment allowed the model to produce much more realistic capillary networks to be generated within minimal rules-based parameters for sprout branching and looping. The model used random motility corrected by chemotaxis to govern cell migration. This model was an improvement in many ways, but was unable to replicate the bush-border effect, indicating that some organizing principle of angiogenesis was still not understood.

An alternative approach from Anderson and Chaplain utilized standard finite-difference methods to discretize the model equations that had been developed for the continuous models [193]. The coefficients produced from this method were used to govern movement of individual endothelial cells by generating movement probabilities resulting in a biased random walk motion. The capillaries behind each tip cell were assumed to simply follow behind. Again, biologically derived rules were used as parameters for branching and anastomoses. These adjustments allowed for haptotaxis to slow migration near the tumor and result in increased branching, yielding the bush-border effect. When cell mitosis was included in this model, very realistic branching networks were observed that are able to successfully vascularize hypoxic regions.

Discretizing equations from continuous modeling is a powerful technique for producing realistic modeling outputs. However, this approach risks the introduction of significant bias during the discretization process. Continuous models are able to account for the full spectrum of intensity of cellular responses; converting to a discrete equation is susceptible to losing that level of nuance.

An additional alternative was first put forward by Othmer et al.[195].They also rely on growth factor gradients to reinforce a random walk style of cell migration, however they use a probability master equation to generate this effect. By fully incorporating probability into the actions of each cell, they were able to replicate the nuance of the continual model with the scientific versatility of the discrete model. In Chapter 3 we will use the same principle to model cell migration in our model.

1.4 The Retina and Retinopathy

1.4.1 Müller Cells

The retinal Müller cell is the principal glial cell of the retina and has several critical functions. First, they span the thickness of the retina radially and serve to provide structure support for the retina. Müller cell bodies lay in the INL and send projections that reach the OLM and ILM on each side of the retina. These cellular projections envelop the neurons of the in both the INL and ONL indicating a close functional relationship.

Retinal neurons and retinal Müller cells share a common progenitor cell but differentiate in separate periods.[196] First, cone photoreceptors, horizontal cells, and ganglion cells arise at the apical edge of the retina. In a second burst of differentiation Müller cells are formed along with rod photoreceptors, bipolar cells and amacrine cells.[197] Müller cells migrate inward from the pigmented epithelium towards their final destination and are thought to guide the innervation of the tissues they enter.

Müller cells can be difficult to identify via immunostaining. They are known to contain glycogen, mitochondria. Their long cellular projections include intermediate filaments that can be stained by vimentin and glial fibrillary acidicprotein (GFAP).

Vimentin and GFAP are normally localized in the inner portion of the retinal Müller cells but in conditions of stress or trauma are dramatically upregulated and found throughout the cell.[198,199]

In addition to providing structural support, Müller cells have several signaling functions. They have been demonstrated to help regulate the supply of angiogenic growth factors during retinal development. In addition to their developmental role, as the primary glial cell in the retina, Müller cells are responsible for maintaining homeostasis of the retinal microenvironment. In response to pathologic stress, Müller cells become 'activated' and undergo a damage-response termed reactive gliosis. In reactive gliosis, the Müller cell population expands and initiates a program of protective actions including uptake of excess glutamate, release of anti-oxidants, and production of neurotophic and angiogenic growth factors.[200] Recently, our collaborators, the Penn lab have carried out an elegant study to underscore the relative importance of Müller cells during oxygen stress; they observed that Müller cells contribute 7X as much hypoxia-induced VEGFA as the next highest source retinal astrocytes.[201]

1.4.2 The retinal vasculature -a model system to study sprouting angiogenesis

Retinal vasculature grows in a unique postnatal, two-dimensional arena that is ideally suited for studies of angiogenic processes; indeed most of the key observations about the molecular basis for angiogenesis have derived from investigations in the retinal vasculature. Extensively characterized vascular patterning including the coinciding sprouting at the vascular periphery and remodeling of more quiescent vasculature near the optic nerve allows for simultaneous study of nearly every aspect of

angiogenesis. The early timepoint for harvesting and easy visualization of the postnatal retinal vasculature make complex studies feasible.[124]

In the mouse, the retina begins as an avascular tissue. Retinal vascularization starts with the development a superficial vascular plexus (SVP) above the GCL near the optic nerve. The vasculature then extends radially and reaches the retinal periphery at approximately postnatal day 8 (P8). At this point the vasculature extends inward and creates the inner and deep vascular plexus. There is some ambiguity about the relative contribution of sprouting angiogenesis and vasculogenesis during the formation of the SVP, but a consensus is emerging for sprouting angiogenesis on the strength of transgenic mouse studies. It is well established that the formation of the SVP is highly regulated and governed by a steep gradient of matrix-embedded VEGFA released by migrating astrocytes ahead of the growing vascular network.[124,202,203]

As the primary vascular plexus continues to expand to reach the retinal periphery, the growth factor gradient in the region close to the optic nerve continues to drop. Consequently, this region is remodeled by pruning and secondary sprouting to form the hierarchical organization of the vasculature. Interestingly key differences between arteries and veins emerge early in this process. The area surrounding arteries is marked by reduced VEGF-A production, and limited secondary vasculature. Presumably this is due to the relative ease of accessing oxygen from the arterial bloodflow. In contrast, the perivenous vasculature remains denser for longer.

The well-characterized nature of postnatal development of the murine retinal vasculature is ideally suited for careful analysis of the role of α2β1 integrin in sprouting angiogenesis.

1.4.3 Retinopathy of Prematurity

Retinopathy of prematurity (ROP) remains a significant source of blindness in children today. The condition was initially linked to prematurity by Terry et al. in 1944. Later the use of excessive oxygen in the care of preterm infants gave rise to more extensive incidence of ROP.[204] Additional risk fractors for ROP are gestational age and birth weight.[205]

ROP occurs in two phases. Initially, hyperoxia causes an initial vessel regression response that affects the microvessels near the optic nerve. This initial stage is followed by a second proliferative phase in which pathologic neovascularization occurs. In humans, unlike mice, retinal blood vessel development occurs in utero; retinal plexus formation begins in the fourth month and the retina is completely vascularized just before birth.[206] Consequently, premature birth leaves newborns with incompletely vascularized retinas that are susceptible to ROP. Each additional week of gestational age, decreases the size of the avascular zone – hence identification of low gestational age as a risk factor.[207] The difference between the relative hypoxia of the uterine environment and the external environment can cause regression of existing vessels before VEGF production is recalibrated and the non-vascularized retina becomes fully active. Use of external oxygen can exacerbate this effect.[207]

The pathologic neovascularization in the second, proliferative, stage of ROP is caused by local tissue hypoxia. In animal models it has been extensively documented that in the first, hyperoxic, stage of ROP, retinal VEGF expression is significantly downregulated.[208–210] The subsequent, hypoxic, stage of ROP is marked by aberrant upregulation of VEGF in the retina.[203,209–212] The effectiveness of anti-VEGF treatments have extensive records of success in limiting pathologic neovascularization in animal

studies.[213–216] This model for the pathogenesis of ROP has been validated in limited human studies.[217]

In the clinic, standard treatment protocol for ROP is administration of cryotherapy or laser. Recently, clinical studies of intravitreal injection of an anti-VEGF antibody, bevacizumab, has had significant success in severe cases.[217] The proliferative stage of ROP is considered to have a common molecular basis with other proliferative retinopathies such as proliferative diabetic retinopathy (PDR).

1.4.4 Proliferative Diabetic Retinopathy

With the proliferation of diabetes and metabolic syndrome in the developed world, it is expected that incidence of PDR will rise dramatically in the coming decades. PDR is an expected complication in all Type I diabetic patients, while over 75% of insulin-dependent Type II diabetics will develop PDR within 25 years.[218,219] The pathogenesis of PDR is complex. Initially thickening of the capillary basement membrane and loss of mural cells leads to vascular defects including microaneurysms and capillary occlusion. These defects cause local tissue ischemia which cause growth-factor induced pathologic neovascularization. Comorbidities including retinal vein occlusions, sickle-cell anemia and other vascular diseases can exacerbate tissue hypoxia and lead to aggravated pathologic retinal neovascularization. The central role of VEGF overproduction is clear; intraocular VEGF levels have been found to be substantially higher in patients with PDR compared to patients with non-proliferative disease.[220,221]

The α2β1 integrin has also been linked to diabetic retinopathy through Genome wide association studies. Understanding how the integrin contributes to the progression of retinopathies such as PDR is the focus of the studies described in Chapter 2.

Figure 1.2. Volcano Plot of GWAS Meta-analysis

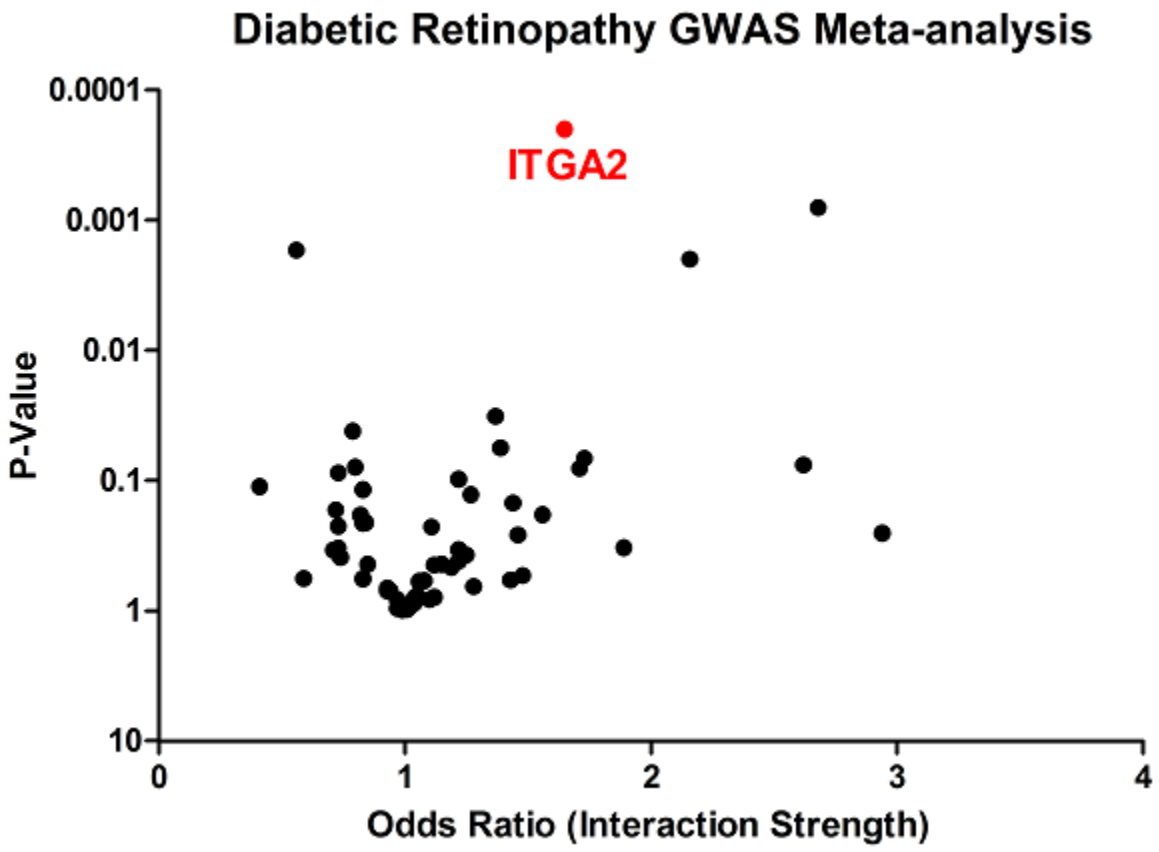

1.4.6 Hypoxia induced angiogenic responses

As we have discussed, angiogenesis is driven largely in response to carefully laid out growth factor gradients. In conditions of tissue hypoxia, overproduction of VEGF and other angiogneic growth factors commonly causes pathologic angiogenesis. This disease process is a hallmark of the tumor microenvironment.

The major regulators of angiogenic growth factor production are the hypoxia-induced factors (HIFs) transcription factors. HIF transcription factors consist of heterodimers composed of the α- and β-subunits. In normoxic conditions, intracellular HIF levels are maintained at low levels by rapid degradation of the α-subunits. In hypoxic conditions, the activity of the oxygen-dependent prolyl hydroxylases (PHD) is suppressed and as a result increased stabilization of α-subunits, leads to the formation of active of heterodimers with the β subunit.

The HIF-1 and Hif-2 transcription factors both induce transcriptional upregulation of genes that contain hypoxia response elements (HRE) in their promoters. Transcription of these genes causes a coordinated, multi-tiered adaptive response. Amongst the most massively upregulated genes in the hypoxia response are phosphoglycerate kinase (PGK) and Vegfa. PGK facilitates decreased oxygen consumption through metabolic changes involving decreased oxidative phosphorylation. Increased VEGF-A rapidly stimulates angiogenesis to improve oxygen supply [222].

There are a number of curious links between α2β1 integrin and the HIF transcription factors. Induction of α2β1 integrin in response to hypoxia has been reported in many cell types.[223] Additionally, Cheli et al. have identified PARP-1, a regulator of HIF transcription factor activation, as a transcriptional coactivator for α2β1 integrin.[116,224] Based on these reports it seems likely that HIF transcription factors may have some role in hypoxia-induced upregulation of α2β1 integrin. Similarly, the p38 MAP kinase, which is reported to be activated downstream of α2β1 integrin in mammary epithelial cells, has been widely implicated in activation of HIF family member, HIF-1α, although the role of p38 in activating HIF-2α is not yet established.[185,225–227] This association is briefly examined in Chapter 3 of this dissertation.

1.4.6 Oxygen-induced retinopathy (OIR) mouse model

OIR is the most popular and well-established animal model for studying pathological retinal angiogenesis. First described in 1994 this model has been adapted for use in a number of animals which have incomplete retinal vascularization at birth.[228] In recent years, the murine model has emerged as the most popular system due to ease of reproducibility, quantifiability and ready availability of genetic tools.[229]

In the OIR model, mice are removed from room air and exposed to 75% oxygen from P7 until P12. The P7 timepoint is used in mice because at this stage the vasculature resembles pre-term infants because of the presence of maximal hyaloid vascular regression and minimal retinal vascular development. The hyperoxic period between P7 and P12 is marked by increased vessel regression in capillaries near the optic nerve along with termination of radial vessel outgrowth. This period closely resembles the preliminary stages of ROP. Mice can be harvested at P12 and the area of vaso-obliteration can be quantified in retinal whole mounts. Mice that continue the OIR protocol are returned to room air for 6 days and harvested at P18. The OIR model, as initially popularized by Smith et al, measures neovascularization at P17; recently, some groups have observed peak neovascularization at P18 and adopted that timepoint as their OIR endpoint.[230–232]

In room air, the newly avascular regions of the retina experience local ischemia and induce the expression of angiogenesis stimulating growth factors, most prominently VEGF-A. Growth factor overproduction in this period triggers pathologic neovascularization which can be measured in retinal cross-sections by the formation of neovascular nuclei extending into the vitreous, and in whole mounts by the area of

vascular tufts. The proliferative stage of OIR mimics analogous phase in human ROP, and recapitulates in an accelerated fashion many elements of PDR.[207]

Chapter 2

MITIGATION OF OXYGEN-INDUCED RETINOPATHY IN α2β1 INTEGRIN-DEFICIENT MICE

This chapter is reprinted from:

Madamanchi A, Capozzi M, Geng L, Li Z, Friedman RD, Dickeson SK, et al. Mitigation of oxygen-induced retinopathy in α2β1 integrin-deficient mice. Invest Ophthalmol Vis Sci. 2014;55: 4338–4347.

2.1 Abstract

PURPOSE. The α2β1 integrin plays an important but complex role in angiogenesis and vasculopathies. Published GWAS studies established a correlation between genetic polymorphisms of the α2β1 integrin gene and incidence of diabetic retinopathy. Recent studies indicated that α2-null mice demonstrate superior vascularization in both the wound and diabetic microenvironments. The goal of this study was to determine whether the vasculoprotective effects of α2-integrin deficiency extended to the retina, using the oxygen-induced retinopathy (OIR) model for retinopathy of prematurity (ROP).

METHOD. In the OIR model, wild type (WT) and α2-null mice were exposed to 75% oxygen for 5 days (P7-P12) and subsequently returned to room air for 6 days (P12-P18). Retinas were collected at postnatal day 7, day 13 and day 18 and examined via H&E and Lectin staining. Retinas were analyzed for retinal vascular area, neovascularization, VEGF expression and Müller cell activation. Primary Müller cell cultures from wild type and α2-null mice were isolated and analyzed for hypoxia-induced VEGF-A expression.

RESULTS. In the retina, the α2β1 integrin was minimally expressed in endothelial cells and strongly expressed in activated Müller cells. Isolated α2-null primary Müller cells demonstrated decreased hypoxia-induced VEGF-A expression. In the OIR model, α2-

null mice displayed reduced hyperoxia-induced vaso-attenuation, reduced pathological retinal neovascularization (NV), and decreased VEGF expression as compared to WT counterparts.

CONCLUSIONS. Our data suggest that the α2β1 integrin contributes to the pathogenesis of retinopathy. We describe a newly identified role for α2β1 integrin in mediating hypoxia-induced Müller cell VEGF-A production.

2.2 Introduction

Angiogenesis, the growth of capillaries from extant blood vessels, is a tightly regulated process and the major mechanism for expansion of the vascular network. Dysregulated angiogenesis is a hallmark of many diseases ranging from cancer to diabetes. In the retina, chronic, pathologic angiogenesis, termed retinal neovascularization (NV), is a central feature of ocular diseases including diabetic retinopathy, and retinopathy of prematurity (ROP).[233]

Retinal NV is often preceded by local tissue hypoxia stemming from capillary loss.[234–236] Hypoxia initiates stabilization of the hypoxia inducible factor (HIF) transcription factors which coordinate cellular responses to hypoxia.[237] In Müller cells, the glial cell type that is responsible for maintaining retinal homeostasis and modulating the growth factor microenvironment, retinal hypoxia triggers a HIF-2α-mediated protective program of vasoactive factor secretion.[200,238,239] In pathological conditions overproduction of growth factors, most prominently vascular endothelial growth factor (VEGF) stimulates retinal NV. Chen et al. suggests that α2β1 integrin may have an important role in regulating VEGF production in endothelial cells under conditions of hyperglycemia.[240] In the retina, endothelial cells and many other cell types including

astrocytes, retinal pigment epithelial cells, and ganglion cells contribute to VEGF overproduction; however, animal models have identified Müller cells as the predominant source of VEGF during retinal NV.[201,241–247]

Integrins, a class of obligate α/β heterodimers that serve as cell surface receptors for extracellular matrix ligands, have emerged as important actors in many vascular diseases.[248] The α2β1 integrin, a collagen and laminin receptor, has been associated with risk of diabetic retinopathy; multiple Genome-Wide Association Studies (GWAS) independently identified an increased risk of diabetic retinopathy among patients with high α2β1 integrin expressing polymorphisms of the ITGA2 gene.[117,249,250] Interesting new work using the diet-induced obesity mouse model indicates that α2-null mice have decreased skeletal muscle capillary rarefaction in the diabetic context.[177] As pathological retinal NV is precipitated by capillary loss, the phenotype reported by Kang et al. along with the GWAS data, suggested that α2-integrin deficiency may be protective against retinal NV in ocular diseases.[228,251]

To investigate the hypothesis that α2-integrin deficiency can attenuate retinal NV, we characterized the α2β1 integrin-deficient mouse in the established oxygen-induced retinopathy (OIR) model for retinopathy of prematurity (ROP). Our findings suggest that α2-integrin deficiency indeed protects the developing retina from oxygen-induced retinopathy; this protective effect appears to be a result of a novel role for α2β1 integrin in mediating hypoxia-induced Müller cell VEGF production.

2.3 Materials and methods

2.3.1 Animals and animal models

All animals were housed in pathogen-free conditions at Vanderbilt University Medical Center. All animal experiments were approved by the Vanderbilt University School of Medicine Animal Care and Use Committee, and they were conducted according to the principles expressed in the ARVO Statement for the Use of Animals in Ophthalmic and Vision ResearchGeneration of α2 integrin-deficient mice on a C57BL6/ was previously described.[30] The mice used in these experiments were 99% genetically C57BL/6. All animals were appropriately age-matched.

For OIR, litters were exposed to 75% oxygen for five days from (P7 to P12) and returned to room air for six days from (P12 to P18).[228,229] At P12 and P18 mice were euthanized and their eyes or retinas were harvested for molecular biology studies, gene expression studies or morphological analysis. The OIR model, as initially popularized by Smith et al, measures neovascularization at P17; recently some groups have observed peak neovascularization at P18 and adopted that timepoint as their OIR endpoint.[230–232] The central avascular area at P12 and extent of neovascularization at P18 was quantitated using ImageJ (NIH). All morphological analyses were conducted in a blinded manner.

2.3.2 qPCR analysis

For developmental and OIR studies, pairs of wild type and α2-null retinas were harvested. Total RNA was recovered following manufacturer's protocol. Quantitative PCR (qPCR) was performed on an Applied Biosystems 7900HT qPCR machine using a 384-plate system, as per manufacture's protocol. Relative fold change in gene expression was defined using the comparative $2^{-\Delta\Delta CT}$ method (including the amplification efficiency correction factor). Relative RNA quantities were normalized to either HPRT,

RPP30 or TBP based on the gene, determined by NormFinder, to represent the optimum normalization gene for the set of samples analyzed. Primer pairs for mRNA expression (Supplemental Methods Table 1) analysis were designed using Primer Express 3.0™ (Applied Biosystems) and published murine DNA and mRNA sequences (UCSC Genome Bioinformatics).

2.3.3 Immuno-analyses

For H&E staining, orbits were removed, fixed in 4% paraformaldehyde (PFA), paraffin-embedded and sectioned into 6 µm sagittal sections. For whole mount analysis, retinas were dissected and permeabilized.[212] For cryosections, orbits were enucleated, fixed in 4% PFA and OCT-embedded and sectioned (10 µm).[252] Both cryosections and whole mounts were evaluated using immunofluorescence microscopy for identification and quantitation of $CD31^+$ and α2β1 $integrin^+$ endothelial cells, or $GFAP^+$ and α2β1 $integrin^+$ Müller cells using antibodies listed in Supplemental Methods Table 2.[212] Immunofluorescence images were captured with a Nikon Eclipse 80i fluorescence microscope. Quantitation was performed using ImageJ (NIH).

2.3.4 Primary Müller cell Isolation

Cultures of Primary Müller retinal cells were established from retinas of P7 wild type and α2-null mice according to previously reported methods.[253] Briefly, eyes were enucleated and soaked overnight in medium (Dulbecco's modified Eagle's medium low glucose [DMEM]; HyClone, Logan, UT), supplemented with 1× antibiotic/antimycotic solution (Sigma, St. Louis, MO). The next day, eyes were incubated at 37°C in digestion buffer (the soaking medium plus 0.1% trypsin and 70 U/mL collagenase) for one hour before retinas were separated. The retinas were then ground and dissolved in a 10%

fetal bovine serum (FBS) containing DMEM growth media. Approximately four to six retinas were used per isolation. Cell growth was monitored until for four to five days until significant cell growth was observed, after which cells were washed repeatedly until a pure population of flat adherent cells remained. The Müller cell content of the cultures was maintained via staining with the marker glutamine synthase and lack of neuronal markers. Cultures were regularly grown at 37°C in a 5% CO_2/95% air (20.9% oxygen) atmosphere (normoxia) in a humidified incubator (NuAire, Plymouth, MN) and passages three to six were used for experiments.

2.3.5 Müller cell VEGF Induction

Wild type and α2-null mouse Müller cell cultures were grown to 70% subconfluency and then exposed to hypoxia for 0, 4, 8, and 24 h or hypoxia mimetic $CoCl_2$ for 24 hours. VEGF-A protein levels were quantified by ELISA using the Quantikine Immunoassay kit from R&D Systems (MMV00), according to the manufacturer's protocol. VEGFA mRNA levels were analyzed via qPCR.

2.3.6 Microarray analysis

GSE32472 microarray data from blood samples were derived from 120 preterm newborns at five, fourteen or twenty-eight days of age, although not all patients were sampled at all time points.[212] Expression of ITGA2 was correlated with both the incidence and severity of retinopathy. ITGA2 expression for all samples at each time point was averaged and then compared using one-way Anova to determine statistical significance (Detailed statistical analysis is contained in Supplemental Methods).

2.4 Results

2.4.1 α2β1 integrin expression status predicts incidence of severe ROP in human infants

To determine whether GWAS data linking ITGA2 expression levels to PDR had implications for ROP in humans, we analyzed a recent study linking microarray gene expression data of peripheral blood leukocytes in 120 Norwegian preterm infants with information about clinical outcomes including ROP (GSE32472). ITGA2 expression levels are in part genetically determined. Increased ITGA2 expression in circulating leukocytes suggests higher systemic expression including in the retinal vasculature. In the GSE32472 study, 111 out of 120 infants had clinical outcome data about their ROP status. From this group, 60 infants did not suffer ROP. Of the remainder, 14 were classified as having 'Mild ROP' indicating a diagnosis of ROP not requiring laser therapy, while 37 infants were classified with 'Severe ROP' indicating a diagnosis of ROP requiring laser therapy. Severity of ROP was associated with increased ITGA2 expression (P=0.0002; One-way ANOVA) (Figure 2.1A). When classified according to tertile of ITGA2 expression, the tertiles of high ITGA2

Figure 2.1

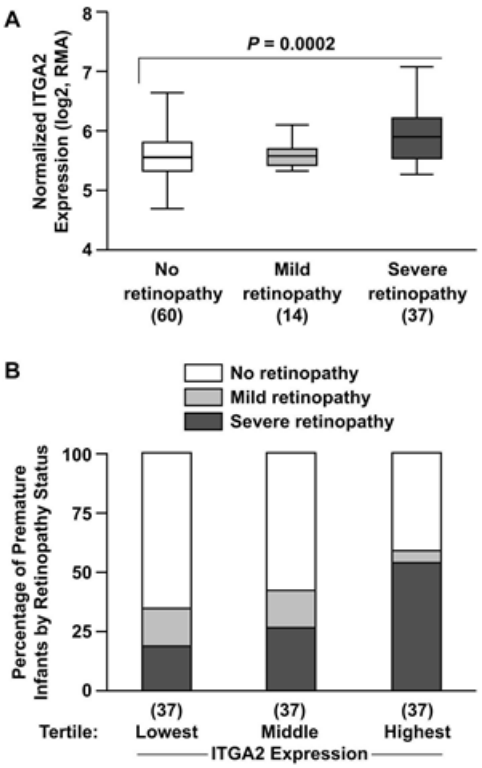

Figure 2.1. ITGA2 expression predicts incidence and severity of Retinopathy of Prematurity in preterm infants.
(A) ROP severity is associated with significantly higher ITGA2 expression. **(B)** Higher tertiles of ITGA2 expression have higher incidences of ROP.

expression showed increased incidence and severity of ROP (Figure 2.1B). This analysis represents the first link between ITGA2 expression and incidence of ROP in human.

2.4.2 In the retina, α2β1 integrin is most strongly expressed in activated Müller cells

Earlier reports from our laboratory and our colleagues suggested that the α2β1 integrin was expressed on growth factor-stimulated endothelial cells, but only modestly or not expressed on quiescent adult vessels.[238] To temporally define expression during retinal development the level of α2β1 integrin expression during retinal maturation in wild type animals was determined. By qRT-PCR analysis, α2 subunit mRNA was detected at the highest levels at P5 and P7. Only low levels of α2 subunit mRNA were observed in the adult at P18 (Figure 2.2A). For comparison, minimal α2 subunit mRNA was detected in α2-null (ITGA2 -/-) mice. This data was confirmed via immunofluorescence analysis of α2β1 integrin (red) expression in cross-sections of P5, P7 and P18 retinas (Figure 2.2B). In accordance with the mRNA results, α2-integrin staining was broadest at P5 and more limited at P18. Interestingly, at P5 and P7 the α2 integrin subunit (red) was expressed not only at the superficial vascular plexus, where endothelial cells were found, but also in the inner nuclear layer. Interestingly, the α2 integrin subunit (red) was prominently expressed on cells spanning from the inner limiting membrane to the outer limiting membrane in a pattern characteristic of Müller glia (Figure 2.2B). At P18 cell type-specific localization of the integrin was evaluated. In the P18 adult retina, α2β1 integrin (red) was only weakly expressed on CD31+ endothelial cells (green) (Figure 2.2C). Staining with glial fibrillary acidic protein (GFAP)

(green), a well-established marker of Müller cells, strongly colocalized with α2-integrin staining (red) (Figure 2.2D).

Figure 2.2

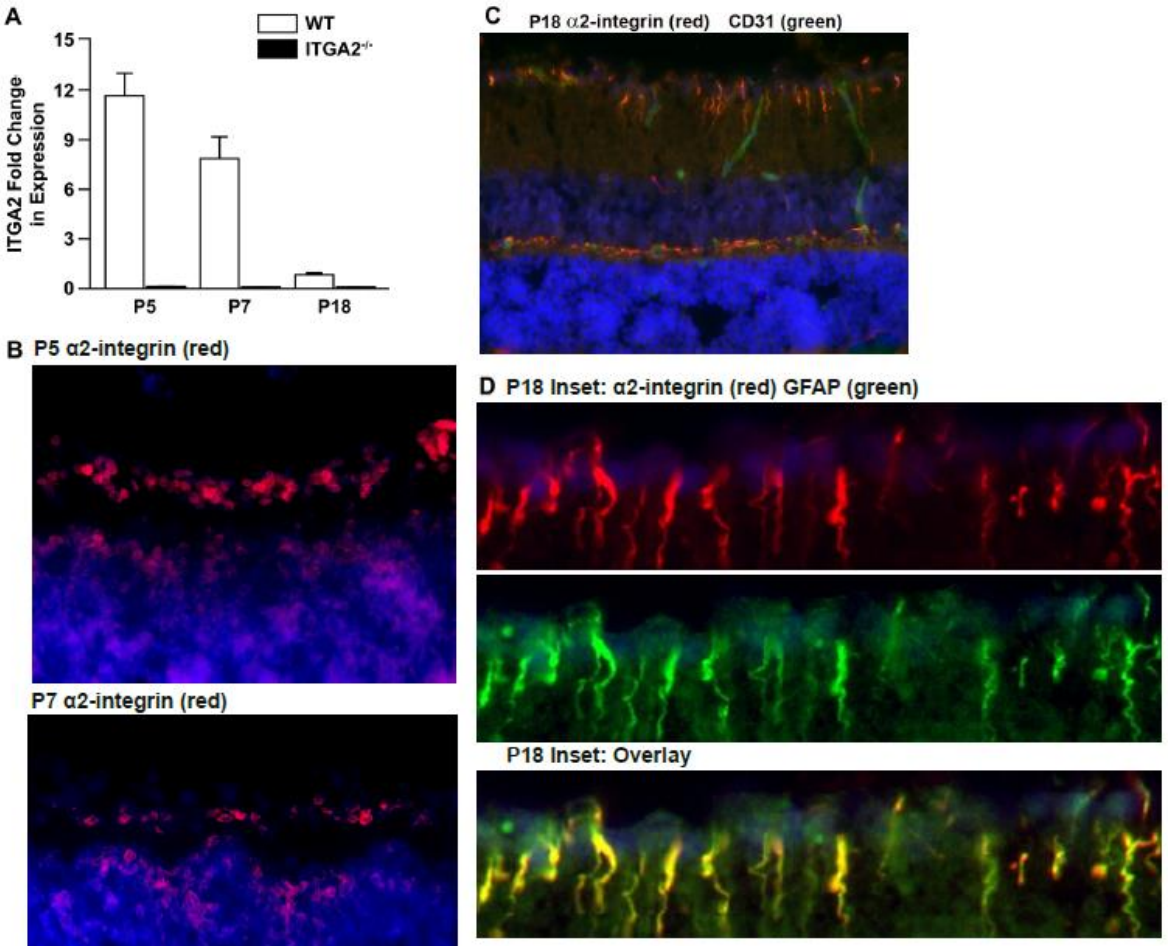

Figure 2.2. α2β1 integrin expression in retinal endothelial and Müller cells
(A) The level of α2-integrin subunit mRNA expression in total retina of wild type (WT) and α2-null (ITGA2 -/-) mice at P 5, 7, 18, was determined by qRT-PCR. Values are normalized to HPRT or RPP30 and displayed relative to WT at P18. Values represent mean +/- SEM.
(B) Immunofluorescence analysis of α2β1 integrin (red) expression in cross-sections of P5, P7 and P18 wild type retinas from unchallenged mice. Integrin expression suggests a pattern indicative of retinal Müller cells. P5 and P7 images were taken at 60X magnification. P18 images were taken at 40x magnification and are representative of 5 or more retinas taken in three separate trials from separate litters.
(C) Immunofluorescence analysis demonstrated limited co-localization of α2β1 integrin expression (red) and CD31 (green) on the vessels in the cross-sections of retinas from P18 wild type mice grown in normal air. Nuclei are stained with DAPI (blue). Images were taken at 40X magnification.
(D) Analysis of P18 retina cross-section from inset in (B) at 4 times magnification. Staining of α2β1 integrin in red (top) and GFAP in green (middle) are merged to show colocalization in yellow (bottom) of α2β1 integrin and GFAP expression in retinal Müller cells.

2.4.3 α2-integrin deletion impairs hypoxia-induced VEGF-A production in Müller cells *in vitro*

Given the strong expression of α2β1 integrin in retinal Müller cells we questioned determine whether α2β1 integrin deletion affected Müller cell function. We evaluated the *in vitro* response to hypoxia in wild type and α2-null primary retinal Müller cells. Wild type Müller cells secreted significantly higher levels of VEGF-A after 24 hours of incubation in hypoxia than α2-null Müller cells (665.7 vs. 419.6 pg/mL, P = 0.0286 at 24 h) (Figure 2.3A). Similarly, VEGF-A mRNA expression, as measured by qRT-PCR, was higher in wild type than α2-null Müller cells after 8 and 24 hours of incubation in hypoxia (5.35 vs 3.13 fold, P= 0.045 at 8 h; 9.38 vs 6.46 fold, P= 0.019 at 24 h) (Figure 2.3B). All fold changes were normalized to VEGF-A expression in WT wild type cells at 0 hours of hypoxia exposure. To determine whether the difference in hypoxia-induced VEGF-A production was HIF transcription factor-dependent, we tested the effect of treatment with 200 µM $CoCl_2$, a hypoxia-mimetic known to specifically activate HIF transcription factors. A 24-hour treatment with 200 µM of $CoCl_2$ induced VEGF-A secretion at similar levels in both wild type and α2-null Müller cells (551.7 vs 496.8 pg/mL, P>> 0.05) suggesting that the role for α2β1 integrin in the regulation of VEGF-A lies upstream, rather than downstream of HIF transcription factor activity (Figure 2.3C). To confirm differential hypoxia-induced HIF-2α activation in wild type and α2-null primary retinal Müller cells we used immunoblot analysis to quantitate HIF-2α levels after 24 hours of culture in normoxic or hypoxic conditions (Figure 2.3D). HIF-2α is significantly higher in hypoxia-treated WT compared to α2-null primary retinal Müller cells. Additionally, we evaluated the effect of hypoxia on α2-integrin expression and found substantially higher

levels of the integrin after 24 hours of culture in hypoxic conditions (Figure 2.3D). These results were confirmed using In-Cell Western analysis (Supplemental Figure 2).

Figure 2.3

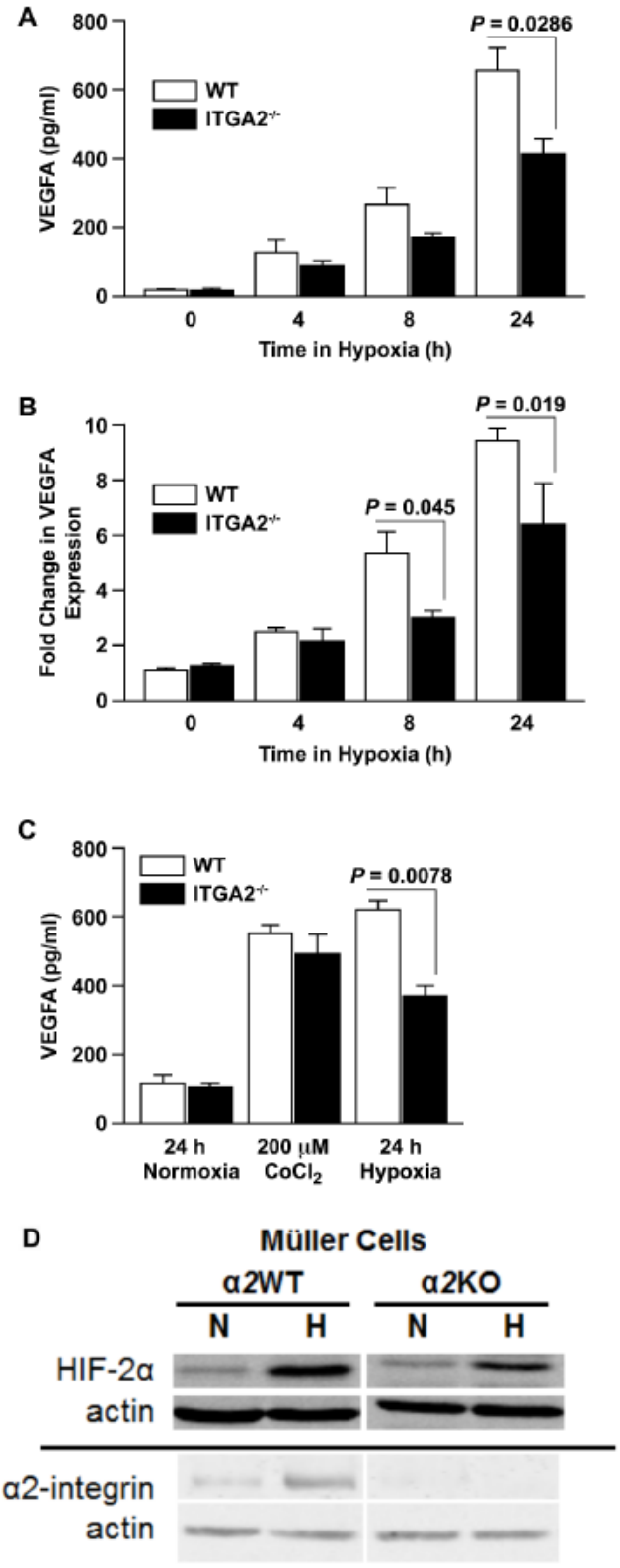

Figure 2.3 α2β1 deletion impairs hypoxia-dependent VEGF production in Müller cells in vitro

(A) Levels of VEGF-A protein in conditioned media from primary WT and α2-null (ITGA2-/-) Müller cells after incubation in hypoxia for 0, 4, 8 or 24 hours, as determined by ELISA. Data is shown as mean +/- SEM for a representative experiment of five separate trials taken with separate isolates of primary Müller cells.

(B) Fold changes of VEGF-A mRNA expression from primary WT and ITGA2-/- Müller cells incubated in hypoxic conditions for 0, 4, 8 or 24 hours, as determined by qRT- PCR. Fold changes are relative to WT at 0 hours (mean +/- SEM). Data are representative of six separate trials with separate isolates of primary Müller cells.

(C) VEGF-A protein in conditioned media from primary WT and ITGA2-/- Müller cells after 24 hours in normoxic conditions, treatment with 200 µM CoCl2, or hypoxic challenge. VEGF-A concentration was determined by ELISA. Data are shown as a mean +/- SEM for a representative of three separate trials with separate isolates of primary Müller cells.

(D) Immunoblot analysis of primary WT and ITGA2-/- Müller cells for HIF-2α and α2-integrin expression after 24 hours of culture in normal air and hypoxia.

2.4.4 α2β1 integrin-deletion mitigates Müller cell activation and VEGF production *in vivo*

To determine whether the difference in hypoxia-induced Müller cell VEGF production also occurs *in vivo*, we examined retinas from wild type and α2-null mice in the OIR model. Consistent with published literature, Müller cell GFAP expression increased robustly at P18 in response to relative hypoxia in wild type mice.[254,255] In contrast, GFAP expression had a more modest increase at P18 in α2-null mice following hypoxia (Figure 2.4A). To determine whether the hypoxia-induced upregulation of α2-integrin expression that we observed *in vitro* was also found *in vivo,* we performed immunoflourescence analysis on retinal cross sections from WT mice in 'relative hypoxia' following the hyperoxia phase of OIR, compared to normal air controls. Specifically, we used P14 mice from the OIR model (P14 is two days post-hyperoxia, labeled in the figure as Hypoxia) and from normal air litters. As expected we observed visibly higher α2-integrin in the 'hypoxia-treated' mice.

Since Müller cells are the primary source of VEGF in the retina, and our *in vitro* data suggested decreased VEGF production in α2-null Müller cells, we evaluated VEGF-A levels during the different stages of OIR.[201,254,255] At P13, one day post-hyperoxia, VEGF-A protein and mRNA levels were significantly increased in retinal lysates from wild type, compared to α2-null lysates (151.9 vs 90.7 pg/mL, P= 0.001 at P13; 2.51 vs 1.64 fold, P= 0.011) (Figure 2.4C-D). At P18, VEGF-A protein remained elevated in the wild type relative to the α2-null animals (113.9 vs 66.4 pg/mL, P= 0.001) (Figure 2.4B). At this later time point, the hypoxia-induced increases in VEGF mRNA levels had diminished in both wild type and α2-null animals (Figure 2.4D). VEGF mRNA

fold changes are displayed relative to P12 wild type. These results were consistent with our *in vitro* experiments with primary retinal Müller cells.

Figure 2.4

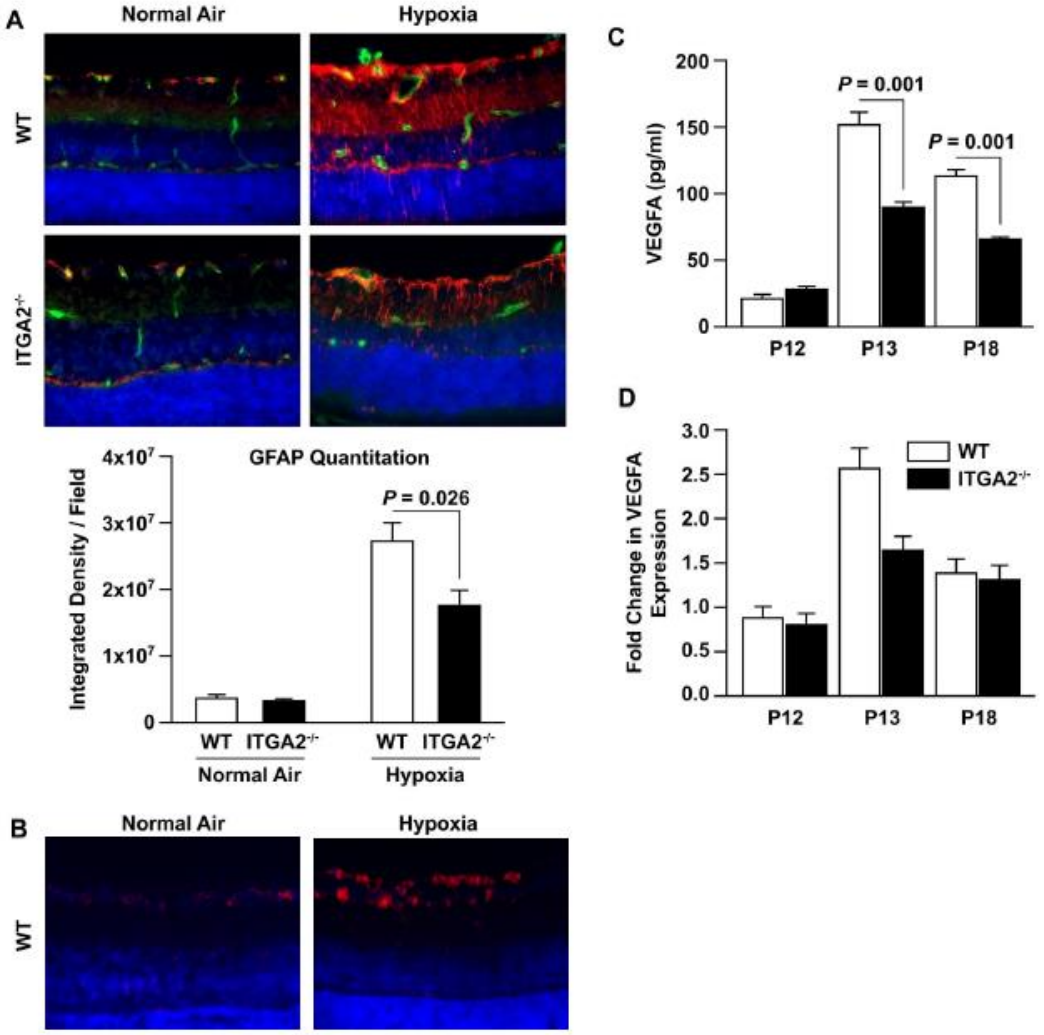

Figure 2.4 α2β1 integrin-deletion mitigates Müller cell activation and VEGF production in oxygen-induced retinopathy.

(A) Cross-sections of retinas from age-matched P18 WT and α2-null (ITGA2-/-) mice raised in normal air or relative hypoxia (6 days after hyperoxia in oxygen-induced retinopathy (OIR)) were evaluated by immunoflourescence microscopy using anti-GFAP (Müller cells-red) or anti-CD31 (ECs-green) and DAPI (nuclei-blue). Images were taken at 40x magnification and representative of three separate trials. The intensity of GFAP 2 staining was quantified and is shown below images (mean +/- SEM). Images are at 40X magnification.

(B) Cross-sections of retinas from age-matched WT and α2-null ITGA2-/- P14 mice in normal air or relative hypoxia (two days after hyperoxia in oxygen-induced retinopathy (OIR)) were evaluated by immunoflourescence microscopy using anti-α2β1 integrin (red) and DAPI (nuclei-blue). Images were taken at 60x magnification.

(C) Lysates from age-matched WT and ITGA2-/- mice in the after OIR injury at P12, P13 and P18 after was quantified by ELISA (mean +/- SEM).

(D) The level of VEGF-A mRNA expression in age-matched WT and ITGA2-/- retinas at P12, P13, P18 retinas after OIR was determined by qRT-PCR. Fold changes are relative to WT P12 (mean +/- SEM). Results in **(B-C)** are derived from represent 3 similar experiments.

2.4.5 α2β1 integrin-deletion protects against oxygen-induced retinopathy

Reduction in Müller cell VEGF production has been demonstrated to be protective in the OIR model.[254,255] To determine whether α2β1-deletion also has a protective phenotype we examined retinas from wild type and α2-null pups exposed to the mouse OIR model. After five days of hyperoxic challenge the central retina was avascular in the wild type retina, as expected from published results (Figure 2.5A).[212,228,254,255] Although α2-null retinas also developed a central avascular area due to capillary loss near the optic nerve, the avascular region was significantly diminished compared to the wild type (Figure 2.5A), indicating that α2β1 integrin deletion protected from early vessel attenuation during hyperoxia. At P18, after return to the relatively hypoxic room air environment for six days, pathologic NV was significantly increased in wild type compared to α2-null retinas (Figure 2.5A). This result was corroborated by the observed increase in pathologic neovascular tuft formation in H&E stains (Figure 2.5B). In summary, deletion of the α2β1 integrin attenuates retinal vessel loss resulting from hyperoxia and protects from subsequent neovascularization.

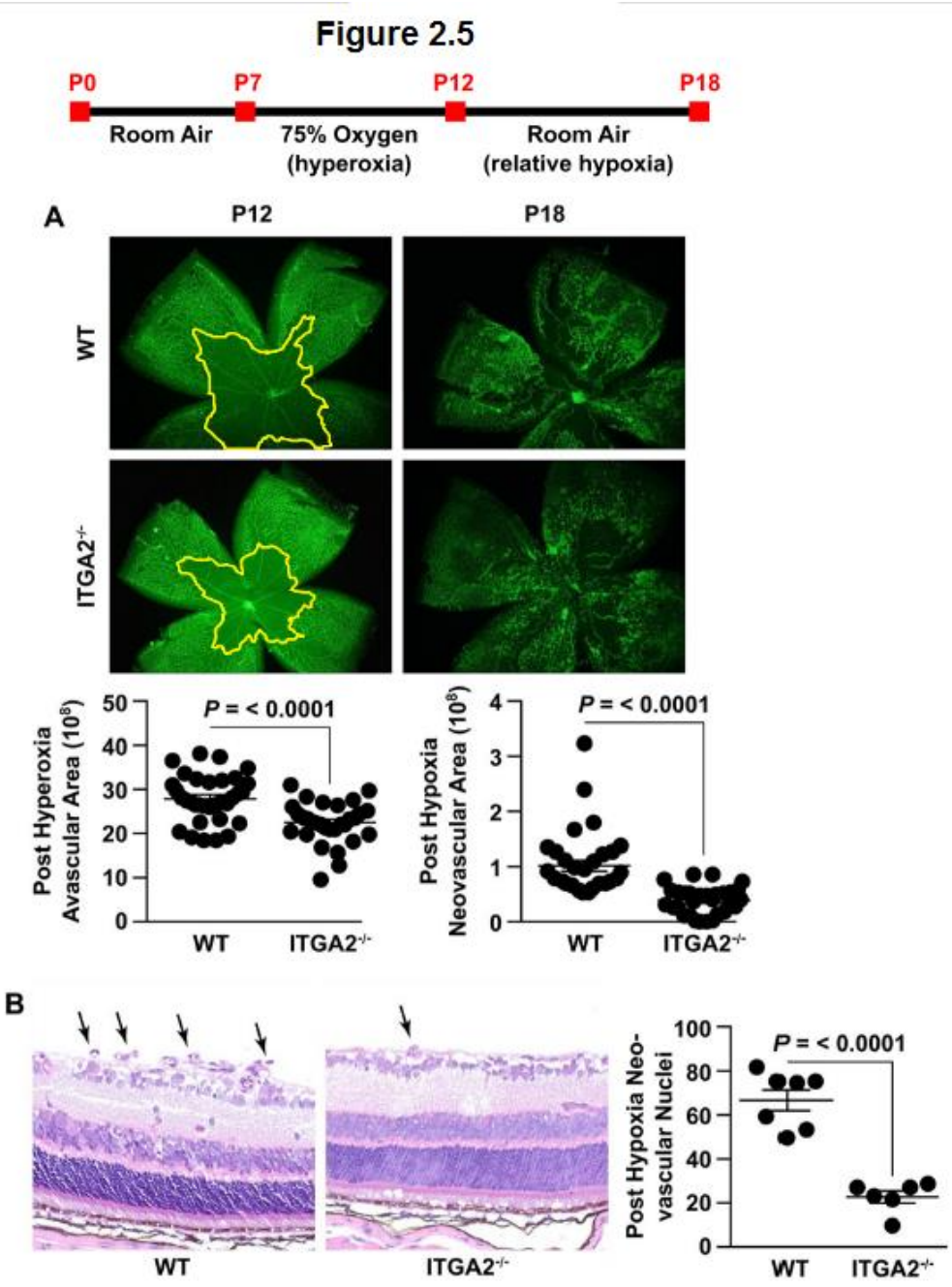

Figure 2.5. α2β1 integrin deletion protects against oxygen-induced retinopathy.
Cartoon: The experimental protocol for oxygen-induced retinopathy (OIR) is shown as a timeline.
(A) Representative immunofluorescence images of retinal flat mounts of age-matched wild type (WT) and α2-null (ITGA2-/-) mice at P12 (after 75% hyperoxia), and P18 (after return to room air and relative hypoxia). Vessels are identified by GS Lectin (green) staining. Quantitation of central avascular area and neovascular area was determined as described and illustrated (mean +/- SEM). Images are 4X.
(B) Representative photograph of H&E stained retinal cross-section of age-matched WT and ITGA2-/- at P18 following OIR injury. Neovascular nuclei are indicated by arrows. The number of nuclei per retinal area was quantitated (mean +/- SEM). Images are 40X.

2.4.6 α2β1 integrin protection against OIR is not a consequence of developmental defects

In addition to their role during vascular stress, Müller cells play a critical role in regulating the growth factors that drive vascularization during retinal development.[254] Because α2β1 was important in hypoxia-induced VEGF production in retinal Müller cells, we explored the possibility that a developmental defect in retinal vascularization accounted for the mitigated OIR phenotype in α2-null mice.

Examination of the retinal vasculature at P5 and P7 revealed a modest but statistically significant difference in vascular outgrowth between wild type and α2-null retinas (Figure 2.6A). Vascular outgrowth was quantitated by comparing the remaining avascular area beyond the vasculature periphery, relative to total retinal area. Deletion of the α2 subunit led to increased avascular area in α2-null compared to wild type mice at P5 and P7 (61% vs. 48%, P= 0.0361 at P5 and 27% vs. 18%, P= 0.0011 at P7). By P7 the difference in vascularization between the wild type and α2-null retinas was diminished compared to P5. At P18 after scheduled vascular outgrowth was completed, differences in vascularization was assessed by measuring vascular density in P18 retinas and revealed no differences (Figure 2.6A). Analysis of vascular density at P9 and P12 also revealed no differences (Supplemental Figure 1).

Although interesting, the magnitude of this subtle developmental difference was not considered to be sufficient to influence the OIR phenotype. To ascertain whether the delayed retinal angiogenesis at P5 and P7 was indicative of baseline differences in Müller cell function during development, we examined VEGF levels during normal development. VEGF-A protein and mRNA levels in retinal lysates at P5, P7 and P18 were similar in wild type and α2-null mice (Figure 2.6B-C). The absence of VEGF-A

differences at these timepoints indicated that α2β1 integrin-deficiency does not affect the growth factor microenvironment, and by extension Müller cell function, under normal conditions.

Figure 2.6

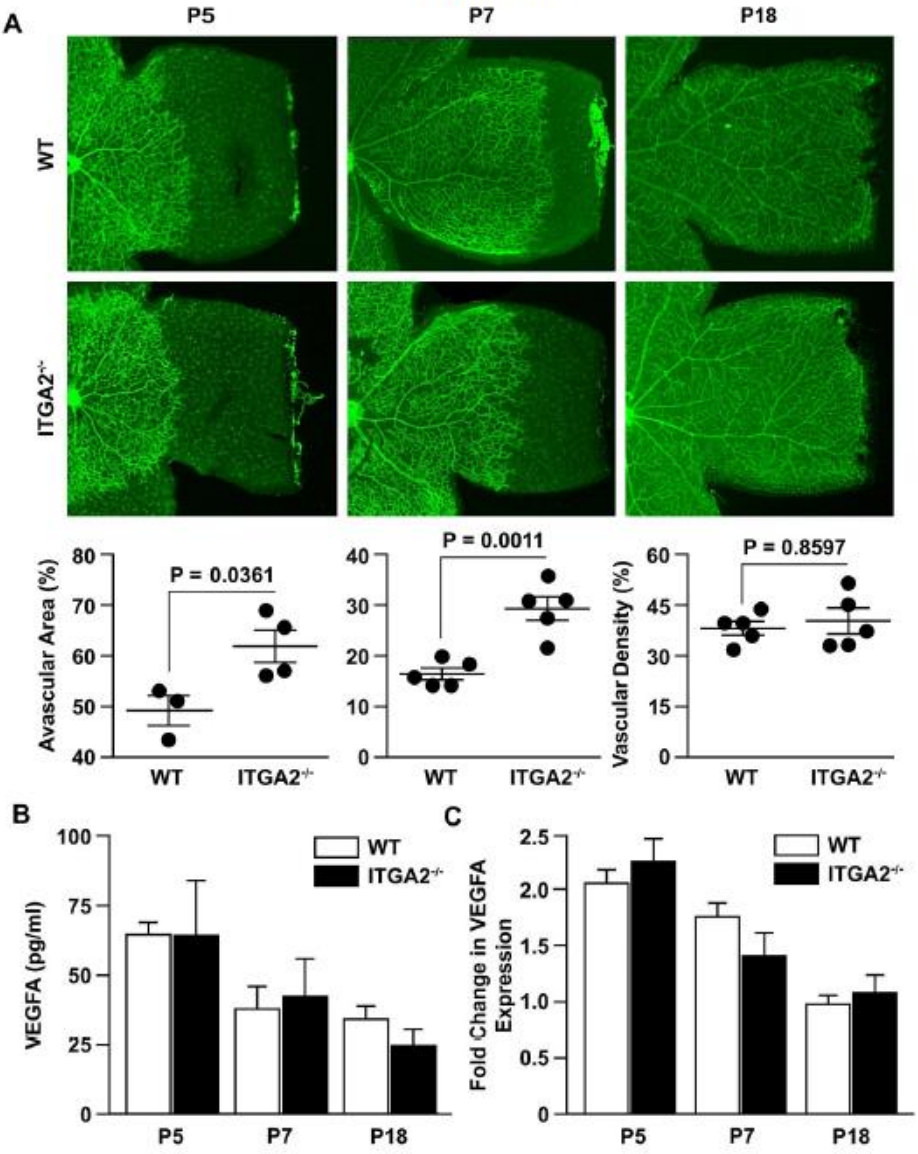

Figure 2.6 No significant differences in vascularization or VEGF levels were identified during development

(A) Retinal flat mounts of age-matched wild type (WT) and ITGA2-/- mice at P5, P7 and P18. Vessels were visualized by GS Lectin (green) via immunofluorescence microscopy. For P5 and P7 vascularization was measured by radial vascular outgrowth, as quantitated by pixel percentage of Avascular Area at retinal periphery relative to total retina area. At P18 radial vascular outgrowth was complete, and so vascularization was measured by Vascular Density, as quantitated by pixel percentage of vessel area relative to total retina area. Each data point represents the average result from an experiment with a litter of at least 4 mice (data represent mean +/- SEM). The results are representative of 3 separate trials. Images are 4X.

(B) The level of VEGF-A protein in retinal lysates of P5, P7 and P18 WT and ITGA2-/- animals under normal conditions, as determined by ELISA (Mean +/- SD).

(C) The fold change in mRNA expression of VEGF-A in developing retinas at P5, P7 and P18 was determined by qRT-PCR. Fold changes are relative to WT day 18 and shown as mean +/- SEM. All results (B-C) are representative of three similar experiments.

2.5 Discussion

The mouse OIR model mimics pathologic neovascularization observed in retinopathy of prematurity and is analogous to proliferative diabetic retinopathy. Epidemiologic studies suggested an association between ITGA2 polymorphisms and diabetic retinopathy in clinical cohorts where pre-retinal neovascularization is a defining pathologic feature.[117,249,250] These epidemiologic studies suggested that sequence variants associated with high levels of α2β1 integrin expression were an independent risk factor for the development of diabetic retinopathy in individuals with type II diabetes, in addition to other cardiovascular diseases in younger patients (less than age 50).[256] Our goal for testing α2-null mice in the OIR model was to evaluate the integrin's effect on retinal NV in a preclinical model of ocular vasculopathy.

In OIR experiments, deletion of the α2β1 integrin provided significant protection against both hyperoxia-induced vascular regression and subsequent neovascular proliferation. The α2-null retina demonstrated less reactive gliosis and substantially decreased VEGF-A secretion. Under other experimental challenges including wound-healing and tumor-implantation the α2-null mouse demonstrated increased neoangiogenesis.[30,90,176] However, in the diabetic microenvironment α2-null mice exhibited decreased capillary rarefaction. In the OIR model, as in many ocular vasculopathies, pathological retinal NV is preceded by capillary loss and hypoxia. On this basis we originally hypothesized that the α2-null mice would be protected in the OIR model because of superior resistance to hyperoxia-induced capillary loss. However, our survey of α2β1 expression in the retina uncovered very modest levels of CD31 positive, α2β1 positive cells suggesting low levels of integrin expression in capillaries and other endothelial cells. The expression of α2β1 integrin in a classic Müller glia pattern, and

strong colocalization with Müller cell marker GFAP led us to investigate the effect of α2-integrin deficiency in Müller cell function.

In vitro studies with primary retinal Müller cell cultures demonstrated a decreased ability for α2-null Müller cells to produce VEGF-A in response to hypoxia. Given that NV in OIR is considered to be primarily driven by VEGF-A overproduction, our findings strongly suggest that the integrin's contribution to the pathogenesis of OIR is from the Müller compartment.[212,252,255] However, without cell-type specific α2-null mice it is not possible to rule out contributing roles in the endothelium or other cell types.

Differences in vascularization and vascular development at P7 can influence response to OIR. Our experiments identified a subtle but statistically significant difference in vascular outgrowth between wild type and α2-null retinas. The modest scope of this difference in vascular outgrowth is unlikely to be large enough to influence the OIR phenotype that we observed. Hyperoxia-induced vaso-attenuation of capillaries is most prominent in the central area surrounding the optic nerve, an area in which we observe no significant differences between wild type and α2-null vasculature.Further, the absence of differences in VEGF mRNA and protein levels between wild type and α2-null retinas suggest normal Müller cell function during retinal development. Previously, Stenzel et al, reported that there were no differences in vascular development in α2-null mice.[152] They observed similar vascular sprouting and vascular density at P5 in α2-null mice and heterozygous littermates. Our metric of vascular outgrowth was not reported in their study, and we compared wild type mice to α2-null rather than heterozygous α2+/- mice.

These results provide the basis for future investigations into the mechanistic role of the α2β1 integrin in ocular diseases featuring pathologic retinal neovascularization.

Our study identified a novel role for the α2β1 integrin in regulating Müller cell function. This newly identified link to glial function may shed new light on studies linking ITGA2 polymorphisms with ischemic stroke.

Full characterization of the molecular mechanism by which the α2β1 integrin is required for hypoxia-induced, Müller cell-mediated VEGF-A induction is outside the scope of this study, but represents another intriguing area for further research. A connection between α2β1 integrin function and VEGF-A induction was first reported by Chen et al, who showed in HUVECs that inhibitory antibodies to α2β1 integrin blocked hyperglycemia-induced VEGFA expression.[240] Our observation of the same phenomena in a distinct cell type (Müller cells as opposed to endothelial cells), in a different species (mouse versus human), with a different stimulus (hypoxia versus hyperglycemia) raises the possibility of a broadly applicable role for the α2β1 integrin in regulating VEGFA expression. Interestingly, both hyperglycemia and hypoxia are reported to stimulate stabilization and activation of HIF transcription factors.[257] To evaluate whether the difference between wild type and α2-null Müller function occurred upstream or downstream of HIF transcription factor activation we tested VEGFA production after treating Müller cells with $CoCl_2$, an established hypoxia mimetic and chemical inducer of HIF transcription factors. Treatment with $CoCl_2$ caused similar levels of VEGF-A production by wild type and α2-null Müller cells, which indicates that the α2-null Müller cells have no defects in VEGF-A expression or secretion, and that the difference must occur upstream of activation of HIF transcription factors.

Recent work indicates that HIF-2α is the HIF family member that is most responsible for Müller cell function during retinopathy.[238,239] Culturing in hypoxia for 24 hours caused higher levels of HIF-2α protein in wild type compared to α2-null Müller

cells. Interestingly we also observed significant upregulation of α2-integrin expression during hypoxia. Induction of α2β1 integrin in response to hypoxia has been reported in other cell types.[223] Additionally, Cheli et al. have identified PARP-1, a regulator of HIF-2α activity, as a transcriptional coactivator for α2β1 integrin.[116,224] Based on these reports it seems likely that HIF-2α may be involved in hypoxia-induced upregulation of α2β1 integrin; however, the potential mechanism by which α2β1 integrin may promote hypoxia-induced HIF-2α activation remains unclear. Recent work characterizing cellular signaling pathways in Müller and other microglial cells offer interesting hypotheses about potential mechanisms for α2β1 regulation of Müller cell-dependent VEGF-A production. The p38, a MAP kinase reported to be activated downstream of α2β1 integrin in mammary epithelial cells, was shown to be phosphorylated in rat Müller cells during hypoxia.[185,258] Similarly, phosphorylation of p38 was demonstrated to be critical for VEGF production in mouse embryonic fibroblasts, as well as retinal pigment epithelium.[226,258] Interestingly, p38 phosphorylation has been widely implicated in activation of HIF family member, HIF-1α, although the role of p38 in activating HIF-2α is not yet established.[225,227] It is tempting to speculate that α2β1 integrin and HIF-2α exist in a feed-forward loop in which hypoxia-induced activation of HIF-2α upregulates α2β1 integrin, potentially in a PARP-1-mediated mechanism. In turn, α2β1 integrin could conceivably promote the stabilization and activation of HIF-2α via P38 phosphorylation or some other downstream signal. Crosstalk between α2β1 integrin and HIF-2α warrants further investigation as a potential mechanism through which the α2β1 integrin mediates hypoxia-induced VEGF-A production in Müller cells.

2.6 Supplemental Figures and Methods

Supplemental Figure 1

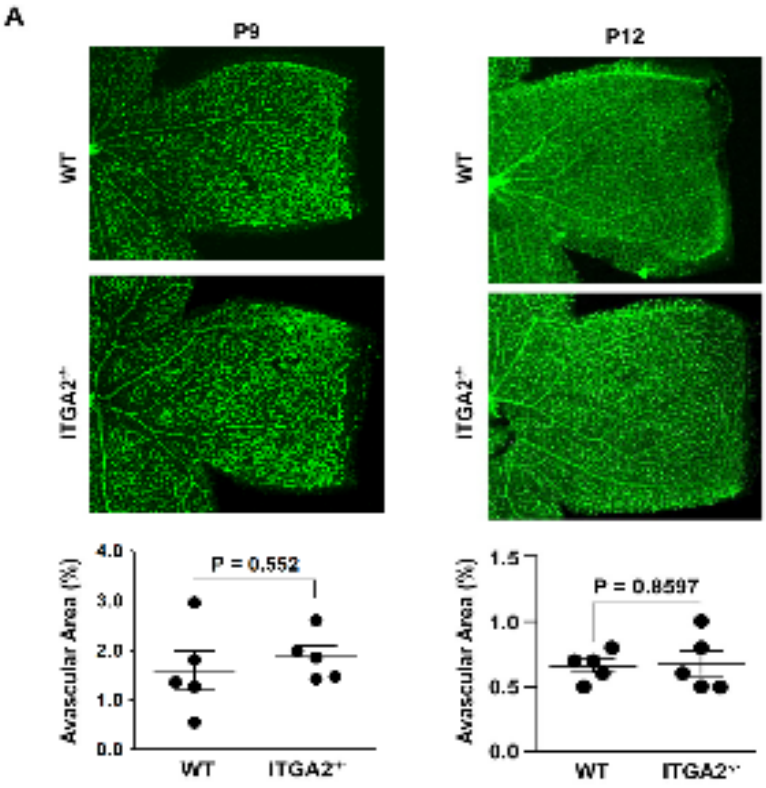

Supplemental Figure 1

(A) Retinal flat mounts of age-matched wild type (WT) and ITGA2-/- mice at P9 and P12. Vessels were visualized by GS Lectin (green) via immunofluorescence microscopy. At P9 and P12 radial vascular outgrowth was complete, and so vascularization was measured by Vascular Density, as quantitated by pixel percentage of vessel area relative to total retina area. Each data point represents the average result from an experiment with a litter of at least 4 mice (data represent mean +/- SEM). The results are representative of 3 separate trials.

Supplemental Figure 2

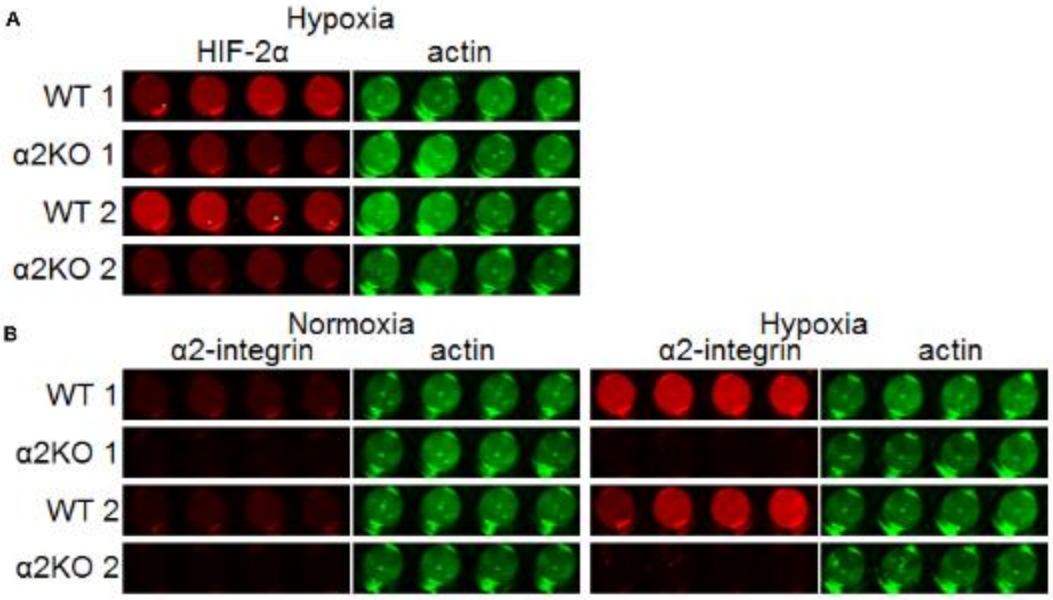

Supplemental Figure 2

(A) In-cell western analysis of HIF-2α expression in two primary WT and α2KO (ITGA2-/-) Müller cells after 24 hours of culture in hypoxia conditions. HIF-2α expression shown in Red and actin shown in Green.

(B) In-cell western analysis of HIF-2α expression in two primary WT and α2KO (ITGA2-/-) Müller cells after 24 hours of culture in hypoxia conditions. Expression of α2-integrin in Red and actin expression in Green.

Supplemental Methods - qPCR Analysis

Primer Design and Analysis – Primer pairs for mRNA expression (Table 1) analysis were designed using Primer Express 3.0™ (Applied Biosystems) using published murine gDNA and mRNA sequences (UCSC Genome Bioinformatics). Primer pairs that spanned an introns >500bp were preferred. Primers with binding site that exhibited secondary structures with significant ΔG at 60°C, as determined by UNAfold (Integrated DNA Technologies), were eliminated. After synthesis (MWG Eurofins) amplification efficiencies were determined using a six-step, four-fold dilution series of cDNA. Melt curve analysis on each sample was performed to confirm amplification specificity.

Supplemental Table 1

Gene	Primer Sequence	Amplicon Size (bp)
ITGA2 Forward	GCAAAACAATCAAGTAGCCATCCT	180
ITGA2 Reverse	TCAGAGGGCTTCTGTATGCTAATG	
VEGFA* Forward	GTCCTGTGTGCCGCTGATG	122
VEGFA* Reverse	GCTGGCTTTGGTGAGGTTTG	
HPRT Forward	CTCATGGACTGATTATGGACAGGAC	123
HPRT Reverse	GCAGGTCAGCAAAGAACTTATAGCC	
RPP30 Forward	GCTGCCGTGTCCACAAATT	182
RPP30 Reverse	AGGCAGTGCGTGGAGACTCA	
TBP Forward	GCCAGACCCCACAACTCTTC	180
TBP Reverse	AGCCAAGATTCACGGTAGATACAAT	

* Primer taken from Ehlken et al., 2011.[1]

qPCR Sample Preparation

For developmental studies pairs of retinas from P5, 7, 12, and 18 WT and KO mice were harvested. For OIR studies pairs of retinas from P12, 13 and 18 WT and KO mice were harvested. Retina harvests occurred immediately after sacrifice and were followed by dounce homogenization in 200µl Trizol (Life Technologies). Total RNA was recovered following manufactures protocol. RNA concentrations were measured using a

Nanodrop 1000 (Nanodrop Inc.). The RNA samples (three µg in a 30µl reactions) were converted to cDNA using SuperScript®VILO™ cDNA Synthesis Kit following manufacturers protocol (Life Technologies). 10µl reactions were prepared, in triplicate, using Power SYBR Green 2X Master Mix (Applied Biosystems), 250µM forward and reverse primers, 1.0µl cDNA and RNase-free water. Quantitative PCR (qPCR) was done on an Applied Biosystems 7900HT qPCR machine using a 384-plate system. qPCR amplification protocols were performed as per manufacturers protocol including post amplification melt curve analysis to confirm the absence of nonspecific amplification products.

Relative fold change in gene expression was completed using the comparative 2-ΔΔCT method (including the amplification efficiency correction factor). Relative RNA quantities were normalized to either HPRT, RPP30 or TBP based on the gene, determined by NormFinder, to represent the optimum normalization gene for the set of samples analyzed.

2.6.2 Oxygen induced retinopathy (OIR) experimental mouse model for retinopathy of prematurity (ROP)

Pups are allowed to live in normal conditions with their nursing mothers for the first 7 days. At postnatal day 7 (P7), pups from each genetic background (WT and a2-null) are taken with their nursing mothers and placed in a plexiglass chamber in a hyperoxic oxygen concentration of 75% O2 (Oxycycler Model A84, Biospherix, Lacona, N.Y.). After 5 days (P7-P12), pups are either sacrificed for retina dissection and analysis or returned to 'relatively hypoxic' room air conditions for 6 days (P12-P18). At this point remaining pups are sacrificed for retinal dissection and analysis.

Hyperoxic conditions from P7-P12 causes in vaso-obliteration around the optic nerve resulting in a central avascular area. Exposure to the 'relatively hypoxic' room air conditions from P12-P18 causes VEGF-A induced neovascularization.

Retinas from each group of mice were processed as follows [2]:
Mice from OIR experimental groups and normal air controls were euthanized by decapitation on P12 or P18. Eyes were enucleated, and the retinas were dissected and fixed in 4% neutral-buffered PFA at 4°C. One eye was then processed for sectioning, and the other eye was used to evaluate avascular area/neovascularization. The retinal vasculature was stained with 4µg/mL FITC-conjugated isolectin B4 (Sigma-Aldrich; Cat #L2895). Images of isolectin B4–stained retinas were digitized, captured, and displayed at 20x magnification (Photoshop). For P12 retinas, total retinal area and vascularized area were outlined and for P18 retinas, neovascular tufts were outlined with an irregular polygon. The pixels were counted within the area, and the total pixels from each polygon were pooled.

2.6.3 Immunoanalyses

Immunoflourescence images were captured with a Nikon Eclipse 80i fluorescence microscope. Quantification was performed using ImageJ (NIH)**.**

Supplemental Table 2

IF- Frozen Section CD31- α2 integrin colocalization	
CD31 Primary	Rat anti-mouse CD31 (1:100; BD553370)
CD31 Secondary	Alexa Fluor® 488 Goat Anti-Rat IgG (H+L) (1:600; Life A11006)
Alpha2	PE Hamster Anti-Mouse CD49b (1:100; BD 558759)
DAPI	(1:2000; Life D1306)
IF - Frozen Section GFAP- α2 integrin colocalization	
GFAP Primary:	Rabbit polyclonal to GFAP (1:100; abcam ab7779)?
GFAP Secondary	Rhodamine Red Goat Anti-Rabbit IgG (1:600; Invitrogen R6394)
GFAP Secondary	Alexa Fluor® 488 Goat Anti-Rabbit IgG (1:600; Invitrogen A11008)
Alpha2	PE Hamster Anti-Mouse CD49b (1:100; BD 558759)
DAPI	(1:2000; Life D1306)

2.6.4 Immunostaining and quantification

Frozen Sections: 12uM cryosections that were isolated from P18 mice from normal or OIR treated cohorts as described in Geisen et al., 2008 [3]. These sections were analysed via immunofluorescence microscopy for identification and quantitation of CD31+ and α2β1+ endothelial cells, or GFAP+ and α2β1+ Müller cells using antibodies listed in supplements.

H&E Staining: Eyes were enucleated and fixed in 4% paraformaldehyde overnight before storage in 70% EtOH in 4 degrees celsius. The eyes were then paraffin sectioned into 6 um saggital crossections which were prepared by H&E staining as described in Smith et al., 1994 [4].

Flat-mount Retinas: WT and KO Mice from normal conditions were sacrificed at P5, P7 and P18, along with mice treated with OIR from P12 and P18. Retinas were dissected and permeabilized before staining as described in Geisen et al., 2008 [3]. For

Immunoflourescent experiments images were taken with a Nikon Eclipse 80i fluorescence microscope before quantification with ImageJ.

2.6.5 Western Immunoblot Analysis

Protein lysate from hypoxia-cultured or normoxia cultured primary retinal Müller cells were subjected to sodium dodecyl sulfate–polyacrylamide gel electrophoresis (SDS-PAGE) and immunoblotted with either primary anti-HIF2α [NB100-480SS ; Novus Biologicals] or anti-CD49b (α2-integrin) [AB1936; EMD Millipore] antibody and anti-actin antibody [sc-1616; santa cruz biotechnologies] at 4°C followed by secondary antibody treatment. Dual color infrared imaging system (Odyssey; LiCor BioSciences) was used for visualization.

2.6.6 In-Cell Western Analysis

In-cell Western was performed in accordance with manufacturer's specifications. Briefly, primary Müller cells were plated in 96 well plates at a density of 5×10^3 cells/well and incubated until approximately 70% subconfluency. Cells were then cultured in either normoxic [37°C in a 5% CO_2/95% air (20.9% oxygen) atmosphere] or hypoxic conditionsin a humidified incubator (NuAire, Plymouth, MN).

Cells were fixed in 3.7% methanol-free formaldehyde in PBS, rinsed with PBS, blocked with 5% nonimmune rabbit serum in PBS/0.1% Triton X-100 for 1 h, and incubated with primary antibodies, either anti-HIF2α [NB100-480SS; Novus Biologicals] or anti-CD49b (α2-integrin) [HMa2; BDB553819] and anti-actin antibody [sc-1616; santa cruz biotechnologies], for 2hours at 37°C. The cells were then rinsed three times in PBS for 5 min each and then incubated in fluorochrome-conjugated secondary antibody diluted in

PBS/0.1% Triton X-100 for 1 h at room temperature in the dark. The cells were then rinsed three times in PBS for 5 min each and scanned using a Li-Cor Odyssey device**.**

2.6.7 Works Cited in Supplement

1. Ehlken C, Martin G, Lange C, Gogaki EG, Fiedler U, Schaffner F, Hansen LL, Augustin HG, Agostini HT. Therapeutic interference with EphrinB2 signaling inhibits oxygen-induced angioproliferative retinopathy. *Acta Ophthalmol (Copenh)*. 2011;89:82–90.

2. Barnett JM, McCollum GW, Fowler JA, Duan JJ-W, Kay JD, Liu R-Q, Bingaman DP, Penn JS. Pharmacologic and genetic manipulation of MMP-2 and -9 affects retinal neovascularization in rodent models of OIR. *Invest Ophthalmol Vis Sci*. 2007;48:907–915.

3. Geisen P, Peterson LJ, Martiniuk D, Uppal A, Saito Y, Hartnett ME. Neutralizing antibody to VEGF reduces intravitreous neovascularization and may not interfere with ongoing intraretinal vascularization in a rat model of retinopathy of prematurity. *Mol Vis*. 2008;14:345–357.

4. Smith LE, Wesolowski E, McLellan A, Kostyk SK, D'Amato R, Sullivan R, D'Amore PA. Oxygen-induced retinopathy in the mouse. *Invest Ophthalmol Vis Sci*. 1994;35:101–111.

Chapter 3

SIGNAL REGULATION AND NUMERICAL SIMULATION OF SPROUTING IN MOUSE RETINA ANGIOGENESIS

3.1 Abstract

The VEGF-Notch signaling system regulates specification of endothelial cells into migratory ‘tip’ and proliferative ‘stalk’ phenotypes via lateral inhibition. Drugs targeting the VEGF-Notch signaling system have been introduced clinically as anti-angiogenesis medications. However, a more mechanistic understanding of how notch-mediated tip-stalk specification regulates complex vascular phenotypes is needed in order to realize more complex therapeutic goals such as orderly revascularization. Plexus irregularity, a phenotype of increased variability in the radial growth of developing retinal vasculature, is observed in select notch mutant mouse models. It has been hypothesized that increased notch signaling leads to plexus irregularity, but technological hurdles have prevented direct *in vivo* experimentation of this question. In this study we present a hybrid mathematical model to simulate the morphological and signaling features observed in the postnatal development of the retinal vascular network. Using this model, we study how the VEGF-notch signaling system directs the development of morphological features including, retinal vascularization, plexus density, and plexus irregularity. Additionally, we use this model to predict how crosstalk molecules signal to the VEGF-Notch axis to modulate these vascular phenotypes. This work provides insight into the molecular mechanism of retinal sprouting angiogenesis and can help identify potentially synergistic therapeutic approaches.

3.2 Introduction

Sprouting angiogenesis, the expansion of a network of blood vessels in response to local tissue hypoxia, is an area of burgeoning research interest. It is broadly involved in disease processes ranging from tumor progression and metastasis, to retinopathies. Over the last two decades, it has been shown that a complex interplay of growth factor gradients and cellular signaling systems tightly regulate sprouting angiogenesis. Further insights into the nuanced molecular systems that govern this process are of tremendous scientific, and potentially therapeutic value. Sprouting angiogenesis is initiated when hypoxic tissue secretes the chemokine, vascular endothelial growth factor A (VEGF-A), to stimulate the expansion of the vascular network and improve tissue perfusion. Quiescent blood vessels contain equipotent endothelial cells. VEGF-A stimulates these endothelial cells (ECs) to adopt a tip cell phenotype via the endothelial VEGF receptor-2 subtype (VEGFR-2). In tip cells, VEGF-A-mediated VEGFR-2 activation stimulates filopodia extension and chemotactic cell migration along the VEGF-A gradient, and also upregulates both VEGFR-2 and notch ligand, delta-like protein 4 (DLL4). DLL4 is a transmembrane ligand that induces Notch signaling and mediates downstream repression of VEGFR-2, in adjoining cells. These adjoining ECs adopt a proliferative stalk cell phenotype, which fills in behind tip cells and forms new vascular lumen in a VEGF receptor-1 (VEGFR-1) mediated manner. In this way coupled negative and positive feedback loops establish a mechanism of lateral inhibition that spatially organizes tip and stalk cell fates in response to an angiogenic growth factor gradient (Figure 3.1).

The tremendous progress in our understanding of the VEGF-notch axis, has led to pharmacological targeting of VEGFR2 and DLL4 for anti-angiogenesis therapeutics.[259] However, therapeutic approaches that promote orderly neovascularization remain elusive. One promising development is the identification of

Figure 3.1 Notch-mediated lateral inhibition decreases VEGFR2 activation and tip-cell induction in 'stalk cells'

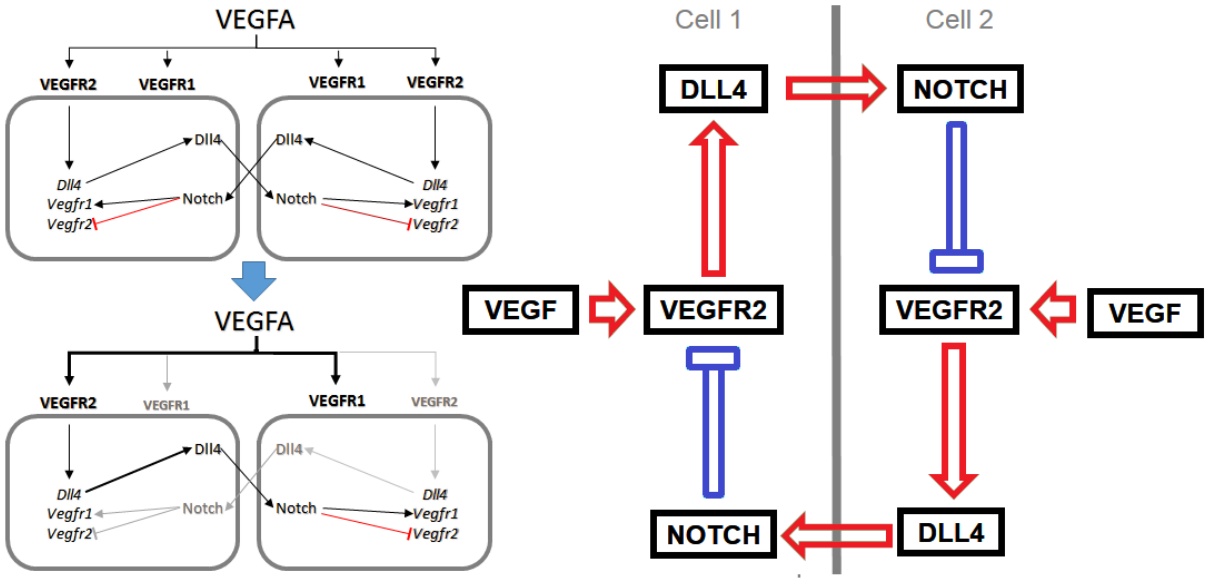

Left: A cartoon representation from Jakobsson 2010 shows how adjacent endothelial cells respond to a VEGFA gradient. The cell exposed to higher VEGFA upregulates VEGFR2 and DLL4. DLL4 downregulates VEGFR2 in neighboring cells. This lateral inhibition causes decreased capacity for VEGFR2 activation. Over time small initial differences result in divergent 'tip' and 'stalk' phenotypes among neighboring endothelial cells.
Right:A minimalist representation of the feedback loop that drives lateral inhibition.

several angiogenic signaling pathways that crosstalk with the VEGF-Notch signaling network. In 2011, Kim et al., described the role of Semaphorin3E-PlexinD1 as a negative regulator of Notch signaling (Figure 3.2).[260] Loss of function mutants in this pathway display decreased plexus density and increased plexus irregularity during postnatal mouse retina development. It is not clear whether these phenotypes in Plexin-null mice can be explained by loss of Plexin-induced notch signaling or whether non-notch mediated effects of Plexin also contribute.

This ambiguity highlights a major challenge in developing neoangiogenesis therapies; the full phenotypic effects of manipulating the notch signaling system are still incompletely understood. In the postnatal mouse retina, the primary experimental model for sprouting angiogenesis, it is technically challenging to provide precise amounts of agonists/antagonists at specific temporal and spatial locations. Rescue experiments of loss-of-function mutants tend to produce exaggerated rather than developmentally normal phenotypes.

Computational modeling of the notch lateral inhibition system has been used to explore how molecular systems drive tissue level changes in the vascular network,

Figure 3.2 Plexin-D1 provides negative feedback to Notch-mediated lateral inhibition

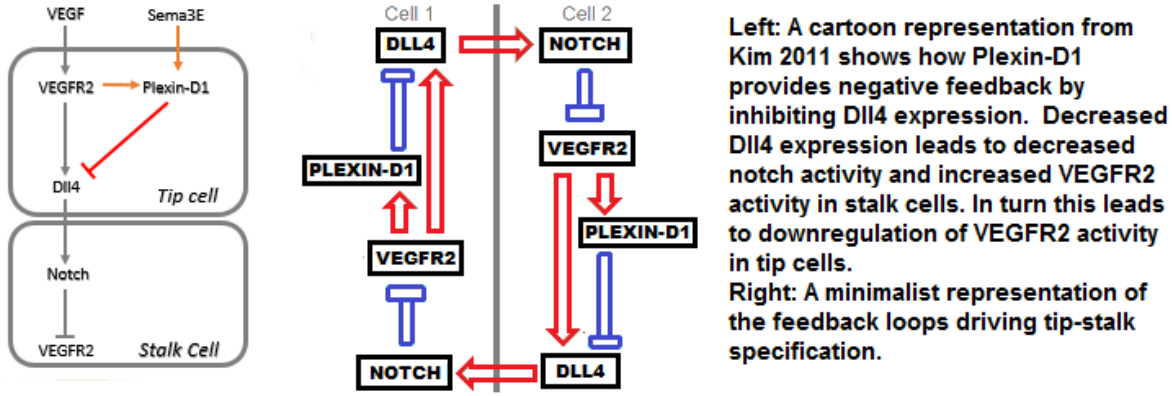

Left: A cartoon representation from Kim 2011 shows how Plexin-D1 provides negative feedback by inhibiting Dll4 expression. Decreased Dll4 expression leads to decreased notch activity and increased VEGFR2 activity in stalk cells. In turn this leads to downregulation of VEGFR2 activity in tip cells.
Right: A minimalist representation of the feedback loops driving tip-stalk specification.

while avoiding the technical challenges inherent to the mouse model. Bentley et al., demonstrated *in silico* that notch signaling is sufficient to explain sprout initiation, tip selection, and vascular branching. Yet, several key questions remain. Does the VEGF-notch axis regulate other sprouting angiogenesis phenotypes such as vascular density or plexus regularity? Also, how does crosstalk from other angiogenic signaling molecules, such as Plexin-D1, affect Notch-mediated sprouting angiogenesis? Do they

simply up or downregulate Notch activity, or do they affect the network complexity of the greater VEGF-Notch axis?

In this study we introduce a hybrid multi-scale model that explores how manipulating VEGF-notch signaling effects retinal vasculature phenotypes. Our model also serves as a platform for evaluating proposed relationships between candidate molecules and the Notch signaling pathway. Here we study how Plexin-D1 affects VEGF-Notch signaling and why its deletion causes the phenotypes observed in Plexin-null mutant mice. Our model focuses on the retina, because there is a long tradition of both experimental and computational analyses of postnatal retinal vascular development in the mouse.

3.2.2 Model Antecedents

Anderson and later Watson developed two-dimensional hybrid partial differential equation models to carefully simulate how growth factor gradients (VEGF) regulate postnatal retinal vascular development.[261,262] Watson et al. model the EC cell movements in sprouting angiogenesis by simulating a VEGF gradient produced by poorly oxygenated astrocytes, and upregulated matrix-degrading enzymes in VEGF-stimulated ECs. The VEGF gradient is produced with a continuous system of partial differential equations describing the changes in EC cell density, and the EC movement is modeled using a discrete random walk simulation of cells over a superimposed grid covering the retina.[261] The simulation gives a graphical representation of the spatio-temporal movement of EC forming the nascent blood vessels between embryonic day 15 and postnatal day 8. Their numerical outcomes show similarities with the *in vivo* development of the vascular network. Watson's model for postnatal retinal vascular development relies on a phenomenological understanding of branching dynamics and

does not incorporate current understandings of the notch-mediated molecular mechanism that regulates vessel branching. Consequently, this model is incapable of making predictions about the phenotypes caused by pharmacological or transgenic manipulation of the VEGF-Notch system.

Katie Bentley, in collaboration with the Gerhardt group, used a hierarchical agent-based model to simulate VEGF and Notch mediated feedback loops.[263] They demonstrated that Notch signaling is sufficient to explain vascular branching via sprouting angiogenesis/lateral inhibition. This *in silico* hypothesis has been validated *in vivo* through experiments showing increased branching with both genetic and pharmacological inhibition of notch signaling. Bentley et al. modeled sprouting angiogenesis in an abstract manner and did not specifically model the postnatal retinal vasculature. This approach is limited in how much can be extrapolated from the model. For example, Bentley's approach correctly predicts that inhibiting Notch signaling leads to a hypersprouting phenotype, but it is unclear what phenotypes arise from increased notch signaling. No predictions about plexus irregularity or rate of vascular expansion can be made with models like this.

Collier et al. have developed a temporal mathematical model that describes interactions between two adjacent cells.[264] They described a Delta-Notch intercellular signaling mechanism based on contact-mediated lateral inhibition. Their work demonstrated how this signaling mechanism could cause a differentiation pattern where a cell's fate differs considerably from its neighbor's fate due to the feedback loop between Notch and Delta. They outline how the strength of Delta-Notch signaling regulates the type of differentiation pattern that emerges. Their work is limited to Delta-Notch signaling which is investigated in a general theoretical framework divorced from a

specific physiological context. This limitation prevents any predictions about complex vascular phenotypes in the retina.

3.2.3 Model Construction

Our hybrid multiscale model simulates how VEGF, Notch, and candidate cross-talk signaling interact at the cellular level to drive tip-stalk cell fate specification, and uses those tip-stalk decisions to inform endothelial cell migration and proliferation across a simulated VEGF gradient.

3.2.3.1 Modeling Domain

In order to facilitate comparison to experimental results from mouse retinas, we use a leaf-shaped modeling domain that resembles a quadrant of a dissected and mounted mouse retina between postnatal day 5 and postnatal day 7. The leaf-shaped domain contains a two-dimensional lattice grid that is uniformly covered with one astrocyte per grid point. Astrocytes are considered hypoxic and produce VEGF unless an endothelial cell is present at that grid point.

VEGF produced by hypoxic astrocytes diffuses across the modeling domain as described by the following partial differential equation:

$$\frac{\partial c}{\partial t} = \alpha_a \bar{a} + D_c \nabla^2 c - \eta_c r c - \sigma_c c \qquad (1)$$

Where $\bar{a}$ is the local average number of hypoxic astrocytes per gridpoint. This average is calculated over a local region containing the site $p = (x, y)$ surrounded by its eight neighboring grid points. The constant α_a is the local VEGF production rate per hypoxic astrocyte and the constants $D_c,\ \eta_c,\ \sigma_c$ are non-dimensional rate parameters referring

respectively to the diffusion, consumption, and decay of VEGF (see [6] and [7] for details).

3.2.3.2 Endothelial Cell Behavior

The model begins with three endothelial cells near the origin (where the annulus of a dissected retina would be located). In biological settings endothelial cell behavior is dictated by Tip/Stalk status; Tip cells migrate in a random biased walk toward greater VEGF concentration, while stalk cells proliferate in their wake. To simulate this biology, Anderson et al., employed a partial differential equation that uses the VEGF gradient diffusion, chemotaxis and tip dynamics to describe the likelihood of a tip or stalk cell occupying a given grid point at a given time.[261] Our model determines Tip/Stalk status by VEGF-Notch signaling, which allows us to use a simplified PDE to probabilistically describe tip cell movement. We determine how likely a tip cell is to move into a given grid point (*x,y*), at time *t*, using the function *r*(*x,y,t*)

$$\frac{\partial r}{\partial t} = D_r \Delta r - \nabla\left(\frac{x_c}{1+\alpha_c c} r \nabla \mathrm{c}\right) \qquad (2)$$

where the function $c(x, y, t)$ measures VEGF concentration at (x, y) and time t. The constant D_r represents the cell random motility coefficient, and the parameters x_c and α_c govern the chemotaxis effect on the cell. Their values are given in Watson et al. (For details on the derivation of this equation from Anderson et al., see appendix I)

The above equation provides a continuous model that describes the movement of *all* tip cells. We are interested in tracking *individual* tip and stalk cells, so we discretize this PDE using a Euler finite difference approximation method. Specifically, we incorporate a cellular automata model to describe the movement of individual

endothelial cells with a set of rules that accounts for tip-stalk cell fate specification and nearest-neighbor cell interactions. In this discrete model the probabilities of movement of a given cell are calculated according to the formulas given below in (3)-(8).

$$r_{l,m}^{q+1} = P_1 r_{l+1,m}^{q} + P_2 r_{l-1,m}^{q} + P_3 r_{l,m+1}^{q} + P_4 r_{l,m-1}^{q} \quad (3)$$

$$P_0 = 1 + \frac{x^{\alpha k}}{4h^2(1+\alpha c)^2}\left((c_{l+1,m}^{q} - c_{l-1,m}^{q})^2 - \left(c_{l,m+1}^{q} - c_{l,m-1}^{q}\right)^2\right) - \frac{x^{k}}{(1+\alpha c)}\left(c_{l+1,m}^{q} + c_{l-1,m}^{q} - 4c_{l,m}^{q} + c_{l,m+1}^{q} + c_{l,m-1}^{q}\right) - \frac{4Dk}{h^2} \quad (4)$$

$$P_1 = \frac{Dk}{h^2} + \frac{x^{k}}{4h^2(1+\alpha c)}(c_{l+1,m}^{q} - c_{l-1,m}^{q}) \quad (5)$$

$$P_2 = \frac{Dk}{h^2} + \frac{x^{k}}{4h^2(1+\alpha c)}(c_{l,m+1}^{q} - c_{l,m-1}^{q}) \quad (6)$$

$$P_3 = \frac{Dk}{h^2} + \frac{x^{k}}{4h^2(1+\alpha c)}(c_{l,m+r}^{q} - c_{l,m-1}^{q}) \quad (7)$$

$$P_4 = \frac{Dk}{h^2} + \frac{x^{k}}{4h^2(1+\alpha c)}(c_{l,m+1}^{q} - c_{l,m-1}^{q}) \quad (8)$$

The value P_0 determines the probability that a given tip/stalk cell at site $(x, y) = (lh, mk)$ and at a given time step $t = qk$ will remain stationary; P_1, P_2, P_3, and P_4 determine the probability that the cell moves left, right, down and up, respectively. As the tip cell migrates, stalk cells proliferate in its wake, resulting in elongation of the vessel branch.

Now that we have a system for describing how a given tip cell will move, we need a mechanism to describe how and where tip cells form. We do this by modeling the VEGF-Notch signaling within each individual cell (as described in the following

section). More details about how this differs from the Anderson approach are provided in section 3.4.

Figure 3.3

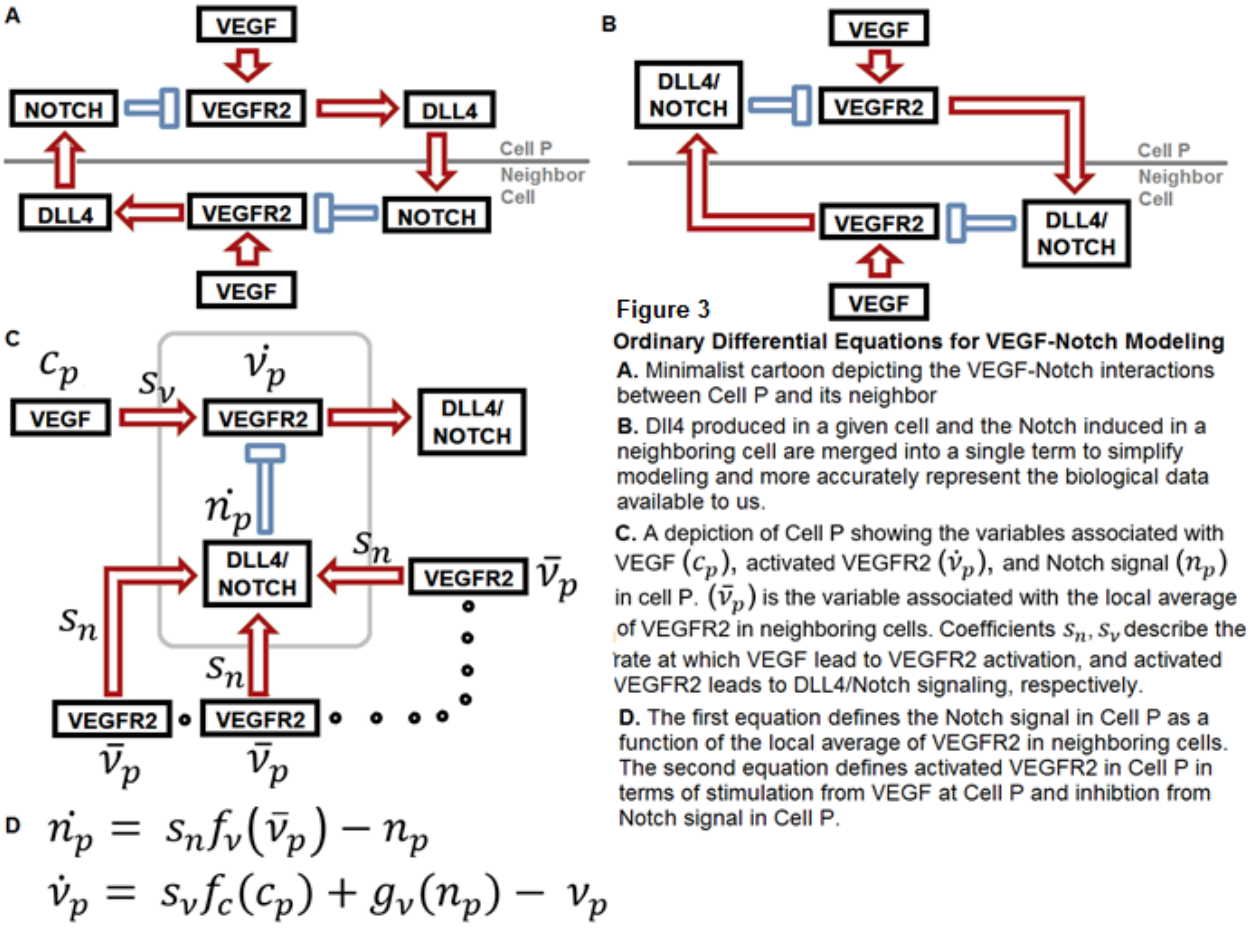

Figure 3
Ordinary Differential Equations for VEGF-Notch Modeling

A. Minimalist cartoon depicting the VEGF-Notch interactions between Cell P and its neighbor

B. Dll4 produced in a given cell and the Notch induced in a neighboring cell are merged into a single term to simplify modeling and more accurately represent the biological data available to us.

C. A depiction of Cell P showing the variables associated with VEGF (c_p), activated VEGFR2 $(\dot{v}_p)$, and Notch signal (n_p) in cell P. $(\bar{v}_p)$ is the variable associated with the local average of VEGFR2 in neighboring cells. Coefficients s_n, s_v describe the rate at which VEGF lead to VEGFR2 activation, and activated VEGFR2 leads to DLL4/Notch signaling, respectively.

D. The first equation defines the Notch signal in Cell P as a function of the local average of VEGFR2 in neighboring cells. The second equation defines activated VEGFR2 in Cell P in terms of stimulation from VEGF at Cell P and inhibtion from Notch signal in Cell P.

3.2.3.3 Cellular Signaling Simulation

This portion of our model uses a system of ordinary differential equations (ODEs) to model the internal signaling milieu of each cell. We model Notch-VEGFR2 signaling interactions at the cellular level with a set of ordinary differential equations. First we

consider the minimal model for Notch-VEGFR2 mediated lateral inhibition (Figure 3.3). In a given Cell P, the activation of VEGFR2 is calculated by balancing the stimulation from the local VEGF concentration (c_p) and inhibition from the amount of DLL4/Notch $(\dot{n}_p)$ in cell P. The DLL4/Notch signal ($\dot{n}_p$) in cell P is calculated based on the local average of activated VEGFR2 in neighboring cells $(\bar{v}_p)$.

$$\begin{aligned} \dot{n_p} &= s_n f_v(\bar{v}_p) - n_p \\ \dot{v}_p &= s_v f_c(c_p) + g_v(n_p) - v_p \end{aligned} \tag{9}$$

Note that although DLL4 and Notch are distinct biological components, they are merged as only the notch-signaling function of DLL4 is modeled. The functions $f_*(u)$ and $g_*(u)$ that are modifying the variables $\bar{v}_p$, c_p, and n_p in equation (9) are sigmoidal Hill functions. They normalize the values of these variables so that molecules with very disparate quantities can be modeled in the same equation. Greater detail on these functions can be found in appendix II. The term S_n is a sensitivity coefficient that describes the rate at which VEGFR2 activation leads to DLL4/Notch signaling. Similarly, S_v is a sensitivity coefficient describing how VEGF levels lead to VEGFR2 activation. The user provides values for these coefficients before solving the system of differential equations.

One goal of this project is to understand how the VEGF-Notch signaling system can be affected by crosstalk from other angiogenic signaling molecules. To do this we expand our system of ODEs (9) to incorporate the variable α_p that represents the level of a candidate angiogenic crosstalk molecule in cell p at a given time. As before, we model the interactions with neighboring cells over time through a system of ordinary differential equations (Figure 3.4).

Figure 3.4

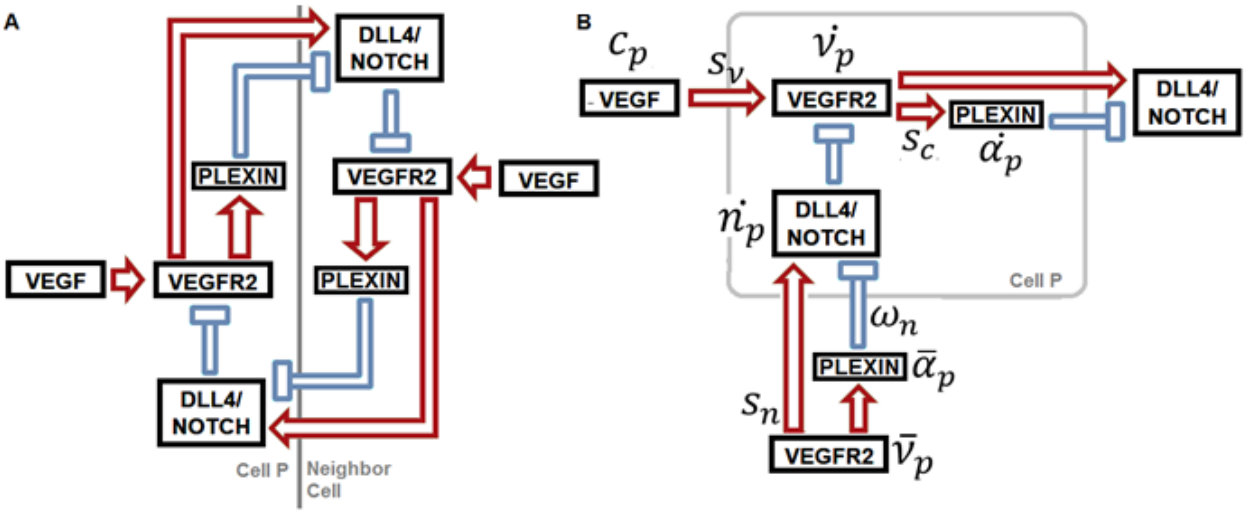

C

$$\dot{n_p} = \tau_n[s_n f_v(\bar{v}_p)\left(1 + \omega_n f_b(\bar{\alpha}_p)\right) - n_p]$$
$$\dot{v_p} = \tau_v[s_v f_c(c_p)\left(1 + s_a f_\alpha(\alpha_p)\right) + g_v(n_p) - v_p\,]$$
$$\dot{\alpha_p} = \tau_\alpha[s_c f_v(v_p\,)\left(1 + s_\alpha g_\alpha(n_p)\right) - \alpha_p\,]$$

Figure 4 Modeling Greater VEGF-Notch Signaling Network using Ordinary Differential Equations
A. Minimalist cartoon depciting the greater VEGF-Notch system in Cell P and adjacent cell. In addition to the core VEGF-Notch network, an accessory component, Plexin, is also included.
B. A cartoon of Cell P as modeled. In addition to the variables and coefficients described in figure 3, the variable ($\dot{\alpha_p}$) represents the level of the accessory notch system component Plexin-D1. The coefficient (ω_n) describes how the local average of Plexin-D1 in adjacent cells ($\bar{\alpha}_p$)influences DLL4/Notch signal (n_p) in Cell P.
C. A system of 3 ODEs describing the values of DLL4/Notch ($\dot{n_p}$), activated VEGFR2 ($\dot{v_p}$), and the accessory component Plexin-D1($\dot{\alpha_p}$)in Cell P at a given time.

$$\dot{n_p} = \tau_n[s_n f_v(\bar{v}_p)\left(1 + \omega_n f_b(\bar{\alpha}_p)\right) - n_p]$$
$$\dot{v_p} = \tau_v[s_v f_c(c_p)\left(1 + s_a f_\alpha(\alpha_p)\right) + g_v(n_p) - v_p\,] \quad (10)$$
$$\dot{\alpha_p} = \tau_\alpha[s_c f_v(v_p\,)\left(1 + s_\alpha g_\alpha(n_p)\right) - \alpha_p\,]$$

The coefficients s_c and s_α describe how activated VEGFR2 and Notch, respectively, lead to the production of the candidate component ($\dot{\alpha_p}$) in cell P. The coefficients ω_n and s_a describe how the candidate component (α_p) affects the rate of production of DLL4/Notch signal and activated VEGFR2, respectively, in cell P. Together these

coefficients can describe the many potential signaling relationships that comprise crosstalk between the candidate accessory components and the core VEGF-Notch signaling system. Here we use Plexin-D1 as our candidate angiogenic signaling molecule. In the literature, Plexin-D1 is reported to be upregulated by VEGFR2 and to inhibit DLL4/Notch signaling. These relationships are captured in the coefficients ω_n and S_c. Plexin-D1 is not reported to activate VEGFR2 or to be inhibited by Notch signaling; to reflect the absence of those relationships the coefficients S_a and S_α are removed by being set to zero. In addition to these coefficients we introduce the constant τ_* to represent a timescale coefficient for each of the three equations. This parameter accounts for each of the VEGFR2 activation, Dll4/Notch or the candidate crosstalk molecule (Plexin-D1) terms may respond faster or slower to changes in the system.

This system of ODEs is solved with the Runge-Kutta method using the MATLAB solver ODE45. Solving this system provides a vector containing the levels of VEGFR2 activation, Dll4/Notch, and candidate crosstalk molecule (Plexin-D1) for each endothelial cell. Based on the level of VEGFR2 throughout the simulated retina, we can use location to determine which endothelial cells are Tip cells at a given time.

3.2.3.4 Analysis

Our model captures graphical snapshots of the model retina at the beginning, middle, and end of the simulation. These snapshots are then analyzed to calculate total vascularized area, endothelial cell density, and plexus irregularity. Those measurements directly correspond to the phenotypic assessments that biologists conduct on dissected P7 mouse retinas.

3.2.3.5 Innovation

By nesting an updated version of Collier's Notch signaling system within a modified version of Watson's model for retinal vascular development, we have developed a model that connects molecular changes in Notch signaling with phenotypic changes in retinal vasculature development. Our work serves as a platform for first exploring the retinal phenotype of increased notch signaling and secondly for evaluating proposed relationships between candidate molecules and the notch signaling pathway by comparing the predicted and the observed retinal phenotype of a given transgenic or pharmacological intervention.

The primary distinction between the present model and the model given by Anderson et al. is the implementation of the vessel branching mechanism. Anderson et al. use a probabilistic branching mechanism in which new tip cells spontaneously materialize to form new vessel branches.[261] This approach allows for the simulation of realistic capillary branching, but it does not allow for prediction of how alterations in VEGF-notch signaling can change retinal vasculature phenotypes. The model that we introduce in this study uses VEGF-Notch signaling to determine Tip cell formation; as a result, our model is able to predict how modulating cellular signaling can affect complex vascular phenotypes such as vessel irregularity.

3.3 Results

3.3.1 Model produces simulated retinas with expected responses to changes in VEGF and Notch

The base model, which incorporates VEGF and DLL4/Notch signals, was run using S_n and S_v coefficients ranging from 0.1 to 0.9 each. Each combination of

coefficients was run 30 times. As discussed in the model overview, S_n, Notch sensitivity, is a sensitivity coefficient that describes the rate at which VEGFR2 activation leads to DLL4/Notch signaling. Similarly, S_V, VEGFR2 sensitivity, is a sensitivity coefficient describing how VEGF levels lead to VEGFR2 activation. For reference Figures 3.5A and 3.5B show the graphical cartoon and the ODEs that describe the VEGF-Notch signaling being modeled. More details about the derivation of these equations are contained in Methods (Section 3.3 and Figure 3.3). In Figure 3.5C (following page) we show representative graphical outputs from the endpoints of simulations with differing levels of the Notch and VEGFR2 sensitivity coefficients. In Figure 3.5D and 3.5E we show the quantified Vessel Density and Vascularized Area from each simulated retina. The Notch and VEGFR2 sensitivity coefficients within the range of 0.5 to 0.7 for each coefficient) result in simulated retinas with vessel density and vascularized area values that are similar to what have observed biologically in WT P7 retinas.[265] Also, the results from our simulation showed that very low VEGFR2 signaling (VEGFR2 sensitivity, S_V < 0.4) results in non-responsiveness to changes in Notch signaling, which is consistent with previously published biological results.

Figure 3.5 A-C

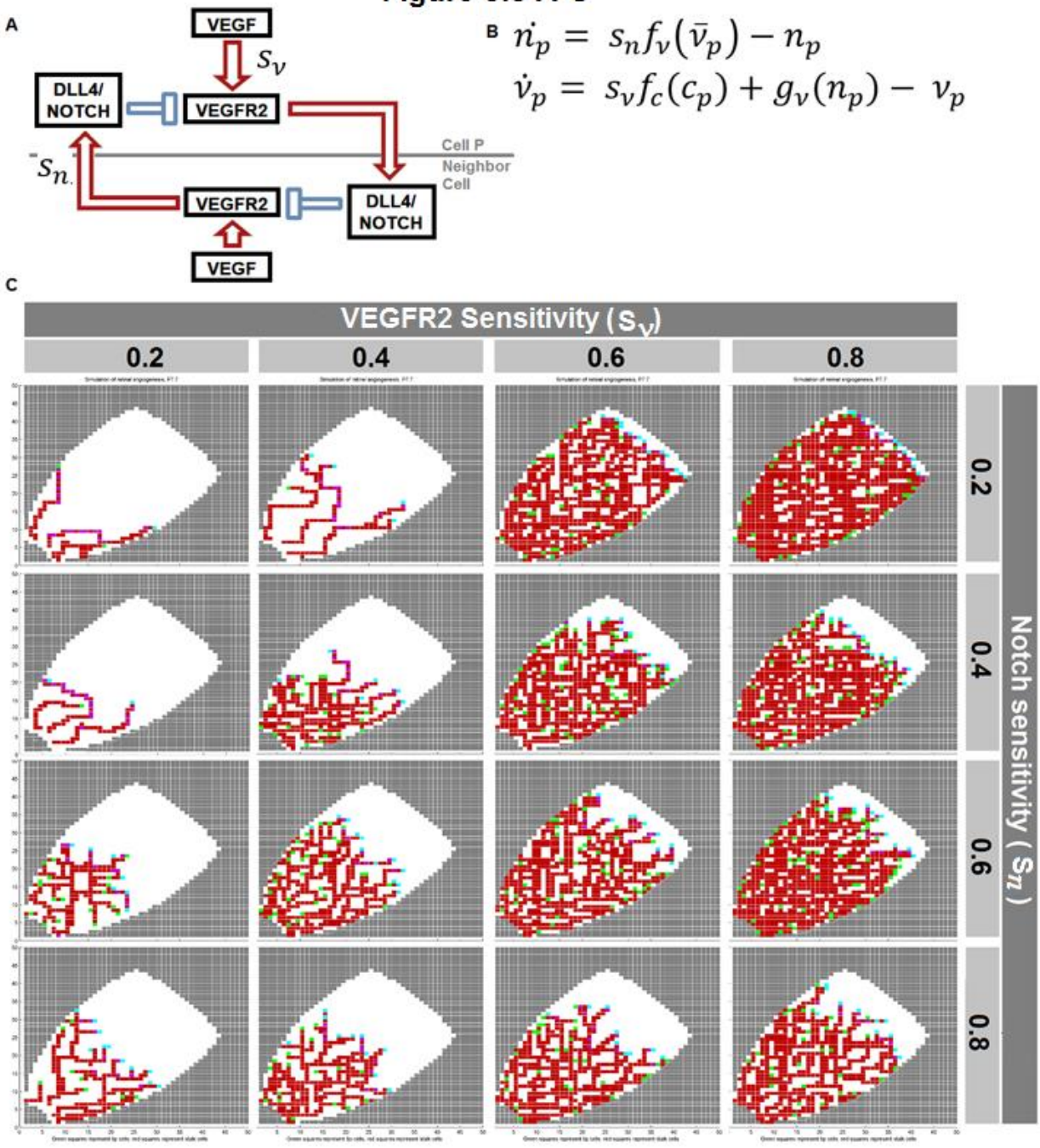

Figure 5 Simulated Retinas Respond to VEGFR2 and DLL4/Notch Modulation as Biologically Predicted

A. Minimalist Cartoon depicting the VEGF-Notch singaling between Cell P and its neighbor as modeled in the Base Model. The VEGFR2 and Notch sensitivity coefficients are both annotated in this model.

B. Ordinary Differential Equations for VEGF-Notch signaling in Base Model

C. Representative simulated retinas produced by the base model with the VEGFR2 and Notch Sensitivity coefficients as indicated on the X and Y axis Bars.

Figure 3.5 D-G

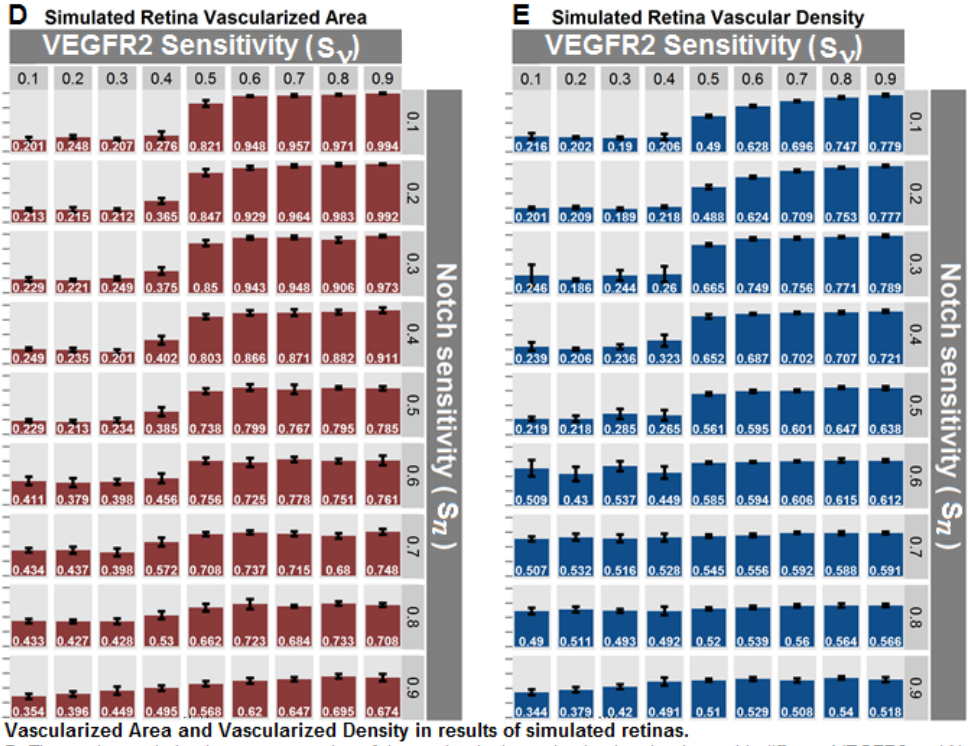

Vascularized Area and Vascularized Density in results of simulated retinas.

D. The total vascularized area as a portion of the total retinal area in simulated retinas with different VEGFR2 and Notch Sensitivities. Values represent mean+SEM of 30 simulated retinas.

E. The vessel density as area covered by endothelial cells relative to total retinal area in imulated retinas with different VEGFR2 and Notch Sensitivities. Values represent mean+SEM of 30 simulated retinas.

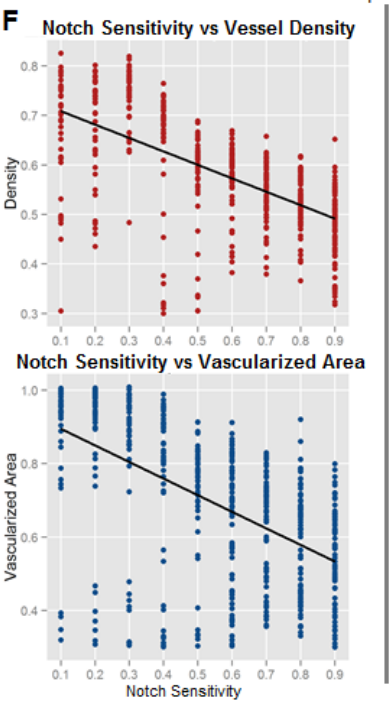

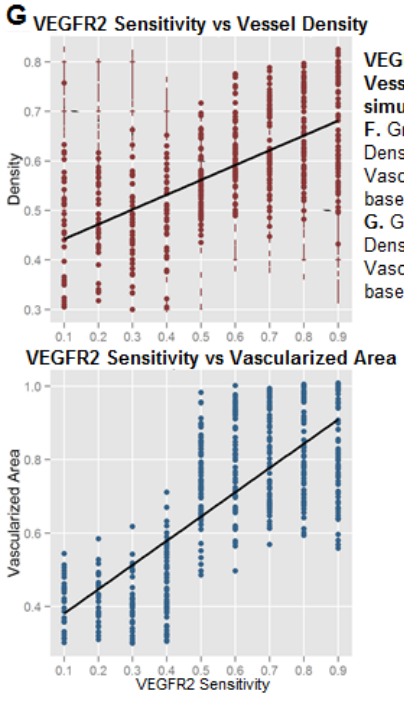

VEGFR2 promotes and Notch downregulates Vessel Density and Vascularized Area within the simulation

F. Graphical display of linear regressions of Vessel Density (Effect size: -.275; $p < .00876$) and Vascularized Area (Effect size: -.458; $p < 2e\text{-}16$) based on Notch Sensitivity.

G. Graphical display of linear regressions of Vessel Density (Effect size: +.292; $p < .000314$)and Vascularized Area (Effect size: +.679; $p < 2e\text{-}16$) based on VEGFR2 Sensitivity.

We used regression analysis to isolate the specific contribution of Notch signaling to the phenotypic metrics of Vessel Density and Vascularized Area in our model. A simple linear regression was calculated to predict vessel density based on the Notch sensitivity coefficient. A significant regression relationship was found with an effect size of -0.275 ($p < 0.00876$). This means a 0.1 step increase in the Notch Sensitivity coefficient is associated with a decrease in vessel density of 2.75%. Similarly, a simple linear regression to predict vascularized area based on the Notch sensitivity coefficient found a significant regression relationship with an effect size of -0.458 ($p <2e-16$). This indicates that a 0.1 step increase in the Notch sensitivity coefficient is associated with a decrease in vascularized area of 4.58%. This finding mirrors the biological findings that increased notch signaling causes decreased vessel density and vascularized area.

Regression analysis was also used to understand how VEGFR2 signaling affected Vessel Density and Vascularized Area in our model. A simple linear regression was calculated to predict vessel density based on the VEGFR2 sensitivity coefficient. A significant regression relationship was found with an effect size of +0.292 ($p < 0.000314$). This finding indicates that a 0.1 step increase in the VEGFR2 sensitivity coefficient is associated with an increase in vessel density of 2.92%. Similarly, a simple linear regression to predict vascularized area based on the VEGFR2 sensitivity coefficient found a significant regression relationship with an effect size of -0.679 ($p <2e-16$). This indicates that a 0.1 step increase in the VEGFR2 sensitivity coefficient is associated with an increase in vascularized area of 6.79%. These results are reflective of the biological findings in the literature. A visual representation of these regression

analyses showing the relationships between Notch and VEGFR2 sensitivity coefficients and Vessel Density and Vascularized Area is shown in Figure 3.5F-G.

3.3.2 Model accurately simulates PlexinD1 role in regulating Vessel Density

We tested whether our model could predict how Plexin-D1 affects the retinal vasculature using only information about how Plexin-D1 interacts with VEGFR2-Notch signaling. To do this we ran our model using S_c and ω_n coefficients ranging from 0.2 to 0.8 and -0.2 to -0.8 respectively. Each combination of coefficients was run 30 times. As discussed in the model overview, S_c is a coefficient that describes the rate at which VEGFR2 activation leads to Plexin-D1 production or expression. Similarly, the coefficient ω_n describes how PlexinD1 levels affect DLL4/Notch signaling. For reference Fig 3.6A and 3.6B (previous page) show the graphical cartoon and the ODEs that describe the role of Plexin-D1 in VEGF-Notch signaling as modeled. More details about the derivation of these equations are contained in Methods (Section 3.3 and in Figure 3.4). In Figure 3.6C and 3.6D we show the quantified Vascularized Area and Vessel Density from each simulated retina. The association between vessel density and plexin-D1 expression reflects Kim et al.'s report that Plexin-D1 deletion causes an increase in vessel density. Kim et al. did not investigate differences in vascularized area during retinal vasculature development.

Figure 3.6

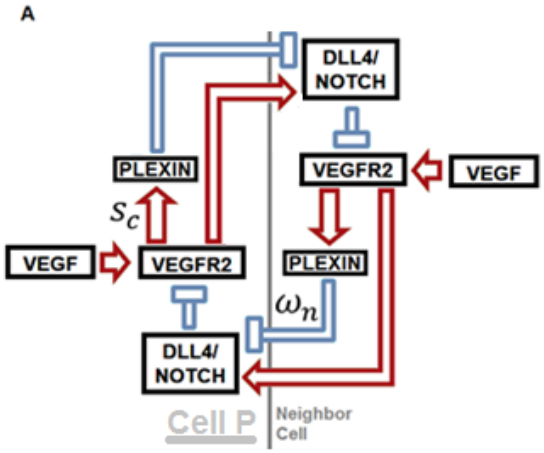

B

$$\dot{n}_p = \tau_n[s_n f_v(\bar{v}_p)(1 + \omega_n f_b(\bar{\alpha}_p)) - n_p]$$

$$\dot{v}_p = \tau_v[s_v f_c(c_p) + g_v(n_p) - v_p]$$

$$\dot{\alpha}_p \doteq \tau_\alpha[s_c f_v(v_p) - \alpha_p]$$

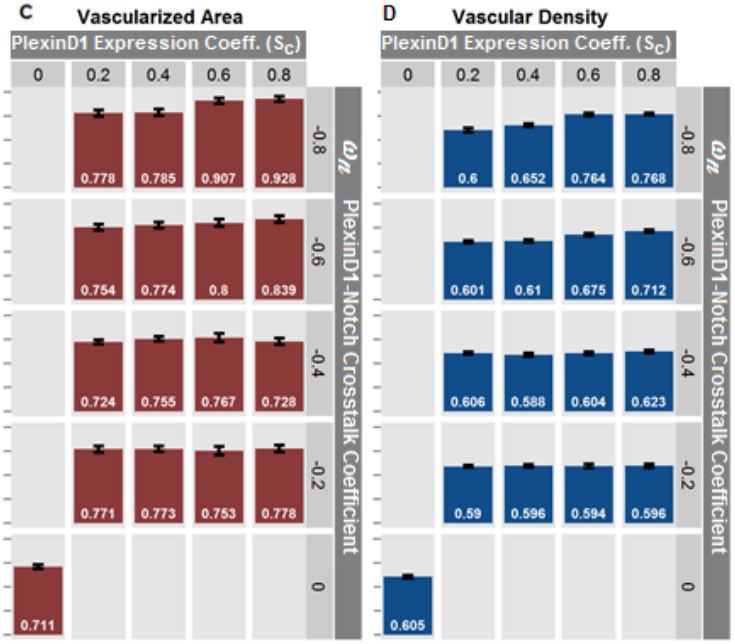

Figure 6

A. Cartoon depicting the greater VEGFR2 signaling network including PlexinD1 as modelled. The coefficient S_c and ω_n show the effect of VEGFR2 on PlexinD1 expression and the effect of PlexinD1 on Dll4/Notch signaling in Cell P.

B. A system of 3 ODEs describing the values of DLL4/Notch, activated VEGFR2, and the accessory component, Plexin-D1 in Cell P at a given time.

C. The total vascularized area as a portion of the total retinal area in simulated retinas with different coefficients controlling Plexin-D1 expression and Plexin-D1 inhibition of Notch signaling. Values represent mean+SEM of 30 simulated retinas.

D. The vessel density as area covered by endothelial cells relative to total retinal area in simulated retinas with different coefficients controlling Plexin-D1 expression and Plexin-D1 inhibition of Notch signaling. Values represent mean+SEM of 30 simulated retinas.

E. Graphical display of linear regressions of Vascularized Area (Effect Size: 0.183; $p < 0.00028$) and Vessel Density (Effect size: 0.155; $p < 0.00042$) based on Plexin-D1 expression.

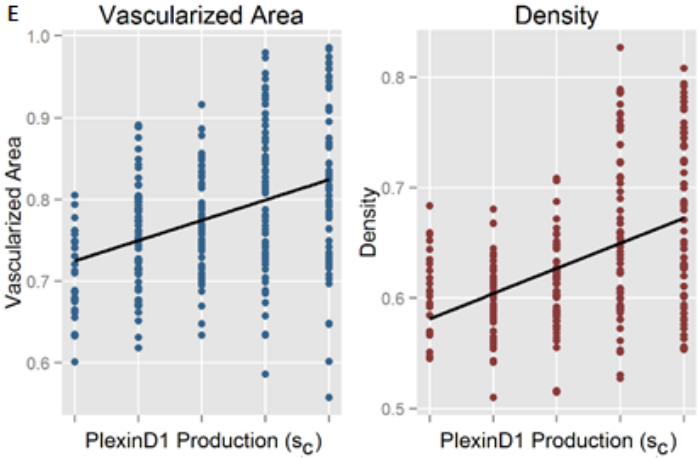

3.3.3 Plexin-D1 Deletion Increases Notch Effect on Plexus Irregularity

Kim et al. observed, *in vivo*, that Plexin-D1 deletion caused an increase in a complex vascular phenotype that they called plexus irregularity. They hypothesized that this phenotype, which they quantified as the difference between the maximum and minimum radial vascular outgrowth (Figure 3.7C), was a direct consequence of increased Notch signaling in Plexus-D1-null vasculature. To test these hypotheses, we examined how Plexin-D1 and Notch signaling affected simulated plexus irregularity. A statistical metric for variability, the Coefficient of Variation (CV), was calculated on the radial vascular extension in the simulated retinas and used to quantify plexus irregularity.

The base model, which simulates only VEGFR2 and DLL4/Notch signals, was run using Notch sensitivity coefficient (S_n) inputs from 0.2 to 1.2 in increments of 0.2, and VEGFR2 sensitivity coefficient (S_v) inputs from 0.6 to 1.2. VEGFR2 sensitivity coefficient inputs less than 0.6 were omitted because they produced stunted vascular plexuses as seen in figure 5B that are not reflective of observations from biological experiments. Each combination of coefficients was run 30 times. For reference, Figures 3.7A and 3.7B show the graphical cartoon and the ODEs that describe the VEGF-Notch signaling as modeled in this simulation. In Figure 3.7D we show the plexus irregularity as quantified by the Coefficient of Variation from each simulated retina. A simple linear regression to predict Coefficient of Variation based on the Notch sensitivity coefficient, S_n, found a significant regression relationship with an effect size of 0.602 ($p<2e\text{-}16$). These results were visualized in Figure 3.7E and indicate that each 0.2 step increase in the Notch sensitivity coefficient is associated with an increase in Coefficient of Variance of 12.04%.

Figure 3.7

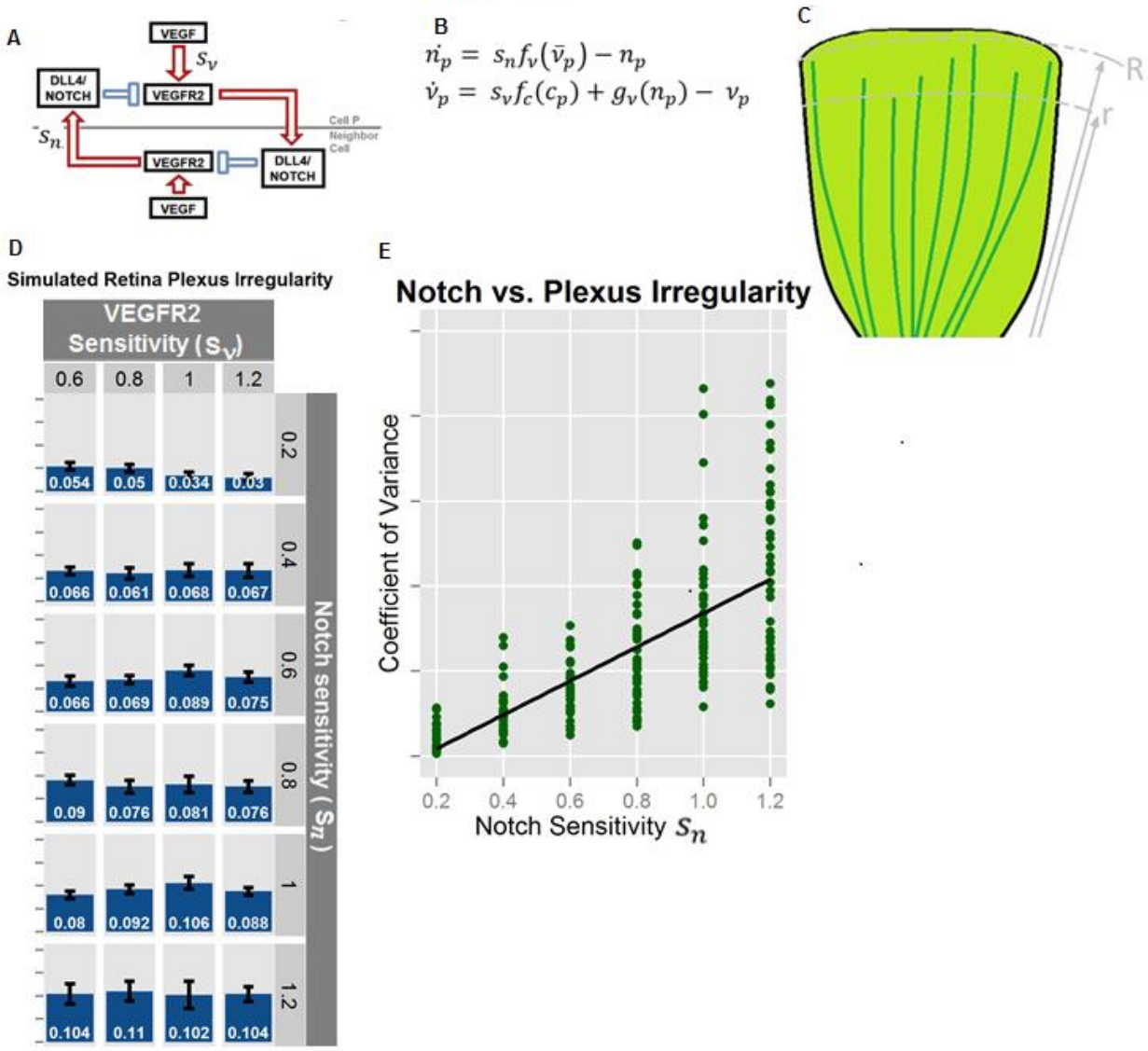

Figure 7
Notch Signaling contributes to Plexus Irregularity in Simulated Retinas
A. Cartoon depicting the VEGFR2-Notch signaling network as modelled.
B. A system of 2 ODEs describing the values of DLL4/Notch and activated VEGFR2 at a given time
C. A graphical cartoon illustrating variation in radial vasculature outgrowth.
D. The plexus irregularity of simulated retinas as quantified by the Coefficient of Variation of radial vascular outgrowth. Retinas were simulated using a range of Notch sensitivity and VEGFR2 sensitivity coefficient inputs. Values represent mean+SEM of 30 simulated retinas.
E. Graphical display of linear regression of Coefficient of Variatiion based on Notch sensitivity coefficient(Effect Size: 0.602; $p < 2e\text{-}16$).

Next we tested whether our model could predict how PlexinD1 deletion affects plexus irregularity. To do this we ran our full model with the coefficient ω_n set to -0.4 indicating a modest inhibition of DLL4/Notch signaling by PlexinD1. We set the PlexinD1 Expression coefficient (S_c) to either 0.5 or 0 indicating modest PlexinD1 expression or PlexinD1 deletion, respectively. Finally, to gather results from a wide array of conditions we used Notch sensitivity coefficient (S_n) inputs from 0.2 to 0.8 in increments of 0.2, and VEGFR2 sensitivity coefficient (S_v) inputs from 0.6 to 0.8. Each combination of coefficients was run 30 times. For reference, Figure 3.8A shows a graphical cartoon that shows the VEGF-Notch signaling as modeled in the conditions with and without PlexinD1. In Figure 3.8B we show the quantified plexus irregularity from each simulated retina. We used a multiple linear regression to understand how the presence of PlexinD1 regulated plexus irregularity. Results (displayed in table form in Figure 3.8C) indicate multiple significant relationships. The presence of PlexinD1 is associated with decreased plexus irregularity (Effect size: -0.144929, $p < 0.000914$). As before, a significant regression relationship shows that Notch sensitivity is associated with increased plexus irregularity (Effect size: 0.294, $p < 2e\text{-}16$), however a significant interaction term Sn:Plexin (Effect size: -0.21, $p < 2e\text{-}16$) indicates that the relationship between Notch signaling and Plexus irregularity is decreased in the presence of PlexinD1.

Figure 3.8

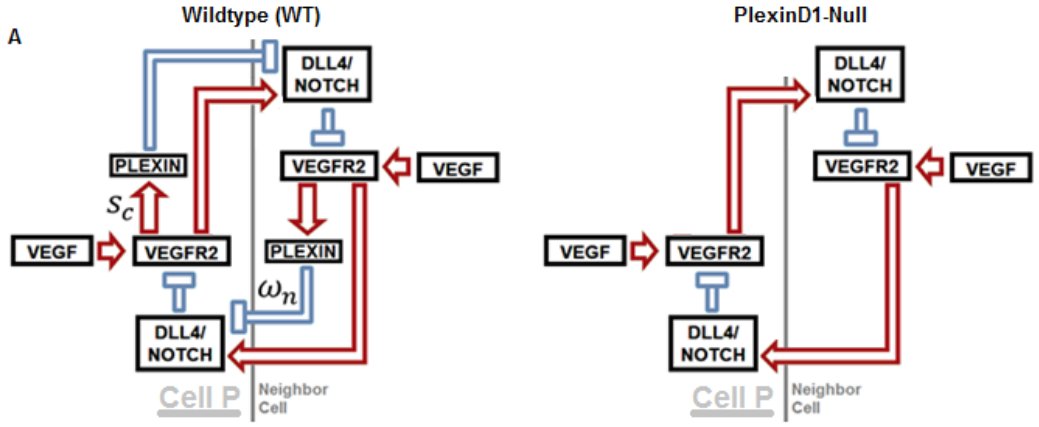

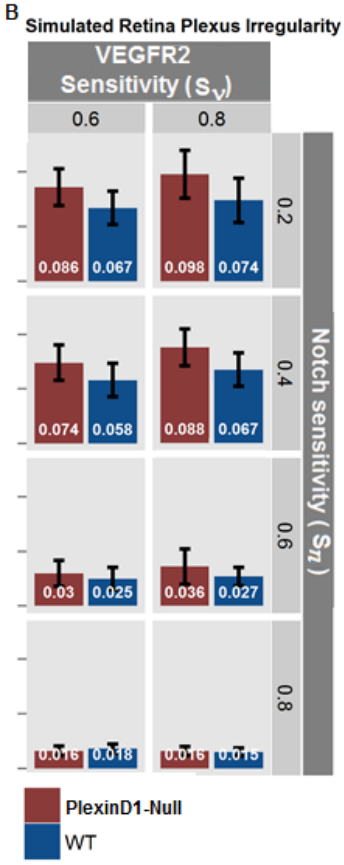

C

Multiple Linear Regression Results

	Estimate	Std. Error	t value	Pr(>|t|)
(Intercept)	0.184347	0.009544	19.316	< 2e-16 ***
Plexin	**-0.144929**	0.013497	-3.329	**0.000914** ***
s_n	**0.294160**	0.031812	9.247	**< 2e-16** ***
s_n:Plexin	**-0.210127**	0.017424	-12.059	**< 2e-16** ***

Signif. codes: 0 '***' 0.001 '**' 0.01 '*' 0.05 '.' 0.1 ' ' 1				
Residual standard error: 0.03117 on 760 degrees of freedom				
Multiple R-squared: 0.4177	Adjusted R-squared: 0.4123	F-statistic: 77.87 on 7 and 760 DF	p-value: < 2.2e-16	

Figure 8
PlexinD1 presence mitigates plexus irregularity and blunts effect of notch signaling.
A. Cartoon (Left) depicting the VEGFR2-Notch signaling network including PlexinD1. Cartoon (right) showing the PlexinD1-Null VEGFR2-Notch signaling network as modelled.
B. The plexus irregularity of simulated retinas as quantified by the Coefficient of Variation of radial vascular outgrowth. Retinas were simulated using a range of Notch sensitivity and VEGFR2 sensitivity coefficient inputs. WT retinas (Blue) were simulated with with PlexinD1 and PlexinD1-Null retinas (Red) were simulated with PlexinD1 expression set to zero. Values represent mean+SEM of 30 simulated retinas.
E. Table results of Multiple linear regression of Plexus irregularity as measured by Coefficient of Variation based on Notch Sensitivity Coefficient (Sn) and PlexinD1 presence.

3.4 Discussion and Future Directions

Using a hybrid multi-scale modeling approach, we were able to produce simulated retinas that respond to modulation of VEGFR2 or Notch signaling in predicted ways. Additionally, our model was able to incorporate published qualitative signaling information about a crosstalk partner of the VEGFR2-Notch network (PlexinD1) and predict phenotypic changes in Vessel Density, Vascularized Area, and Plexus Irregularity. This is a novel achievement in modeling of the retinal vasculature and will aid biologists in evaluating future reports of new Notch crosstalk signaling mechanisms.

A second goal in this project was to gain insight into the mechanistic causes of the complex vascular phenotype of plexus irregularity. Our results indicate that in our model, increased Notch signaling, as modeled by inputs into the Notch sensitivity coefficient, contributes to increased plexus irregularity. Results of our study also indicate that the presence of PlexinD1 decreases plexus irregularity. These results support the hypothesis put forward by Kim et al. that PlexinD1 deletion increases plexus irregularity by increasing Notch signaling. However, we also observed that PlexinD1 deletion seems to moderate the effect of notch signaling on plexin irregularity. Because PlexinD1 directly regulates notch signaling, it is difficult to understand whether deleting PlexinD1 increases plexus irregularity simply by increasing notch sensitivity or through some other intrinsic effect. Interestingly, theoretical work by Nguyen et al. indicate that nested negative feedback loops can have the effect of damping oscillation.[266] This raises the intriguing possibility that the presence of PlexinD1 as a regulatory node has an intrinsic effect on plexus irregularity – beyond the effect of simply lowering Dll4/Notch signaling.

To test this intriguing hypothesis, we must compare plexus irregularity in Wild type simulations that include PlexinD1 signaling with the plexus irregularity of PlexinD1-null simulations that have artificially lower DLL4/notch signaling. If we match the DLL4/Notch signaling between those two conditions, we can isolate the intrinsic effect of PlexinD1 as a regulatory node from its effects as a simple Notch inhibitor. To do this we need to convert the ODEs used in this project to a linear form that will allow for calculating notch compensation. Understanding how different inhibitors control complex vascular phenotypes such as plexus irregularity can help us understand how to design synergistic pharmacological strategies to meet needs such as therapeutic neovascularization.

Our modeling approach had multiple limitations. First, we did not have much quantitative signaling data from *in vivo* retinal vasculature, and the signaling data that were available did not have cellular localization. This limitation prevented quantitative derivation of the different coefficients in our model. To work around this limitation, we used a wide range of coefficient inputs whenever possible to ensure that our results were representative of a wide range of conditions. The second major limitation was the high computational load in our MATLAB models. This forced us to limit the size of our retinas to a 100 by 100 grid. This accommodation prevented direct comparison to real biological retinas, and limited our comparison to crude phenotypic descriptions such as vessel density and vascularized area.

3.5 Appendix I

The tip/stalk cell density is represented by the function $r(x, y, t)$ at the grid point (x, y), and time t, and its time rate of change depends on three terms describing respectively the diffusion, chemotaxis and tip kinetics according to the following partial differential equation:

$$\frac{\partial r}{\partial t} = \delta_n \Delta r - \lambda_V \nabla(r \nabla c_V) + f(r, s, c_V, c_D). \qquad (1)$$

We assume that vessel branching is only dictated by the movement of tip cells that are positioned at the end of the sprout. We also assume that tip cells do not reproduce or die significantly between day 5 and day 7 of the postnatal retinal development. Due to the short period of time elapsed, the haptotactic response to the cellular fibronectin concentration gradient is neglected, and the matrix degrading enzymes are assumed to have a minimal effect on the structure of ECM and EC density; Therefore the terms that are governing their action are ignored in this study. The variation of the cell density over time is assumed to depend only on random migration and the chemotactic response to VEGF concentration gradient. Using non-dimensional parameters equation (1) reduces to:

$$\frac{\partial r}{\partial t} = D_r \Delta r - \nabla\left(\frac{x_c}{1 + \alpha_c c} r \nabla \mathrm{c}\right) \qquad (2)$$

where the function $c(x, y, t)$ measures VEGF concentration at (x, y) and time t. The constant D_r represents the cell random motility coefficient, and the parameters x_c and

α_c are governing the chemotaxis effect on the cell. Their values are given in Watson et al.

3.7 Appendix II

$$f_*(x) = \frac{x^{k_*}}{a_* + x^{k_*}} \tag{11}$$

$$g_*(x) = \frac{1}{1 + b_* x^{h_*}}$$

Where the first function f expresses activation and the second function g represents inhibition. The star symbol denotes respectively c, n, α and ν indices. Most of the values of the parameters a_*, b_*, k_*, h_* are taken from Collier's model, where the argument x represents successively c_p, n_p, α_p and ν_p.

Chapter 4

THE α2β1 INTEGRIN MODULATES SPROUTING ANGIOGENESIS VIA MULTIPLE LEVELS OF CROSSTALK WITH THE ENDOTHELIAL NOTCH NETWORK

4.1 Abstract

Our group has recently observed delayed radial vascular outgrowth during postnatal development of the α2-null retina. Intriguingly, this phenotype runs counter to previous reports of enhanced angiogenesis in α2-null mice in tumor, obese or wound-healing microenvironments. To investigate this unique finding we conducted a careful morphological and molecular characterization of the α2-null retinal vasculature during postnatal retinal development. We discovered that despite the established role of α2β1 integrin in upregulating DLL4 expression, the α2β1 integrin-deletion resulted in vascular patterning defects characteristic of transgenic notch network mutants with increased rather than decreased DLL4 expression and Notch signaling. Using a combination of *in vitro* experiments and *in silico* computational modeling we suggest that the morphological and signaling features of the α2-null vasculature are caused by diminished VEGFR2 activation as a result of a loss of α2β1 integrin-mediated VEGFR1 repression and/or filopodia function. The involvement of α2β1 integrin in VEGFR1 repression and filopodia function had been previously reported, but had not before been considered as mechanisms for increased Notch signaling.

4.2 Introduction

Angiogenesis is coordinated by a complex interplay between endothelial cells and their microenvironment. Integrins, obligate α/β heterodimers that serve as cell

surface receptors for extracellular matrix ligands, mediate this process.[248] Numerous integrins including αvβ3, αvβ5, α4β1, α5β1, and α1β1 integrins have been implicated in regulation of angiogenesis.[267–272]

The role of the α2β1 integrin, a collagen and laminin receptor, in angiogenesis has been highly controversial. Several labs, including our own, reported that genetically modified α2β1 integrin-null mice exhibit normal developmental angiogenesis while increased neoangiogenesis was found in wound healing and diet-induced obesity models.[273,274] Similarly, we demonstrated that α2β1 integrin-deletion increases tumor angiogenesis in a growth factor-dependent manner via modulation of VEGFR-1 signaling.[275] The anti-proliferative role for endothelial cell-specific, α2β1 integrin was supported by in vitro experiments showing that α2β1 integrin engagement by laminin promotes endothelial cell cycle arrest and quiescence.[276] In contrast, directly targeting the α2β1 integrin using small molecule inhibitors (SMI) blocked both endothelial tube formation in vitro and sprouting angiogenesis in zebrafish.[277] That line of inquiry has resulted in the deployment of an α2β1 integrin inhibitor in phase II clinical trials as an adjuvant anti-angiogenesis cancer therapy.[278–280] A deeper understanding for the role of the α2β1 integrin in angiogenesis that integrates the paradoxical data from transgenic and inhibitor experiments offers potential advances for novel therapeutics for cancer and proliferative retinopathies. Additionally, insight into the molecular underpinnings for the ‘α2-null’ vascular phenotype is in itself of significant interest, as pharmacological recapitulation of this phenotype would be valuable in the wound-healing and obese microenvironments.

The emerging understanding of notch signaling as a master regulator of angiogenesis offers a fresh perspective for interpreting the role of α2β1 integrin in

angiogenesis. The notch pathway is a highly conserved signaling system that coordinates sprouting angiogenesis by organizing endothelial cells into migratory 'tip' and proliferative 'stalk' cell conformations with differential capacity to respond to VEGF stimulation. Estrach et al. report that, in an in vitro context, α2β1 integrin-mediated laminin signaling is necessary but not sufficient for induction of the tip cell determinant, Dll4.[280] The *in vivo* signaling picture appears to be more complex; microarray analysis of 'tip cells' isolated from retinas via laser microdissection shows increased α2β1 integrin gene expression.[259,278,281] This supports a role for the integrin in tip cell determination. However, DLL4 deletion has proven to be embryonic lethal whereas α2β1 integrin-deletion has only minor differences in vascular development. This key distinction suggests that perhaps the α2β1-integrin role in tip cell determination is more complex than the reported 'necessary but not sufficient for DLL4 expression.' Notch signaling in α2β1 integrin-deficient mouse model has not yet been investigated.

The murine postnatal retinal development model has been the primary system for advancing our understanding of endothelial notch signaling in sprouting angiogenesis. Work by Betsholtz, Eichmann, Wiegand, and others in this system was critical in establishing our current 'tip-stalk' paradigm for notch regulation of sprouting angiogenesis.[282–284] A significant challenge of the retina model is the technical difficulty of interventional experiments. Recently *in silico* computational models based on *in vitro* experimental data have emerged as an alternative approach for providing mechanistic insight into complex angiogenesis phenomena. For example, using *in vitro* experimental data to simulate feedback between VEGF and notch signaling, the initial sprouting process has been accurately replicated *in silico*, indicating that VEGF/notch regulation is sufficient to pattern tip cell selection, sprout initiation and branching.[263,281]

In the current study we use *in vitro, in vivo, and in silico* approaches. Our group has recently observed a statistically significant delay in radial vascular outgrowth as characterized by significantly increased total avascular area of the retina in α2-null compared to wild type mice at P5 and P7.[265] First we follow up on this observation with a detailed characterization of *in vivo* postnatal retinal development and notch signaling in α2-null mice. Second we use *in vitro* notch signaling experiments and an *in silico* model of notch-mediated sprouting angiogenesis to qualitatively and quantitatively test our understanding of α2β1 integrin-notch crosstalk in retinal angiogenesis.

4.3. Materials and Methods

4.3.1 Animals

Generation of α2β1 integrin-deficient mice on a C57BL6/ was previously described.[273] The mice used in these experiments were 99% genetically C57BL/6. Animals were housed in pathogen-free conditions at Vanderbilt University Medical Center and all experiments were conducted in compliance with institutional animal care and use committee regulations. All animals were appropriately age-matched.

Wild type (wild type) and α2β1 integrin-deficient animals were harvested at P5 and P7. For whole mount analysis, retinas were dissected and permeabilized as described before.[265] Careful morphological analysis was conducted and phenotypic differences were quantitated by measuring density and vessel irregularity at the vascular front. In each retina, four 20x fields were randomly chosen, each coming from a ‘different lobe’ of the whole mount. These fields were quantified for density by measuring vessel area / total area of the vascularized region. Morphological analysis/quantitation was done in a blinded manner separate from retina

isolation/random field selection. Vessel irregularity was measured as defined by Kim et al. as the vertical distance between the farthest projection and the shortest growth in vessel area.[260] For both metrics, values for the four measured areas per retina were averaged. Example measurements are included in the supplement.

4.3.2 Endothelial cell isolation and culture

Primary endothelial cells (ECs) were prepared as described.[273] Briefly, the lung vasculature was perfused with PBS/2.5mM EDTA, then 0.25% trypsin/2.5 mM EDTA. ECs were recovered, cultured in endothelial cell growth media, and when greater than 90% pure, used for experiments. For *in vitro* analysis, Notch-ligand coated plates were generated as described.[285] ECs were plated on 2.5µg/mL mouse Dll4-His (R&D Systems #1389-D4), rat Jag1Fc (R&D Systems #599-JG), or control 0.2% gelatin for 48 hours. The γ-secretase inhibitor (DAPT) (10µM) (Sigma Aldrich, Inc. D5492) was added for 8 hours to inhibit Notch signaling.

4.3.3 qPCR analysis

Total RNA was recovered following manufacturer's protocol. Quantitative PCR (qPCR) was performed on an Applied Biosystems 7900HT qPCR machine using a 384plate system, as per manufacture's protocol. Relative fold change in gene expression was completed using the comparative $2^{-\Delta\Delta CT}$ method (including the amplification efficiency correction factor). Relative RNA quantities were normalized to either HPRT, RPP30, or TBP, as determined by NormFinder to represent the optimum normalization gene for the set of samples analyzed. Primer pairs for mRNA expression (Supplemental Table 3) analysis were designed using Primer Express 3.0™ (Applied

Biosystems) and published murine DNA and mRNA sequences (UCSC Genome Bioinformatics).

4.3.4 Microscopy

Immunofluorescence microscopy was used for identification and quantitation of DLL4, VEGFR2, VEGFR1 and α2β1 with antibodies listed in Supplemental Methods Table 2. Immunofluorescence images were captured with a Nikon Eclipse 80i fluorescence microscope. Quantitation was performed using ImageJ (NIH). Confocal microscopy of retinal whole mounts was conducted using a Zeiss LSM 710 META Inverted Confocal Microscope (Vanderbilt Cell Imaging Shared Resource).

4.3.5 Computational Modeling

Computational modeling was done in MATLAB software.

4.3.5.1 Model Construction – Conceptual Summary

Our modeling approach is explained in detail in Chapter 3. Briefly, we have adapted a model of VEGF-induced lateral inhibition developed by Collier et al., to describe VEGFR2-Notch signaling in endothelial cells.[264] Output of this model can be used to determine 'Tip' and 'Stalk' cell fates for an individual cell exposed to a given growth factor environment. These tip and stalk cell fate decisions are then used in a tissue level model for retinal vasculature development adapted from Watson et al.[262] By nesting a model of endothelial cell notch signaling within a discretized model for retinal vascular development, we can conduct simulated experiments to see how different changes to the greater VEGFR2-Notch signaling network may affect retinal vasculature phenotypes.

4.3.5.2 Modeling of Endothelial cell notch signaling.

In chapter 3 we introduced a set of ordinary differential equations (ODEs), which describe VEGFR2 activation ($\dot{v}_p$), DLL4/Notch signaling signal ($\dot{n}_p$), and crosstalk from a candidate angiogenic signaling molecule ($\dot{\alpha}_p$) in cell p at a given time.

$$\begin{aligned} \dot{n_p} &= \tau_n[s_n f_v(\bar{v}_p)\left(1+\omega_n f_b(\bar{\alpha}_p)\right) - n_p] \\ \dot{v_p} &= \tau_v[s_v f_c(c_p)\left(1+s_a f_\alpha(\alpha_p)\right) + g_v(n_p) - v_p\,] \\ \dot{\alpha_p} &= \tau_\alpha[s_c f_v(v_p\,)\left(1+s_\alpha g_\alpha(n_p)\right) - \alpha_p\,] \end{aligned} \qquad (1)$$

Within this system of ODEs, the coefficients S_n, S_v, and S_c describe the expression level of their corresponding term. Specifically, S_n is a sensitivity coefficient that describes the rate at which VEGFR2 activation leads to DLL4/Notch signaling. Similarly, S_v is a sensitivity coefficient describing how VEGF levels (C_p) lead to VEGFR2 activation. The user provides values for these coefficients before solving the system of differential equations.

The coefficients S_c and S_α describe how activated VEGFR2 and Notch, respectively, lead to the production of the candidate component ($\dot{\alpha_p}$) in cell P. The coefficients ω_n and S_a describe how the candidate component (α_p) affects the rate of production of DLL4/Notch signal and activated VEGFR2, respectively, in cell P. Together these coefficients can describe the many potential signaling relationships that comprise crosstalk between the candidate accessory components and the core VEGF-Notch signaling system.

4.3.5.3 Retina Model

The retinal vascular development model simulates sprouting angiogenesis between p5 and p7 using a discrete random walk based simulation of cell migration over a grid, which we superimpose over the retina. In the present

study we considered a modified version of the model presented by Watson et al.[261,262] For simplicity, we discarded the simulation of astrocyte development and assumed a uniform initial distribution of VEGF growth factor. As our model only covered a two-day period of sprouting angiogenesis, this simplification does not cause meaningful deviation from the biological situation of the retina It is increasingly clear that sprouting angiogenesis during retinal development was driven, not by secreted VEGF, but rather by matrix entrapped VEGFA laid out by advancing astrocytes.[279] Between P5 and P7, the distance between the front of the advancing vasculature and the advancing astrocyte network did not change appreciably.

Our major modification to Watson et al.s' work was the replacement of their rules-based vessel branching mechanism with a dynamic DLL4/Notch signaling mechanism that was described above. In our system, the cell-signaling model (described above in equation 1) allows endothelial cells to dynamically switch between 'tip' and 'stalk' cell fates based on the signaling and growth factor environment. The resulting model allows us to examine the effect of modulating DLL4/Notch expression on overall capillary network development. The details of our model for retinal vascular development are described in the previous chapter.

4.4 Results

4.4.1 Vascular patterning defects in α2-null retinas

We have previously reported that α2β1 integrin-deletion caused delayed retinal vascular outgrowth at P5 and P7. To follow up on this finding we conducted careful morphological analysis of vessel patterning at these time points, as shown in representative images of wild type and α2-null p7 retinas (Figure 4.1A). The α2-null vascular plexus demonstrated decreased density (46% compared to 54% for the wild type, P=0.0004) and increased irregularity at the vascular front (Figure 4.1B).

Figure 4.1

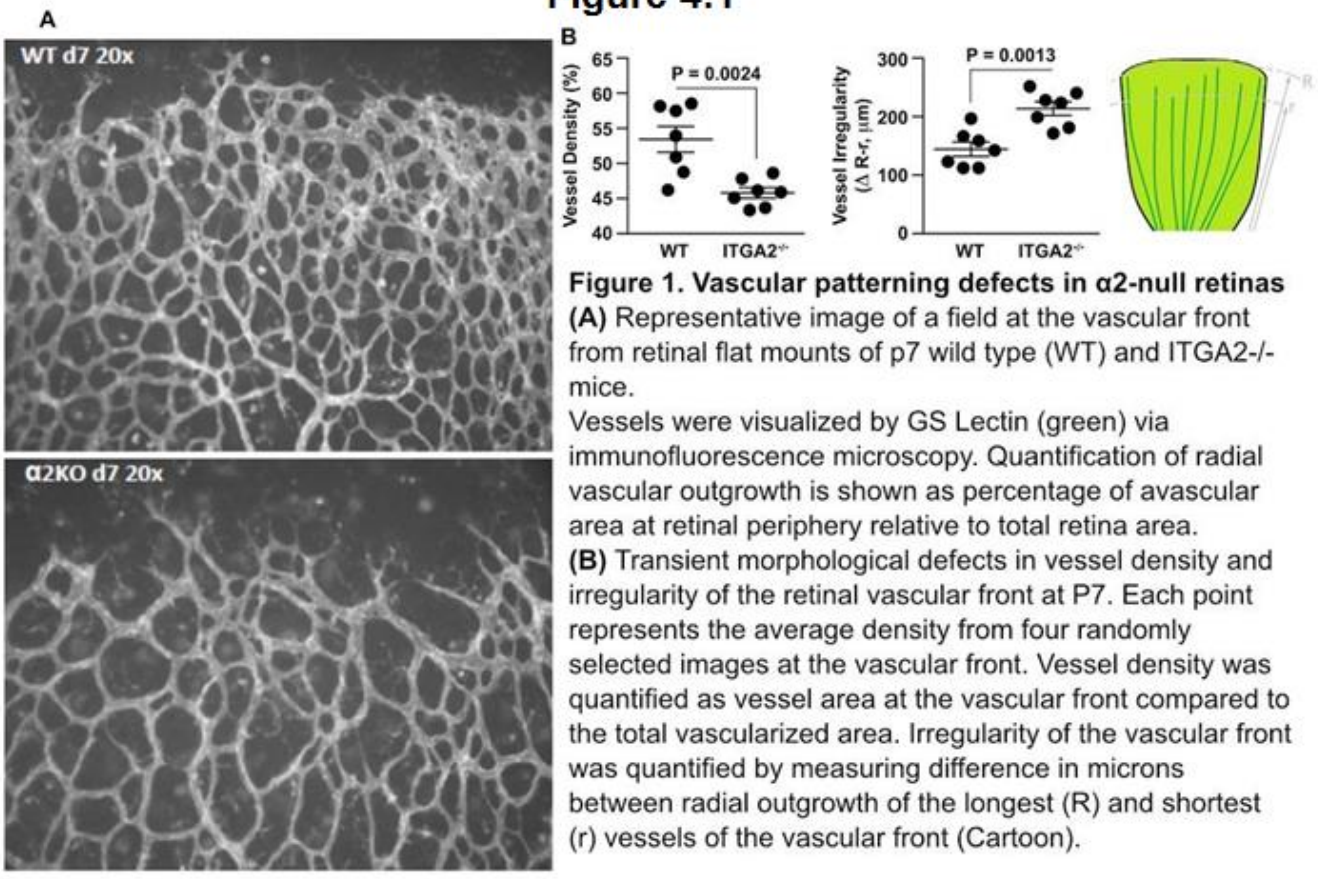

Figure 1. Vascular patterning defects in α2-null retinas
(A) Representative image of a field at the vascular front from retinal flat mounts of p7 wild type (WT) and ITGA2-/- mice.
Vessels were visualized by GS Lectin (green) via immunofluorescence microscopy. Quantification of radial vascular outgrowth is shown as percentage of avascular area at retinal periphery relative to total retina area.
(B) Transient morphological defects in vessel density and irregularity of the retinal vascular front at P7. Each point represents the average density from four randomly selected images at the vascular front. Vessel density was quantified as vessel area at the vascular front compared to the total vascularized area. Irregularity of the vascular front was quantified by measuring difference in microns between radial outgrowth of the longest (R) and shortest (r) vessels of the vascular front (Cartoon).

Measurement of vessel irregularity was defined as the distance between the farthest and shallowest vascular extension at the vascular front, as reported by Kim et al. Using

this metric, vessel irregularity in the α2-null was significantly greater than in the wild type retina (Figure 4.1B). These data suggest that α2β1 integrin expression contributes to normal retinal angiogenesis.

Figure 4.2 Comparison of Retinal Patterning Defects in Notch Pathway Mutants

Genotype	Branching	Growth Delay	Regularity of Vascular Plexus	Plexus Density	Tip cells	Dll4	Notch signaling
Dll4+/-	Higher	Not Reported	unknown	Higher	More	Less	Decreased
DAPT	Higher	NA	NA	Higher	More	More	Blocked
Lama4 -/-	Higher	Not Reported	unknown	Higher	More	Less	Decreased
Sema 3E -/-	Lower	Not Reported	More Irregular	Lower	Less	More	Increased
PlexinD1 -/-	Lower	Not Reported	More Irregular	Lower	Less	More	Increased
Jag1iΔEC	Lower	Slower Growth	unknown	Lower	Less	More	Increased
Itga2-/-	No change	Slower Growth	More Irregular	Lower	?	?	?

A literature search revealed that the morphological defects observed in the α2-null vasculature (increased vessel irregularity and decreased vascular density) are changes that are characteristic of transgenic mutants with increased Notch signaling (Figure 4.2). Defects in the frequency of vessel branching are common in notch pathway mutants, but we observed no statistically significant differences in this area.

4.4.2 Increased notch signaling in α2-null background

Based on prior literature, which established that α2-integrin promotes DLL4 expression and Notch signaling, we initially hypothesized that α2-null retinas would show decreased notch signaling. However morphological characterization demonstrated that the vascular patterning of α2-null retinas was more closely aligned with transgenic mice characterized by increased notch signaling. To test the possibility that notch signaling was increased in α2-null retinas, we used immunofluorescence microscopy to evaluate expression of Dll4 in wild type and a2-null retinas *in vivo*. Dll4 protein was

expressed at significantly elevated levels by endothelial cells in α2-null compared to wild type mice (Figure 4.3A). To assess whether the increased Dll4 expression in the α2-null retinal vasculature represented a cell-intrinsic signaling property of α2-null endothelial cells, primary endothelial cells (ECs) from wild type and α2-null animals were stimulated in vitro with immobilized notch-stimulating, murine Dll4-His, Notch-inhibiting rat Jag1-Fc, or control. As expected, expression of Dll4 mRNA was significantly decreased in both wild type and α2-null ECs when stimulated with DLL4 ligand, compared to control. However, in both control and DLL4-stimulated conditions, Dll4 mRNA expression was significantly greater in α2-null ECs compared to wild type counterparts (Figure 4.3B).

Figure 4.3

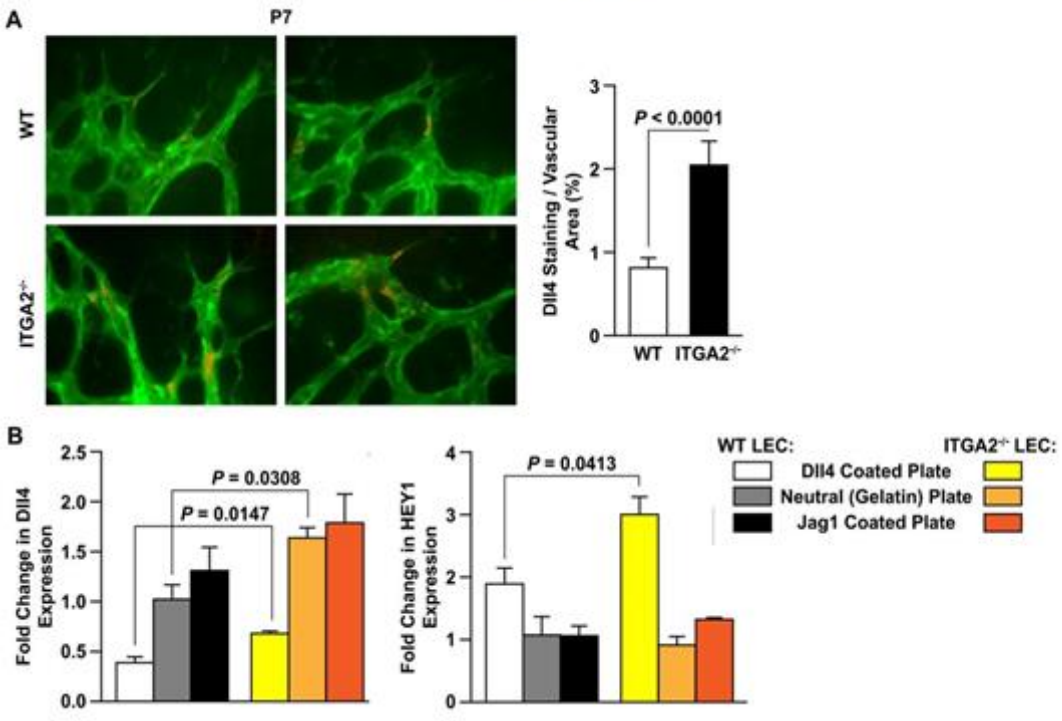

Figure 3 α2β1 deletion dysregulates endothelial notch signaling.
(A) Immunoflourescence images with GS Lectin (green) and DLL4 (red). Quantification of DLL4 stain given in Mean+-SD and reflects values from 4 or more images 5 separate retinas.
(B) Fold change in mRNA expression for Dll4 and Hey1 in primary lung endothelial cells grown on notch-ligand coated plates, as determined by qRT-PCR. Values are normalized to HPRT or RPP30 and displayed relative to WT LEC grown on Neutral plates as Mean+-SEM.
All results **(A, B)** are representative of three or more similar experiments.

Under conditions of notch inhibition by JAG1, Dll4 expression was slightly, but not significantly, greater in α2-null ECs. Hey1, a transcriptional repressor and downstream target of notch, was induced in both wild type and α2-null ECs incubated with the notch-activating Dll4 ligand. However, Hey1 mRNA expression was significantly increased in the α2-null ECs compared to wild type (Figure 4.3B). Together, these data indicate enhanced notch signaling in α2-null LECs. Similar results were obtained with immortalized retinal endothelial cells.

4.4.3 α2β1 integrin supports Dll4 induction in murine retinal endothelium

Contrary to our initial hypothesis, α2-null retinas and primary endothelial cells demonstrated increased notch signaling. This unexpected result required us to reexamine our a priori expectations. Estrach et al. reported that adhesion of primary human endothelial cells to laminin-111 triggered Dll4 expression, and that siRNA-mediated knockdown of α2β1 integrin abolished Dll4 induction.[280] To determine whether these findings were applicable to murine cells, we analyzed α2β1 integrin regulation of DLL4 in primary retinal endothelial cells and the retinal vasculature.

To test the effect of α2β1 integrin on DLL4 induction we used In-cell western analysis to compare VEGFA-induced DLL4 expression in wild type immortalized RECs on laminin and BSA-coated wells (Figure 4.4A). Our data indicate significantly higher VEGFA-induced DLL4 expression in laminin-bound RECs, which confirmed the findings of Estrach et al. We also examined α2β1 integrin localization in primary retinal endothelial cells and the retinal vasculature. Estrach et al. report α2β1integrin expression in tip cell filopodia in embryoid bodies using a 3D matrigel sprouting assay.[280] Similarly, microarray results from del Toro et al. showed enriched α2 integrin

subunit gene expression in retinal tip cells.[286] In immortalized primary retinal endothelial cells grown on matrigel-coated surfaces, we also observed strong α2β1 integrin expression in filopodia (Figure 4.4B). In the *in vivo* setting, we were unable to visualize strong α2β1integrin expression in cells with classic tip morphology; however we observed intense integrin staining in protruding structures extending from the superficial vascular plexus toward the intermediate and deep vascular plexuses (Figure 4.4C and supplemental image). If these protrusions are interpreted as early-stage tip cells invading along the z-dimension, then this matches both the microarray results reported by del Toro et al. and the *in vitro* data of Estrach et al. Together, these findings suggest that the previously reported role for the α2β1 integrin in promoting VEGF-mediated DLL4 expression and tip cell induction accurately portrays one element of α2β1 integrin crosstalk with the Notch network in murine endothelial cells.

So, if α2β1 integrin indeed promotes the upregulation of DLL4, how then does α2β1 integrin deletion result in increased expression of DLL4 and enhanced notch signaling? One possibility is the presence of compensatory changes in notch signaling components upstream of DLL4 expression. We have previously reported that VEGFA growth factor expression is unchanged between wild type and α2-null retinas during development. We used immunofluorescence analysis to examine α2-null retinas for potential changes in growth factor receptor expression upstream of DLL4. There was statistically significantly increased protein expression of VEGFR1, but not VEGFR2, in the vasculature of α2-null retinas when compared to wild type mice (Figure 4.4D-E).

Figure 4.4 α2β1 Integrin-Notch Crosstalk. (Figure on following page)
(A) In-Cell Western analysis of VEGFA-induced Dll4 expression in Immortal Retinal Endothelial Cells on Laminin- and BSA-coated wells of a 96 well plate
(B) A representative immunofluorescence image of wild type immortalized REC grown on matrigel coated glass coverslip. Stained with Phalloidin-488 (Green), anti-α2 integrin antibodies (red) and DAPI (blue)
(C) reconstruction of confocal z-stack using anti-CD31 (green) and anti-α2 integrin antibodies (red)
(D) Representative immunofluorescence image and quantification of retinal whole mounts of age-matched wild type and ITGA2-/- mice at P7 labeled with GS Lectin (green) and VEGFR2 (red).
(E) Representative immunofluorescence image and quantification of retinal whole mounts of age-matched wild type and ITGA2-/- mice at P7 labeled with GS Lectin (green) and VEGFR1 (red).
Quantification of VEGFR2 and VEGFR1 stain reflects values from 4 or more images from 5 separate retinas (mean+-SEM).

Figure 4.4

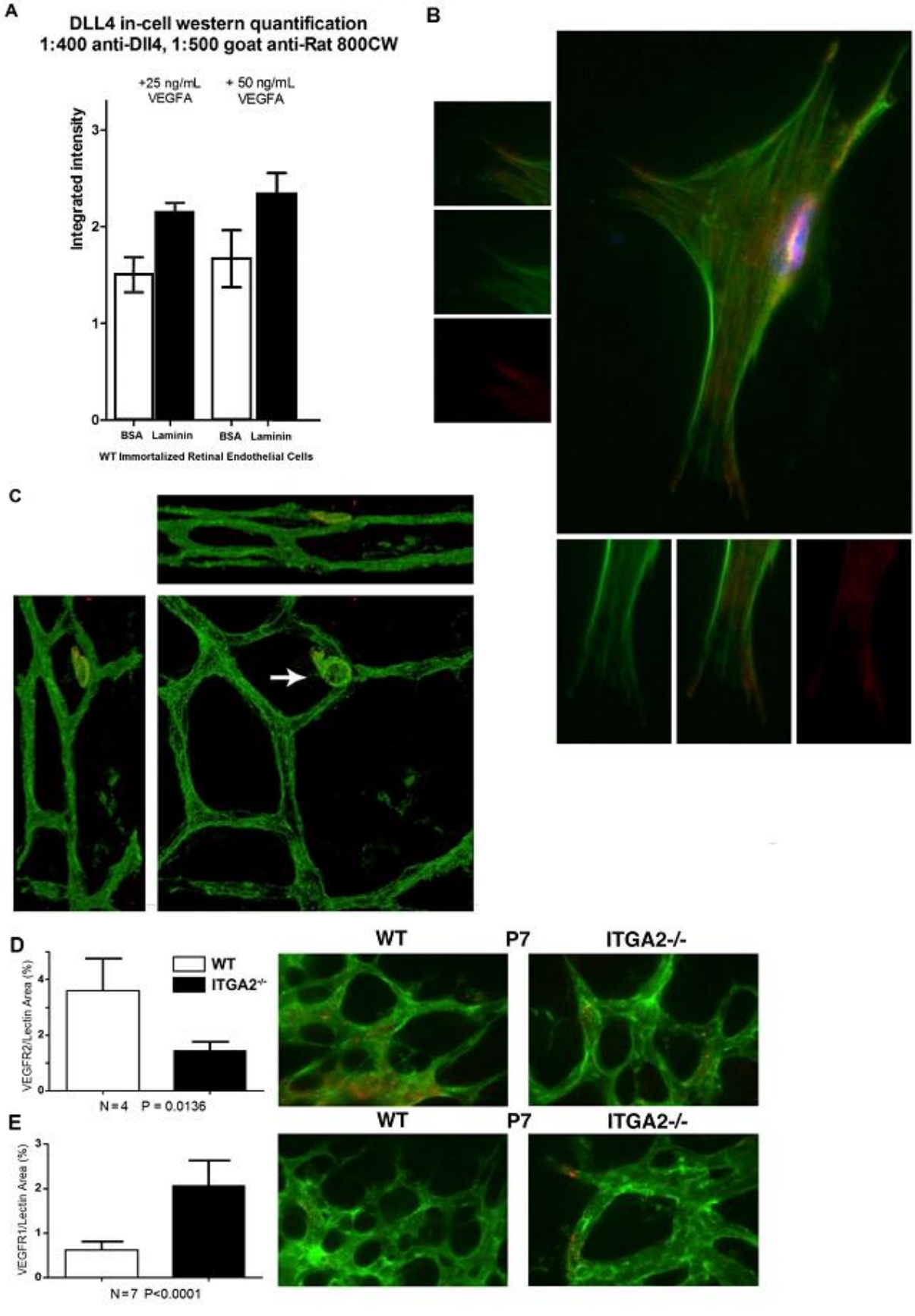
A
DLL4 in-cell western quantification
1:400 anti-Dll4, 1:500 goat anti-Rat 800CW
+25 ng/mL VEGFA
+ 50 ng/mL VEGFA
Integrated intensity
0
1
2
3
BSA
Laminin
BSA
Laminin
WT Immortalized Retinal Endothelial Cells
B
C
D
WT
ITGA2-/-
VEGFR2/Lectin Area (%)
0
2
4
N=4 P=0.0136
P7
WT
ITGA2-/-
E
VEGFR1/Lectin Area (%)
0
1
2
3
N=7 P<0.0001
P7
WT
ITGA2-/-

4.4.4 Computational Modeling of α2β1 integrin-notch crosstalk

Despite evidence that the α2β1 integrin has an important role in supporting DLL4 expression and endothelial notch signaling, we observe enhanced Notch signaling and a vascular morphology consistent with upregulated Notch signaling in α2-null retinas. Our group has previously reported that α2β1 integrin specifically represses VEGFR1 expression. This raises the possibility that α2β1 integrin deletion causes changes in VEGF receptor composition upstream of DLL4 that ultimately result in an enhanced Notch phenotype. In chapter 3 we described a hybrid multiscale model that can predict how modulation of the VEGFR2-Notch signaling system by outside angiogenic signaling molecules can cause specific morphological changes to the developing murine retinal vasculature. Here we use this model as a platform to evaluate whether our proposed mechanism for α2β1-Notch crosstalk is compatible with the enhanced Notch phenotype of α2-null retinas.

To test this hypothesis, we simulated murine retinal vascular development with and without α2β1 integrin under several scenarios. We tested (1) what we term the 'Established molecular model' in which α2β1 integrin only supports DLL4 expression, (2) an α2-null retina in which there is no expression of α2β1 integrin, and (3), what we call the 'alternate hypothesis' in which α2β1 integrin not only supports DLL4 expression but also negatively regulates VEGFR2 activation. Graphical cartoons depicting these three signaling conditions are shown in Figure 4.5A. The system of ODEs used to model each of these signaling relationships is shown in Figure 4.5B.

First we tested whether there were any VEGFR2 or Notch signaling conditions under the 'Established model' in which loss of α2β1-notch crosstalk could result in an enhanced Notch signaling phenotype. We ran wildtype and α2-null simulations under

the established model using S_n and S_v coefficients ranging from 0.2 to 1.2 each. Each combination of coefficients was run 30 times. As discussed in the model overview, S_n is a sensitivity coefficient that describes the rate at which VEGFR2 activation leads to DLL4/Notch signaling. Similarly, S_v, is a sensitivity coefficient describing how VEGF levels lead to VEGFR2 activation. The coefficient S_c describes the rate of α2β1 production, and the coefficient ω_n describes how α2β1 supports DLL4 expression. In Figure 4.5C, results of this simulation are displayed as vessel density, quantitated as area covered by endothelial cells relative to total retinal area in simulated retinas. Values represent Mean+SEM of 30 simulated retinas. Under conditions of weak VEGFR2 activation and weak Notch signaling, there is no statistically significant difference in vessel density between wildtype and α2-null simulated retinas (marked with an asterisk). In all other conditions, α2-null simulated retinas had increased vessel density compared to wildtype counterparts. This result is incongruous with the biologically observed results.

Next we tested whether, under the 'established model', there was any level of α2β1 integrin expression or signaling in which the presence of α2β1 integrin lowered vessel density. To accomplish this, we ran Wildtype (blue) and α2-null (red) simulations under the 'old hypothesis' model using S_c inputs ranging from 0.2 to 0.8 and ω_n inputs ranging from 0.2 to 0.8. In Figure 4.5D, the vessel density of the simulated retinas from this trial are displayed. Values represent Mean+SEM of 30 simulated retinas. No combination of coefficients caused the presence of α2β1 integrin to decrease vessel density. Together with the results from 5C, these results show that the 'established model' for α2β1 integrin crosstalk with Notch signaling is incomplete and does not fit the observed biological data.

Next we tested whether the alternative hypothesis, which incorporates α2β1 integrin-mediated activation of VEGFR2 (via repression of VEGFR1 expression) can produce conditions in which the presence of α2β1 integrin decreases VEGFR2 expression. We ran Wildtype (blue) and α2-null (red) simulations under the 'old hypothesis' model using S_α inputs ranging from 0.2 to 0.8 and ω_n inputs ranging from 0.2 to 0.8. Figure 4.5E shows the results of this simulation in terms of vessel density of simulated retinas. Values represent Mean+SEM of 30 simulated retinas. The results show that the VEGFR2 activating effect and the DLL4 upregulating effects of the α2β1 integrin are in opposition. If the DLL4 upregulating effect of the integrin is higher, then the presence of α2β1 integrin causes decreased vessel density (see bottom left corner of Figure 4.5E). If the VEGFR2 activating effect of the α2β1 integrin is more significant, then the presence of α2β1 integrin causes increased vessel density (see top right corner of Figure 4.5E) – what we observe in the developing murine retinal vasculature.

The developing retinal vasculature is a low VEGF setting compared to other vascular microenvironments. As mentioned in the introduction, although the α2β1integrin deletion is associated with decreased angiogenesis in the developing retina, it is associated with increased angiogenesis in higher VEGF settings such as the obese and wound-healing microenvironments. We ran Wildtype (blue) and α2-null (red) simulations under the 'alternative hypothesis' model in a range of VEGF concentrations (from 0.2 to 1.2). The vessel densities of the simulated retinas are displayed in Figure 4.5F. Values represent mean+SEM of 10 simulated retinas. At lower VEGF concentrations, simulated α2-null retinas have decreased vessel density compared to simulated WT retinas. At high VEGF concentrations, the α2-null condition has higher vessel density. (Figure 4.5).

Figure 4.5

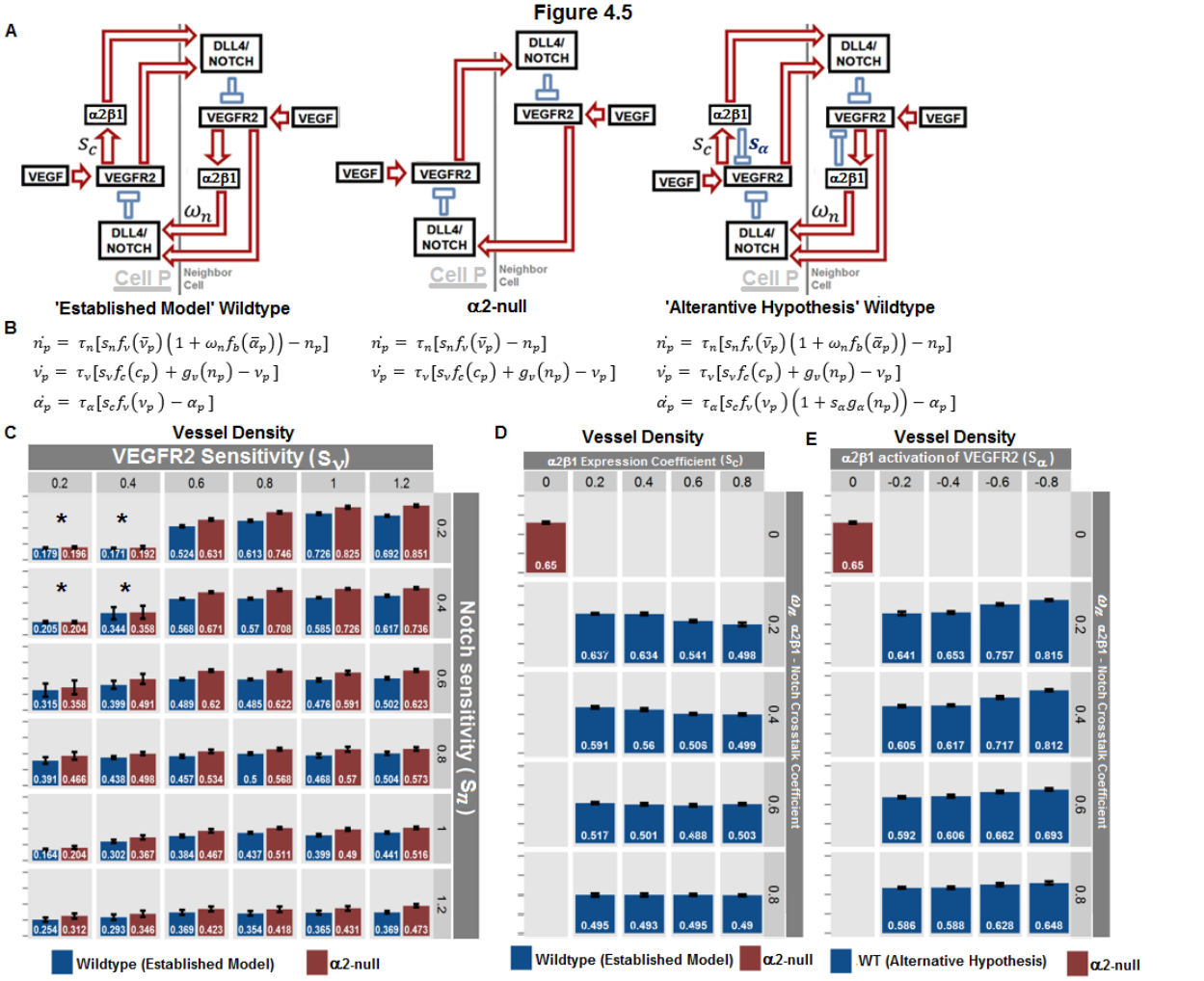

Figure 5. Computational modeling of α2β1-Notch Crosstalk Mechanism

A. Cartoon representation of α2β1-Notch Crosstalk signaling as modelled. (Left) Depicts the "Old Hypothesis" where the role of α2β1 integrin is only in supporting DLL4 expression. (Middle) is the α2-null signaling as modelled. (Right) Depicts the "Alt Hypothesis where the role of α2β1 integrin is in both supporting DLL4 expression and in downregulating VEGFR2 activation.

B. The set of ODEs used for simulating each proposed signaling scenario.

Simulating Established Hypothesis predicts incongrous vascular phenotype regardless of conditions

C. Vessel density as quantitated as area covered by endothelial cells relative to total retinal area in simulated Retinas. Simulations used established model and used the indicated range of coefficients controlling Notch and VEGFR2 signaling. Values represent Mean+SEM of 30 simulated retinas.

D. Vessel density in simulated retinas from established model. Simulations used the indicated range of coefficients controlling α2β1-DLL4 signaling and α2β1 integrin expression. Values represent Mean+SEM of 30 simulated retinas.

Modeling of Alt. hypothesis suggests that in low VEGF settings or with high levels of α2β1-mediated VEGFR2 repression, α2-null retinas have lower vessel density than Wildtype.

E. Vessel density in simulated retinas from Alt. hypothesis model. Simulations used the indicated range of coefficients controlling α2β1-DLL4 signaling and α2β1 integrin expression. Values represent Mean+SEM of 30 simulated retinas.

F. Vessel density in simulated retinas from Alt. hypothesis model. Simulations took place in a broad range of VEGF expression. Values represent Mean+SEM of 30 simulated retinas.

4.5 Discussion

Our work identified novel mechanisms for regulation of the Notch network by α2β1 integrin. We also demonstrate that our computational model, introduced in Chapter 3, can be used as a platform for testing proposed interactions between candidate molecules and the Notch network in the context of sprouting angiogenesis in the developing retina. In the case of α2β1 integrin, application of this model indicates that loss of the previously reported role for the integrin in promoting DLL4 expression is insufficient to predict the *in vivo* molecular and morphological phenotype seen in α2-null retinas. Further, our model predicts that in the retinal endothelium, the previously unidentified role for α2β1 in VEGFR2 activation, upstream of DLL4, is greater than its reported role in facilitating DLL4 induction. In α2-null endothelial cells, loss of this role in VEGFR2 activation outweighs the loss of α2β1 integrin-mediated DLL4 induction and results in increased notch signaling.

Our proposed role for the α2β1 integrin in supporting VEGFR2 activation via repression of VEGFR1 and/or filopodia formation is entirely consistent with the work of Estrach et al. who first reported α2β1 integrin crosstalk with Notch signaling. Like Estrach et al., we observed integrin expression in filopodia in *in vitro* settings. In the *in vivo* developing retina we do not observe the integrin expressed on filopodia, but instead find strong expression in z-axis oriented protrusions that may be lamellipodialike structures in vertical tip-cells. We previously reported the challenges of visualizing endothelial α2β1 integrin against a backdrop of other cell types with higher integrin expression. Integrin expression in lamellipodia may be more easily visualized because of the larger, more physically robust profile of those structures. Expression of the α2β1 integrin on lamellipodia, actually supports a role for the integrin in filopodia as well,

considering that both forms of membrane protrusions are ‘communicating cables’ and share many molecular components.

Perhaps the broadest implication of this work is our proposal that impairment of VEGFR2 activation may act as a mechanism for enhancing notch signaling. Our modeling predicts that VEGFR2 inhibition would have the effect of increasing notch activation. We have not yet had the opportunity to test this prediction but it is suggestive that increased notch signaling is widely observed in patients treated with anti-VEGF therapies. Traditionally, notch upregulation in these patients has been assumed to be a result of evolving tumor resistance to anti-VEGF therapies. However, Kesisis et al. report that even a single dose of anti-VEGF treatment, Bevacizumab, is sufficient to induce upregulation of Notch target genes in colon cancer patients.[287] This intriguing result invites follow-up studies.

Based on the work of Bentley et al. it is clear that filopodia are critical mediators of VEGFR2 activation in endothelial cells. Our model predicts that chemical filopodia inhibition would upregulate endothelial notch signaling. We have not yet tested this prediction *in vitro* or *in vivo*; However, we have found published reports by Kusuhara et al. that deletion of Arhgef15, a GEF which act to promote filopodia formation by activating CDC42 and potentiating RhoJ inactivation downstream of VEGFR2 activation, causes defects in radial vascular outgrowth in the developing retina.[288] Interestingly, Arghef15-null mice also display decreases in plexus density and increased plexus irregularity; the retinal changes phenocopy the vessel patterning defects of the α2-null animals.

Arghef15-null mice have not been investigated for changes in Notch signaling. Like α2-null mice, these animals lack the classic branching phenotype associated with

changes in notch signaling. The previously reported PlexinD1-null mouse serves as an interesting contrast. PlexinD1 loss-of-function mutants also exhibit increased Notch signaling and plexus irregularity and decreased plexus density. However, unlike α2-null and Arhgef15-null retinas, PlexinD1-null mice do not have a decrease in radial vascular outgrowth, and do exhibit differences in branching. These key differences may arise because although deletion of both PlexinD1 and α2β1 integrin cause increased Notch signaling, these molecules have precisely the opposite relationship with the notch network. PlexinD1 is reported to inhibit DLL4 induction and inhibits VEGFR2 activation by promoting filopodia retraction, whereas the α2β1 integrin promotes DLL4 induction and promotes VEGFR2 activation. Both molecules provide coupled positive and negative feedback loops for the notch network. It is tempting to speculate that branching defects only arise if the proximal cause of the phenotype comes from upstream of DLL4/notch rather than VEGFR2. Alternatively, it is possible that delayed vascular outgrowth in α2-null and Arhgef15KO retinas obscure a real difference in vessel branching.

In summary, our results offer a new context for interpreting longstanding inconsistencies in the α2β1 integrin and angiogenesis. We update the current understanding of α2β1 integrin crosstalk with notch signaling by proposing that the integrin provides both positive and negative feedback for sprouting angiogenesis; the integrin supports VEGF-stimulated VEGFR2 activation via its roles in filopodia function and VEGFR1 repression and it inhibits VEGFR2 activation by supporting DLL4-Notch mediated negative feedback. In low VEGF environments such as the developing postnatal retina, impaired VEGFR2 activation in the α2-null vasculature retards angiogenesis. In contrast, in high VEGF environments, such as in wound-healing, or

obese skeletal muscle, the upstream differences in VEGF receptor activation may be less important, allowing for the loss of α2-mediated Notch signaling to support increased vascularization. Indeed, in wound-healing experiments α2-null wounds have similar neovascularization at day 5, and increased neovascularization at day 10.[274]

To therapeutically recapitulate the α2-null endothelial phenotype, which is advantageous in obesity or wound-healing, would require the development of small-molecule inhibitors that specifically impede the VEGFR1 repression or filopodia function of α2β1 integrin. The development of such small molecule inhibitors may also have significant therapeutic value in different growth factor microenvironments associated with different tumors. Additional study using inducible, tissue-specific models is needed to fully realize the potential synergies from targeting different combinations of actors within the Notch network to treat dysregulated angiogenesis in different contexts.

Chapter 5

IMPLICATIONS AND FUTURE DIRECTIONS

Angiogenesis has pathological roles in almost every human disease. The widely heralded advent of anti-angiogenic therapies in the early 2000s has yielded a mixed record of clinical results. The first generation of anti-angiogenic therapies directly targeting VEGF-VEGFR2 signaling, but there is currently great interest in targeting 'accessory' angiogenesis signaling molecules to provide more nuanced therapeutic effects. The α2β1 integrin plays a complex role in angiogenesis. Data from *in vitro* and *in vivo* inhibitor experiments portray a pro-angiogenic role for this integrin, and yet in a transgenic deletion model, vascular beds in the wound-healing, obese skeletal muscle and select tumor microenvironments show enhanced angiogenesis. The studies in this dissertation are aimed at dissecting the molecular basis for these differences in the hopes of providing clinically relevant therapeutic insight. In this chapter, I will summarize some of the key findings that have broadened our understanding of the α2β1 integrin in angiogenesis as well as propose future research directions**.**

5.1 Retinopathy

Although many GWAS have linked higher expressing polymorphisms of the ITGA2 gene with increased incidence of diabetic retinopathy, the biological causes underlying this association have been unknown. In Chapter 2 I describe our studies using the OIR mouse model of retinopathy of prematurity to investigate the role of the α2β1 integrin in the retinopathy disease process. In accordance with the human data from GWAS studies, we found that α2β1 supported pathogenesis in this model; wild

type animals showed greater levels of hyperoxia-induced vaso-obliteration, and consequently increased VEGFA production and pathologic neovascularization. Mechanistic investigations found that the highest level of integrin expression was found not in the vascular compartment, but rather in a glial cell type known as retinal Müller cells. *In vitro* experiments revealed that α2-null Müller cells produce significantly less hypoxia-induced VEGFA as compared to wild type. Current work in the field indicates that differences in angiogenic growth factor levels, and particularly VEGF, are critical determinants of the severity of proliferative retinopathies, and that retinal Müller cells are the key regulators of the retinal growth factor responsible for as much as 70% of the VEGF produced in the retina. Consequently, the observed attenuated production of VEGF in the α2-null Müller compartment is sufficient to explain the protective phenotype in the α2-null mouse.

This work is the first mechanistic study to explore the functional role of the α2β1 integrin in retinopathy, and revealed a novel role for the integrin in regulating Müller cell function. As the OIR model is thought to recapitulate the proliferative phase of a number of retinopathies, this work may be informative in proliferative diabetic retinopathy in addition to ROP. However, to reach clinical relevance, further research is needed in a number of dimensions.

The primary limitation to our study comes from our use of a global α2- integrin subunit deletion model. Although our findings in the Müller compartment are sufficient to explain the OIR phenotype, we were not able to tease apart the contributing effects of the α2β1 integrin in the endothelium or the immune system. Even though the magnitude of α2β1 integrin's effects are likely larger in retinal Müller cells, pharmaceutical agents that target the integrin may be much more bioavailable to endothelial or immune cells.

Finally, we have not identified the precise molecular nature of the interaction between α2β1 integrin and HIF-2α. It is tempting to speculate that the α2β1 integrin and HIF interact in a positive feed-forward loop to accelerate signal sensitivity. Testing this possibility would require carefully controlled time course experiments to evaluate expression and localization of α2β1 integrin, HIF-2α and candidate molecules including P38 and PARP1. Identifying the molecular interactions that drive this interaction will aid in developing targeted therapies.

5.2 Sprouting Angiogenesis

In Chapter 3 we describe interdisciplinary work that characterizes the sprouting angiogenesis in the α2-null retina on a morphological, molecular, and systems level. We describe a multi-scale computational model to predict vascular patterning, specifically plexus density and irregularity, in the developing retina on the basis of notch-regulated tip-stalk dynamics. We used this model to evaluate the current paradigm for α2β1 integrin-notch crosstalk. Our model predicts that an explanation of the vessel patterning defects in the α2-null retina requires enhanced notch signaling. The model dictates that for deletion of α2β1 integrin to result in enhanced notch signaling, the α2β1 integrin must play a regulatory role in VEGFR2 activation, in addition to its established role in DLL4 induction downstream of VEGFR2. It is suggested that α2β1 integrin deletion causes impaired VEGFR2 activation, and results in delayed tip-cell specification leading to a higher DLL4 ‘setpoint’. We have confirmed that DLL4 expression is higher in α2-null endothelial cells in both *in vitro* and *in vivo* settings. We are in the process of assessing DLL4 induction kinetics to determine whether the model’s predictions for the time course of VEGFR2 activation and DLL4 induction are correct.

5.2.1 α2β1 integrin and VEGFR2 activation

We are also interested in determining the mechanism through which α2β1 integrin supports VEGFR2 activation. Our group has long suspected that there was a signaling relationship between these molecules based on the observation that the α2β1 integrin is only strongly expressed in growth factor activated endothelial cells. The identification and characterization of VEGFR2-α2β1 integrin positive feed-forward loop would be valuable in designing sophisticated anti-angiogenesis therapies in cancer, retinopathy and many other diseases.

One potential mechanism for α2β1 integrin regulation of VEGFR2 activation is through modulation of VEGFR1 expression. One of the major functions of VEGFR1 is to act as a trap or decoy for VEGF to modulate VEGFR2 activation. In low VEGF contexts, such as the developing retina where only 3% of VEGFR2 receptors are bound by VEGF, changes in the expression of VEGFR1 would significantly impact VEGFR2 activation.[289] Our group previously reported studies showing that α2β1 integrin specifically represses VEGFR1 expression; loss of VEGFR1 repression may be a source of impaired VEGFR2 activation in the α2-null background. This explanation could be tested by evaluating postnatal vascular development in VEGFR1-overexpressing mice, but this may be technically unfeasible because of confounding differences in embryonic vasculogenesis caused by VEGFR1 overexpression. We expect that VEGFR1 upregulation contributes to many of the vessel patterning changes observed in the α2-null retina, however, we do not anticipate that upregulation of VEGFR1 is sufficient to explain the observed delay in radial vascular outgrowth. For this reason, we expect that, in addition to VEGFR1 upregulation, loss of other α2β1 integrin functions may also be involved.

Computational modeling by Bentley et al. has identified filopodia extension as a critical mediator of VEGFR2 activation during notch-regulated tip-cell specification. We and others have localized α2β1 integrin on endothelial filopodia and there is an established role for α2β1 integrin in filiopodia stabilization in other cell types. We are currently in the process of using time course experiments to determine whether α2-null retinal endothelial cells have defects in the size, quantity, or stability of VEGFA-stimulated filopodia extension.

As mentioned in chapter 3, deletion of ArhGEF15, a cdc42 regulator involved in filopodia extension, appears to phenocopy all of the vascular patterning defects in the α2-null retina. Changes in notch signaling in ArhGEF15-null retinas have not been reported, but our computational model predicts increased DLL4 expression. We intend to test the effects of filopodia impairment on notch signaling either through *in vivo* characterization of transgenic mice with impaired filopodia dynamics (such as ArhGEF15-null mice) or through the use of CDC42 inhibitors on wild type endothelial cells in an *in vitro* setting. One of the major contributions of this paper is the assertion that altered filopodia dynamics may be sufficient to cause enhanced notch signaling.

5.2.2 α2β1 integrin and anti-angiogenesis therapies

One of the initial goals of this work was to understand the molecular differences which result in disparate angiogenesis outcomes in α2-null mice compared to antibody or small molecule inhibition of the α2β1 integrin. By more fully understanding crosstalk between α2β1 integrin and the notch network, we are closer to this goal.

Crosstalk with the notch network may also be involved in explaining the efficacy of α2β1 inhibitors. Our experimental data shows increased DLL4 expression in the α2-

null background but completely abrogated DLL4 induction with anti-α2 antibody treatment. This difference may arise from the abrupt loss of α2β1 integrin signals supporting DLL4 induction with antibody/inhibitor treatment.

5.3 Lessons for Tumor Biology

In the course of our studies on notch signaling we discovered that in addition to α2β1 regulation of the notch network, the integrin is itself down regulated by Notch signaling. For many years our group has been interested in understanding how the α2β1 integrin is lost during tumor progression. Recent work from a number of groups has identified a feed-forward loop between notch signaling and the HER2 oncogene. Our group has previously shown that loss of the α2β1 integrin promotes the progression of HER2-driven breast cancers towards metastatic progression. Is it possible that notch-mediated repression of the α2β1 also occurs in epithelial tumors? Our preliminary data indicate that this is a possibility. Following up on these studies is of significant potential clinical interest.

WORKS CITED

1. Hemler, M. E. VLA proteins in the integrin family: structures, functions, and their role on leukocytes. *Annu Rev Immunol* 8, 365–400 (1990).
2. Hemler, M. E., Jacobson, J. G., Brenner, M. B., Mann, D. & Strominger, J. L. VLA-1: a T cell surface antigen which defines a novel late stage of human T cell activation. *Eur J Immunol* 15, 502–8 (1985).
3. Elices, M. J. & Hemler, M. E. The human integrin VLA-2 is a collagen receptor on some cells and a collagen/laminin receptor on others. *Proc Natl Acad Sci U A* 86, 9906–10 (1989).
4. Kirchhofer, D., Languino, L. R., Ruoslahti, E. & Pierschbacher, M. D. Alpha 2 beta 1 integrins from different cell types show different binding specificities. *J Biol Chem* 265, 615–8 (1990).
5. Staatz, W. D., Rajpara, S. M., Wayner, E. A., Carter, W. G. & Santoro, S. A. The membrane glycoprotein Ia-IIa (VLA-2) complex mediates the Mg++-dependent adhesion of platelets to collagen. *J Cell Biol* 108, 1917–24 (1989).
6. Aquilina, A. *et al.* A novel gain-of-function mutation of the integrin alpha2 VWFA domain. *Eur J Biochem* 269, 1136–44 (2002).
7. Emsley, J., Knight, C. G., Farndale, R. W., Barnes, M. J. & Liddington, R. C. Structural basis of collagen recognition by integrin alpha2beta1. *Cell* 101, 47–56 (2000).
8. Jin, M., Andricioaei, I. & Springer, T. A. Conversion between three conformational states of integrin I domains with a C-terminal pull spring studied with molecular dynamics. *Structure* 12, 2137–47 (2004).

9. Shimaoka, M. *et al.* Reversibly locking a protein fold in an active conformation with a disulfide bond: integrin alphaL I domains with high affinity and antagonist activity in vivo. *Proc Natl Acad Sci U A* 98, 6009–14 (2001).
10. Tulla, M. *et al.* Selective binding of collagen subtypes by integrin alpha 1I, alpha 2I, and alpha 10I domains. *J. Biol. Chem.* 276, 48206–48212 (2001).
11. Tulla, M. *et al.* Effects of conformational activation of integrin alpha 1I and alpha 2I domains on selective recognition of laminin and collagen subtypes. *Exp Cell Res* 314, 1734–43 (2008).
12. Van de Walle, G. R. *et al.* Two functional active conformations of the integrin {alpha}2{beta}1, depending on activation condition and cell type. *J Biol Chem* 280, 36873–82 (2005).
13. Kehrel, B. Platelet receptors for collagens. *Platelets* 6, 11–6 (1995).
14. Moroi, M. & Jung, S. M. Platelet receptors for collagen. *Thromb Haemost* 78, 439–44 (1997).
15. Santoro, S. A. & Zutter, M. M. The alpha 2 beta 1 integrin: a collagen receptor on platelets and other cells. *Thromb Haemost* 74, 813–21 (1995).
16. Sixma, J. J. *et al.* Platelet adhesion to collagen: an update. *Thromb Haemost* 78, 434–8 (1997).
17. Ayala, F. *et al.* Genetic polymorphisms of platelet adhesive molecules: association with breast cancer risk and clinical presentation. *Breast Cancer Res Treat* 80, 145–54 (2003).
18. Carlsson, L. E., Santoso, S., Spitzer, C., Kessler, C. & Greinacher, A. The alpha2 gene coding sequence T807/A873 of the platelet collagen receptor integrin

alpha2beta1 might be a genetic risk factor for the development of stroke in younger patients. *Blood* 93, 3583–6 (1999).

19. Casorelli, I. *et al.* The C807T/G873A polymorphism in the platelet glycoprotein Ia gene and the risk of acute coronary syndrome in the Italian population. *Br J Haematol* 114, 150–4 (2001).
20. Dodson, P. M. *et al.* The platelet glycoprotein Ia/IIa gene polymorphism C807T/G873A: a novel risk factor for retinal vein occlusion. *Eye Lond* 17, 772–7 (2003).
21. Gerger, A. *et al.* Integrin alpha-2 and beta-3 gene polymorphisms and colorectal cancer risk. *Int J Colorectal Dis* 24, 159–63 (2009).
22. Langsenlehner, U. *et al.* Integrin alpha-2 and beta-3 gene polymorphisms and breast cancer risk. *Breast Cancer Res Treat* 97, 67–72 (2006).
23. Wu, J. E. & Santoro, S. A. Complex patterns of expression suggest extensive roles for the alpha 2 beta 1 integrin in murine development. *Dev Dyn* 199, 292–314 (1994).
24. Werr, J. *et al.* Integrin alpha(2)beta(1) (VLA-2) is a principal receptor used by neutrophils for locomotion in extravascular tissue. *Blood* 95, 1804–9 (2000).
25. de Fougerolles, A. R. *et al.* Regulation of inflammation by collagen-binding integrins alpha1beta1 and alpha2beta1 in models of hypersensitivity and arthritis. *J Clin Invest* 105, 721–9 (2000).
26. Nieuwenhuis, H. K., Akkerman, J. W., Houdijk, W. P. & Sixma, J. J. Human blood platelets showing no response to collagen fail to express surface glycoprotein Ia. *Nature* 318, 470–2 (1985).

27. Nieuwenhuis, H. K., Sakariassen, K. S., Houdijk, W. P., Nievelstein, P. F. & Sixma, J. J. Deficiency of platelet membrane glycoprotein Ia associated with a decreased platelet adhesion to subendothelium: a defect in platelet spreading. *Blood* 68, 692–5 (1986).
28. Kunicki, T. J., Orchekowski, R., Annis, D. & Honda, Y. Variability of integrin alpha 2 beta 1 activity on human platelets. *Blood* 82, 2693–703 (1993).
29. Santoro, S. A., Walsh, J. J., Staatz, W. D. & Baranski, K. J. Distinct determinants on collagen support alpha 2 beta 1 integrin-mediated platelet adhesion and platelet activation. *Cell Regul* 2, 905–13 (1991).
30. Chen, J., Diacovo, T. G., Grenache, D. G., Santoro, S. A. & Zutter, M. M. The alpha(2) integrin subunit-deficient mouse: a multifaceted phenotype including defects of branching morphogenesis and hemostasis. *Am J Pathol* 161, 337–44 (2002).
31. Jandrot-Perrus, M. *et al.* Cloning, characterization, and functional studies of human and mouse glycoprotein VI: a platelet-specific collagen receptor from the immunoglobulin superfamily. *Blood* 96, 1798–807 (2000).
32. Miura, Y., Ohnuma, M., Jung, S. M. & Moroi, M. Cloning and expression of the platelet-specific collagen receptor glycoprotein VI. *Thromb Res* 98, 301–9 (2000).
33. Moroi, M. & Jung, S. M. Platelet glycoprotein VI: its structure and function. *Thromb Res* 114, 221–33 (2004).
34. Miura, Y., Takahashi, T., Jung, S. M. & Moroi, M. Analysis of the interaction of platelet collagen receptor glycoprotein VI (GPVI) with collagen. A dimeric form of GPVI, but not the monomeric form, shows affinity to fibrous collagen. *J Biol Chem* 277, 46197–204 (2002).

35. Santoro, S. A. Identification of a 160,000 dalton platelet membrane protein that mediates the initial divalent cation-dependent adhesion of platelets to collagen. *Cell* 46, 913–20 (1986).
36. Tsuji, M., Ezumi, Y., Arai, M. & Takayama, H. A novel association of Fc receptor gamma-chain with glycoprotein VI and their co-expression as a collagen receptor in human platelets. *J Biol Chem* 272, 23528–31 (1997).
37. Ichinohe, T. *et al.* Collagen-stimulated activation of Syk but not c-Src is severely compromised in human platelets lacking membrane glycoprotein VI. *J Biol Chem* 272, 63–8 (1997).
38. Kamiguti, A. S. *et al.* Proteolytic cleavage of the beta1 subunit of platelet alpha2beta1 integrin by the metalloproteinase jararhagin compromises collagen-stimulated phosphorylation of pp72. *J Biol Chem* 272, 32599–605 (1997).
39. Keely, P. J. & Parise, L. V. The alpha2beta1 integrin is a necessary co-receptor for collagen-induced activation of Syk and the subsequent phosphorylation of phospholipase Cgamma2 in platelets. *J. Biol. Chem.* 271, 26668–26676 (1996).
40. Suzuki-Inoue, K. *et al.* Rhodocytin induces platelet aggregation by interacting with glycoprotein Ia/IIa (GPIa/IIa, Integrin alpha 2beta 1). Involvement of GPIa/IIa-associated src and protein tyrosine phosphorylation. *J Biol Chem* 276, 1643–52 (2001).
41. Inoue, O., Suzuki-Inoue, K., Dean, W. L., Frampton, J. & Watson, S. P. Integrin alpha2beta1 mediates outside-in regulation of platelet spreading on collagen through activation of Src kinases and PLCgamma2. *J Cell Biol* 160, 769–80 (2003).

42. Hers, I. *et al.* Evidence against a direct role of the integrin alpha2beta1 in collagen-induced tyrosine phosphorylation in human platelets. *Eur J Biochem* 267, 2088–97 (2000).
43. Auger, J. M., Kuijpers, M. J., Senis, Y. A., Watson, S. P. & Heemskerk, J. W. Adhesion of human and mouse platelets to collagen under shear: a unifying model. *Faseb J* 19, 825–7 (2005).
44. Mazzucato, M. *et al.* Distinct spatio-temporal Ca2+ signaling elicited by integrin alpha2beta1 and glycoprotein VI under flow. *Blood* 114, 2793–801 (2009).
45. Marjoram, R. J. *et al.* Suboptimal activation of protease-activated receptors enhances alpha2beta1 integrin-mediated platelet adhesion to collagen. *J Biol Chem* 284, 34640–7 (2009).
46. Dickeson, S. K., Walsh, J. J. & Santoro, S. A. Binding of the alpha 2 integrin I domain to extracellular matrix ligands: structural and mechanistic differences between collagen and laminin binding. *Cell Adhes Commun* 5, 273–81 (1998).
47. Emsley, J., King, S. L., Bergelson, J. M. & Liddington, R. C. Crystal structure of the I domain from integrin alpha2beta1. *J. Biol. Chem.* 272, 28512–28517 (1997).
48. Elices, M. J., Urry, L. A. & Hemler, M. E. Receptor functions for the integrin VLA-3: fibronectin, collagen, and laminin binding are differentially influenced by Arg-Gly-Asp peptide and by divalent cations. *J Cell Biol* 112, 169–81 (1991).
49. Ignatius, M. J. & Reichardt, L. F. Identification of a neuronal laminin receptor: an Mr 200K/120K integrin heterodimer that binds laminin in a divalent cation-dependent manner. *Neuron* 1, 713–25 (1988).
50. Kamata, T., Liddington, R. C. & Takada, Y. Interaction between collagen and the alpha(2) I-domain of integrin alpha(2)beta(1). Critical role of conserved residues in

the metal ion-dependent adhesion site (MIDAS) region. *J Biol Chem* 274, 32108–11 (1999).

51. Raynal, N. *et al.* Use of synthetic peptides to locate novel integrin alpha2beta1-binding motifs in human collagen III. *J Biol Chem* 281, 3821–31 (2006).
52. Tuckwell, D. S. *et al.* Monoclonal antibodies identify residues 199-216 of the integrin alpha2 vWFA domain as a functionally important region within alpha2beta1. *Biochem J* 350 Pt 2, 485–93 (2000).
53. Carafoli, F., Hamaia, S. W., Bihan, D., Hohenester, E. & Farndale, R. W. An activating mutation reveals a second binding mode of the integrin alpha2 I domain to the GFOGER motif in collagens. *PLoS One* 8, e69833 (2013).
54. Chin, Y. K.-Y. *et al.* The Structure of Integrin 1I Domain in Complex with a Collagen-mimetic Peptide. *J. Biol. Chem.* 288, 36796–36809 (2013).
55. Jokinen, J. *et al.* Integrin-mediated cell adhesion to type I collagen fibrils. *J Biol Chem* 279, 31956–63 (2004).
56. Kern, A., Eble, J., Golbik, R. & Kuhn, K. Interaction of type IV collagen with the isolated integrins alpha 1 beta 1 and alpha 2 beta 1. *Eur J Biochem* 215, 151–9 (1993).
57. Calderwood, D. A., Tuckwell, D. S., Eble, J., Kuhn, K. & Humphries, M. J. The integrin alpha1 A-domain is a ligand binding site for collagens and laminin. *J Biol Chem* 272, 12311–7 (1997).
58. Knight, C. G. *et al.* Identification in collagen type I of an integrin alpha2 beta1-binding site containing an essential GER sequence. *J Biol Chem* 273, 33287–94 (1998).

59. Knight, C. G. *et al.* The collagen-binding A-domains of integrins alpha(1)beta(1) and alpha(2)beta(1) recognize the same specific amino acid sequence, GFOGER, in native (triple-helical) collagens. *J Biol Chem* 275, 35–40 (2000).
60. Siljander, P. R. *et al.* Integrin activation state determines selectivity for novel recognition sites in fibrillar collagens. *J Biol Chem* 279, 47763–72 (2004).
61. Eble, J. A. *et al.* Collagen XVI harbors an integrin alpha1 beta1 recognition site in its C-terminal domains. *J Biol Chem* 281, 25745–56 (2006).
62. Grenache, D. G. *et al.* Wound healing in the alpha2beta1 integrin-deficient mouse: altered keratinocyte biology and dysregulated matrix metalloproteinase expression. *J Invest Dermatol* 127, 455–66 (2007).
63. Heikkinen, A., Tu, H. & Pihlajaniemi, T. Collagen XIII: a type II transmembrane protein with relevance to musculoskeletal tissues, microvessels and inflammation. *Int J Biochem Cell Biol* 44, 714–7 (2012).
64. Veit, G. *et al.* Collagen XXIII, novel ligand for integrin alpha2beta1 in the epidermis. *J Biol Chem* 286, 27804–13 (2011).
65. Edelson, B. T. *et al.* Novel collectin/C1q receptor mediates mast cell activation and innate immunity. *Blood* 107, 143–50 (2006).
66. Chan, B. M. & Hemler, M. E. Multiple functional forms of the integrin VLA-2 can be derived from a single alpha 2 cDNA clone: interconversion of forms induced by an anti-beta 1 antibody. *J Cell Biol* 120, 537–43 (1993).
67. Yebra, M. *et al.* Endothelium-derived Netrin-4 supports pancreatic epithelial cell adhesion and differentiation through integrins alpha2beta1 and alpha3beta1. *PLoS One* 6, e22750 (2011).

68. Goyal, A. *et al.* Endorepellin, the angiostatic module of perlecan, interacts with both the alpha2beta1 integrin and vascular endothelial growth factor receptor 2 (VEGFR2): a dual receptor antagonism. *J Biol Chem* 286, 25947–62 (2011).
69. Goyal, A. *et al.* Endorepellin affects angiogenesis by antagonizing diverse vascular endothelial growth factor receptor 2 (VEGFR2)-evoked signaling pathways: transcriptional repression of hypoxia-inducible factor 1alpha and VEGFA and concurrent inhibition of nuclear factor of activated T cell 1 (NFAT1) activation. *J Biol Chem* 287, 43543–56 (2012).
70. Bidanset, D. J. *et al.* Binding of the proteoglycan decorin to collagen type VI. *J Biol Chem* 267, 5250–6 (1992).
71. Fleischmajer, R. *et al.* Decorin interacts with fibrillar collagen of embryonic and adult human skin. *J Struct Biol* 106, 82–90 (1991).
72. Hedbom, E. & Heinegard, D. Interaction of a 59-kDa connective tissue matrix protein with collagen I and collagen II. *J Biol Chem* 264, 6898–905 (1989).
73. Vogel, K. G., Paulsson, M. & Heinegard, D. Specific inhibition of type I and type II collagen fibrillogenesis by the small proteoglycan of tendon. *Biochem J* 223, 587–97 (1984).
74. Vogel, K. G. & Trotter, J. A. The effect of proteoglycans on the morphology of collagen fibrils formed in vitro. *Coll Relat Res* 7, 105–14 (1987).
75. Kunicki, T. J., Williams, S. A., Diaz, D., Farndale, R. W. & Nugent, D. J. Platelet adhesion to decorin but not collagen I correlates with the integrin alpha2 dimorphism E534K, the basis of the human platelet alloantigen (HPA)-5 system. *Haematologica* 97, 692–5 (2012).

76. Bergelson, J. M., Shepley, M. P., Chan, B. M., Hemler, M. E. & Finberg, R. W. Identification of the integrin VLA-2 as a receptor for echovirus 1. *Science* 255, 1718–20 (1992).
77. Bergelson, J. M., Chan, B. M., Finberg, R. W. & Hemler, M. E. The integrin VLA-2 binds echovirus 1 and extracellular matrix ligands by different mechanisms. *J Clin Invest* 92, 232–9 (1993).
78. Bergelson, J. M. *et al.* The I domain is essential for echovirus 1 interaction with VLA-2. *Cell Adhes Commun* 2, 455–64 (1994).
79. Dickeson, S. K., Mathis, N. L., Rahman, M., Bergelson, J. M. & Santoro, S. A. Determinants of ligand binding specificity of the alpha(1)beta(1) and alpha(2)beta(1) integrins. *J Biol Chem* 274, 32182–91 (1999).
80. Karjalainen, M. *et al.* A Raft-derived, Pak1-regulated entry participates in alpha2beta1 integrin-dependent sorting to caveosomes. *Mol Biol Cell* 19, 2857–69 (2008).
81. Marjomaki, V. *et al.* Internalization of echovirus 1 in caveolae. *J Virol* 76, 1856–65 (2002).
82. Upla, P. *et al.* Clustering induces a lateral redistribution of alpha 2 beta 1 integrin from membrane rafts to caveolae and subsequent protein kinase C-dependent internalization. *Mol Biol Cell* 15, 625–36 (2004).
83. Jokinen, J. *et al.* Molecular mechanism of alpha2beta1 integrin interaction with human echovirus 1. *Embo J* 29, 196–208 (2010).
84. Sato, Y., Morimoto, K., Kubo, T., Yanagihara, K. & Seyama, T. High mannose-binding antiviral lectin PFL from Pseudomonas fluorescens Pf0-1 promotes cell

death of gastric cancer cell MKN28 via interaction with alpha2-integrin. *PLoS One* 7, e45922 (2012).

85. Saarialho-Kere, U. K. *et al.* Cell-matrix interactions modulate interstitial collagenase expression by human keratinocytes actively involved in wound healing. *J Clin Invest* 92, 2858–66 (1993).
86. Pilcher, B. K. *et al.* The activity of collagenase-1 is required for keratinocyte migration on a type I collagen matrix. *J Cell Biol* 137, 1445–57 (1997).
87. Honore, S., Kovacic, H., Pichard, V., Briand, C. & Rognoni, J. B. Alpha2beta1-integrin signaling by itself controls G1/S transition in a human adenocarcinoma cell line (Caco-2): implication of NADPH oxidase-dependent production of ROS. *Exp Cell Res* 285, 59–71 (2003).
88. Ivaska, J. *et al.* Integrin alpha2beta1 mediates isoform-specific activation of p38 and upregulation of collagen gene transcription by a mechanism involving the alpha2 cytoplasmic tail. *J Cell Biol* 147, 401–16 (1999).
89. Messent, A. J. *et al.* Effects of collagenase-cleavage of type I collagen on alpha2beta1 integrin-mediated cell adhesion. *J Cell Sci* 111 (Pt 8), 1127–35 (1998).
90. Zweers, M. C. *et al.* Integrin alpha2beta1 is required for regulation of murine wound angiogenesis but is dispensable for reepithelialization. *J Invest Dermatol* 127, 467–78 (2007).
91. Borza, C. M. *et al.* Inhibition of integrin alpha2beta1 ameliorates glomerular injury. *J Am Soc Nephrol* 23, 1027–38 (2012).

92. Girgert, R. *et al.* Integrin alpha2-deficient mice provide insights into specific functions of collagen receptors in the kidney. *Fibrogenesis Tissue Repair* 3, 19 (2010).
93. Gross, O. *et al.* Preemptive ramipril therapy delays renal failure and reduces renal fibrosis in COL4A3-knockout mice with Alport syndrome. *Kidney Int.* 63, 438–446 (2003).
94. Miller, M. W. *et al.* Small-molecule inhibitors of integrin alpha2beta1 that prevent pathological thrombus formation via an allosteric mechanism. *Proc Natl Acad Sci U A* 106, 719–24 (2009).
95. Xia, H. *et al.* Low alpha(2)beta(1) integrin function enhances the proliferation of fibroblasts from patients with idiopathic pulmonary fibrosis by activation of the beta-catenin pathway. *Am J Pathol* 181, 222–33 (2012).
96. Sasaki, K. *et al.* Differential regulation of VLA-2 expression on Th1 and Th2 cells: a novel marker for the classification of Th subsets. *Int Immunol* 15, 701–10 (2003).
97. Boisvert, M., Gendron, S., Chetoui, N. & Aoudjit, F. Alpha2 beta1 integrin signaling augments T cell receptor-dependent production of interferon-gamma in human T cells. *Mol Immunol* 44, 3732–40 (2007).
98. Aoudjit, F. & Vuori, K. Engagement of the alpha2beta1 integrin inhibits Fas ligand expression and activation-induced cell death in T cells in a focal adhesion kinase-dependent manner. *Blood* 95, 2044–51 (2000).
99. Gendron, S., Couture, J. & Aoudjit, F. Integrin alpha2beta1 inhibits Fas-mediated apoptosis in T lymphocytes by protein phosphatase 2A-dependent activation of the MAPK/ERK pathway. *J. Biol. Chem.* 278, 48633–48643 (2003).

100. Kassiotis, G., Gray, D., Kiafard, Z., Zwirner, J. & Stockinger, B. Functional specialization of memory Th cells revealed by expression of integrin CD49b. *J Immunol* 177, 968–75 (2006).
101. Richter, M. *et al.* Collagen distribution and expression of collagen-binding alpha1beta1 (VLA-1) and alpha2beta1 (VLA-2) integrins on CD4 and CD8 T cells during influenza infection. *J Immunol* 178, 4506–16 (2007).
102. Andreasen, S. Ø. *et al.* Expression and functional importance of collagen-binding integrins, alpha 1 beta 1 and alpha 2 beta 1, on virus-activated T cells. *J. Immunol. Baltim. Md 1950* 171, 2804–2811 (2003).
103. Hanazawa, A. *et al.* CD49b-dependent establishment of T helper cell memory. *Immunol Cell Biol* 91, 524–31 (2013).
104. Arase, H., Saito, T., Phillips, J. H. & Lanier, L. L. Cutting edge: the mouse NK cell-associated antigen recognized by DX5 monoclonal antibody is CD49b (alpha 2 integrin, very late antigen-2). *J. Immunol. Baltim. Md 1950* 167, 1141–1144 (2001).
105. Takahashi, K. *et al.* A murine very late activation antigen-like extracellular matrix receptor involved in CD2- and lymphocyte function-associated antigen-1-independent killer-target cell interaction. *J. Immunol. Baltim. Md 1950* 145, 4371–4379 (1990).
106. McCall-Culbreath, K. D., Li, Z. & Zutter, M. M. Crosstalk between the alpha2beta1 integrin and c-met/HGF-R regulates innate immunity. *Blood* 111, 3562–70 (2008).
107. Sun, H., Santoro, S. A. & Zutter, M. M. Downstream events in mammary gland morphogenesis mediated by reexpression of the alpha2beta1 integrin: the role of the alpha6 and beta4 integrin subunits. *Cancer Res.* 58, 2224–2233 (1998).

108. Zutter, M. M., Sun, H. & Santoro, S. A. Altered integrin expression and the malignant phenotype: the contribution of multiple integrated integrin receptors. *J. Mammary Gland Biol. Neoplasia* 3, 191–200 (1998).
109. Zutter, M. M. *et al.* Collagen receptor control of epithelial morphogenesis and cell cycle progression. *Am. J. Pathol.* 155, 927–940 (1999).
110. Berdichevsky, F., Alford, D., D'Souza, B. & Taylor-Papadimitriou, J. Branching morphogenesis of human mammary epithelial cells in collagen gels. *J. Cell Sci.* 107 (Pt 12), 3557–3568 (1994).
111. D'Souza, B., Berdichevsky, F., Kyprianou, N. & Taylor-Papadimitriou, J. Collagen-induced morphogenesis and expression of the alpha 2-integrin subunit is inhibited in c-erbB2-transfected human mammary epithelial cells. *Oncogene* 8, 1797–1806 (1993).
112. D'souza, B. & Taylor-Papadimitriou, J. Overexpression of ERBB2 in human mammary epithelial cells signals inhibition of transcription of the E-cadherin gene. *Proc. Natl. Acad. Sci. U. S. A.* 91, 7202–7206 (1994).
113. Ramirez, N. E. *et al.* The $\alpha_2\beta_1$ integrin is a metastasis suppressor in mouse models and human cancer. *J. Clin. Invest.* 121, 226–237 (2011).
114. Jacquelin, B. *et al.* Allele-dependent transcriptional regulation of the human integrin alpha2 gene. *Blood* 97, 1721–6 (2001).
115. Kritzik, M. *et al.* Nucleotide polymorphisms in the alpha2 gene define multiple alleles that are associated with differences in platelet alpha2 beta1 density. *Blood* 92, 2382–8 (1998).

116. Cheli, Y., Williams, S. A., Ballotti, R., Nugent, D. J. & Kunicki, T. J. Enhanced binding of poly(ADP-ribose)polymerase-1 and Ku80/70 to the ITGA2 promoter via an extended cytosine-adenosine repeat. *PLoS One* 5, e8743 (2010).
117. Matsubara, Y. *et al.* Association between diabetic retinopathy and genetic variations in alpha2beta1 integrin, a platelet receptor for collagen. *Blood* 95, 1560–4 (2000).
118. Santoso, S., Kunicki, T. J., Kroll, H., Haberbosch, W. & Gardemann, A. Association of the platelet glycoprotein Ia C807T gene polymorphism with nonfatal myocardial infarction in younger patients. *Blood* 93, 2449–53 (1999).
119. Kunicki, T. J., Williams, S. A., Nugent, D. J. & Yeager, M. Mean platelet volume and integrin alleles correlate with levels of integrins alpha(IIb)beta(3) and alpha(2)beta(1) in acute coronary syndrome patients and normal subjects. *Arter. Thromb Vasc Biol* 32, 147–52 (2012).
120. Slavka, G. *et al.* Mean platelet volume may represent a predictive parameter for overall vascular mortality and ischemic heart disease. *Arter. Thromb Vasc Biol* 31, 1215–8 (2011).
121. Habart, D., Cheli, Y., Nugent, D. J., Ruggeri, Z. M. & Kunicki, T. J. Conditional knockout of integrin alpha2beta1 in murine megakaryocytes leads to reduced mean platelet volume. *PLoS One* 8, e55094 (2013).
122. Rossant, J. & Howard, L. Signaling pathways in vascular development. *Annu. Rev. Cell Dev. Biol.* 18, 541–573 (2002).
123. Burri, P. H. & Djonov, V. Intussusceptive angiogenesis--the alternative to capillary sprouting. *Mol. Aspects Med.* 23, S1–27 (2002).

124. Gerhardt, H. *et al.* VEGF guides angiogenic sprouting utilizing endothelial tip cell filopodia. *J. Cell Biol.* 161, 1163–1177 (2003).
125. Marin-Padilla, M. Early vascularization of the embryonic cerebral cortex: Golgi and electron microscopic studies. *J. Comp. Neurol.* 241, 237–249 (1985).
126. Jakobsson, L. *et al.* Endothelial cells dynamically compete for the tip cell position during angiogenic sprouting. *Nat. Cell Biol.* 12, 943–953 (2010).
127. Claxton, S. & Fruttiger, M. Periodic Delta-like 4 expression in developing retinal arteries. *Gene Expr. Patterns GEP* 5, 123–127 (2004).
128. Siekmann, A. F. & Lawson, N. D. Notch signalling limits angiogenic cell behaviour in developing zebrafish arteries. *Nature* 445, 781–784 (2007).
129. Tammela, T. *et al.* Blocking VEGFR-3 suppresses angiogenic sprouting and vascular network formation. *Nature* 454, 656–660 (2008).
130. Lu, X. *et al.* The netrin receptor UNC5B mediates guidance events controlling morphogenesis of the vascular system. *Nature* 432, 179–186 (2004).
131. Holmes, D. I. R. & Zachary, I. The vascular endothelial growth factor (VEGF) family: angiogenic factors in health and disease. *Genome Biol.* 6, 209 (2005).
132. Muller, Y. A. *et al.* Vascular endothelial growth factor: crystal structure and functional mapping of the kinase domain receptor binding site. *Proc. Natl. Acad. Sci. U. S. A.* 94, 7192–7197 (1997).
133. Carmeliet, P. *et al.* Abnormal blood vessel development and lethality in embryos lacking a single VEGF allele. *Nature* 380, 435–439 (1996).
134. Ferrara, N. *et al.* Heterozygous embryonic lethality induced by targeted inactivation of the VEGF gene. *Nature* 380, 439–442 (1996).

135. Ruhrberg, C. *et al.* Spatially restricted patterning cues provided by heparin-binding VEGF-A control blood vessel branching morphogenesis. *Genes Dev.* 16, 2684–2698 (2002).
136. Gerhardt, H. *et al.* Neuropilin-1 is required for endothelial tip cell guidance in the developing central nervous system. *Dev. Dyn. Off. Publ. Am. Assoc. Anat.* 231, 503–509 (2004).
137. Davis, G. E. & Senger, D. R. Endothelial extracellular matrix: biosynthesis, remodeling, and functions during vascular morphogenesis and neovessel stabilization. *Circ. Res.* 97, 1093–1107 (2005).
138. Whelan, M. C. & Senger, D. R. Collagen I initiates endothelial cell morphogenesis by inducing actin polymerization through suppression of cyclic AMP and protein kinase A. *J. Biol. Chem.* 278, 327–334 (2003).
139. Liu, Y. & Senger, D. R. Matrix-specific activation of Src and Rho initiates capillary morphogenesis of endothelial cells. *FASEB J. Off. Publ. Fed. Am. Soc. Exp. Biol.* 18, 457–468 (2004).
140. Hoang, M. V., Whelan, M. C. & Senger, D. R. Rho activity critically and selectively regulates endothelial cell organization during angiogenesis. *Proc. Natl. Acad. Sci. U. S. A.* 101, 1874–1879 (2004).
141. Bayless, K. J., Salazar, R. & Davis, G. E. RGD-dependent vacuolation and lumen formation observed during endothelial cell morphogenesis in three-dimensional fibrin matrices involves the alpha(v)beta(3) and alpha(5)beta(1) integrins. *Am. J. Pathol.* 156, 1673–1683 (2000).

142. Davis, G. E. & Bayless, K. J. An integrin and Rho GTPase-dependent pinocytic vacuole mechanism controls capillary lumen formation in collagen and fibrin matrices. *Microcirc. N. Y. N 1994* 10, 27–44 (2003).
143. Kamei, M. *et al.* Endothelial tubes assemble from intracellular vacuoles in vivo. *Nature* 442, 453–456 (2006).
144. Davis, G. E. & Camarillo, C. W. An alpha 2 beta 1 integrin-dependent pinocytic mechanism involving intracellular vacuole formation and coalescence regulates capillary lumen and tube formation in three-dimensional collagen matrix. *Exp. Cell Res.* 224, 39–51 (1996).
145. Hynes, R. O. Cell-matrix adhesion in vascular development. *J. Thromb. Haemost. JTH* 5 Suppl 1, 32–40 (2007).
146. Costell, M. *et al.* Perlecan maintains the integrity of cartilage and some basement membranes. *J. Cell Biol.* 147, 1109–1122 (1999).
147. Miner, J. H., Cunningham, J. & Sanes, J. R. Roles for laminin in embryogenesis: exencephaly, syndactyly, and placentopathy in mice lacking the laminin alpha5 chain. *J. Cell Biol.* 143, 1713–1723 (1998).
148. Pöschl, E. *et al.* Collagen IV is essential for basement membrane stability but dispensable for initiation of its assembly during early development. *Dev. Camb. Engl.* 131, 1619–1628 (2004).
149. Thyboll, J. *et al.* Deletion of the laminin alpha4 chain leads to impaired microvessel maturation. *Mol. Cell. Biol.* 22, 1194–1202 (2002).
150. Klein, S. *et al.* Alpha 5 beta 1 integrin activates an NF-kappa B-dependent program of gene expression important for angiogenesis and inflammation. *Mol. Cell. Biol.* 22, 5912–5922 (2002).

151. Mettouchi, A. *et al.* Integrin-specific activation of Rac controls progression through the G(1) phase of the cell cycle. *Mol. Cell* 8, 115–127 (2001).
152. Stenzel, D. *et al.* Endothelial basement membrane limits tip cell formation by inducing Dll4/Notch signalling in vivo. *EMBO Rep.* 12, 1135–1143 (2011).
153. Folkman, J. Tumor suppression by p53 is mediated in part by the antiangiogenic activity of endostatin and tumstatin. *Sci. STKE Signal Transduct. Knowl. Environ.* 2006, pe35 (2006).
154. Wickström, S. A., Alitalo, K. & Keski-Oja, J. Endostatin associates with lipid rafts and induces reorganization of the actin cytoskeleton via down-regulation of RhoA activity. *J. Biol. Chem.* 278, 37895–37901 (2003).
155. Hamano, Y. *et al.* Physiological levels of tumstatin, a fragment of collagen IV alpha3 chain, are generated by MMP-9 proteolysis and suppress angiogenesis via alphaV beta3 integrin. *Cancer Cell* 3, 589–601 (2003).
156. Bix, G. *et al.* Endorepellin causes endothelial cell disassembly of actin cytoskeleton and focal adhesions through alpha2beta1 integrin. *J Cell Biol* 166, 97–109 (2004).
157. Roca, C. & Adams, R. H. Regulation of vascular morphogenesis by Notch signaling. *Genes Dev.* 21, 2511–2524 (2007).
158. Hellstrom, M. *et al.* Dll4 signalling through Notch1 regulates formation of tip cells during angiogenesis. *Nature* 445, 776–80 (2007).
159. Artavanis-Tsakonas, S., Rand, M. D. & Lake, R. J. Notch signaling: cell fate control and signal integration in development. *Science* 284, 770–776 (1999).
160. Gridley, T. Notch signaling in vertebrate development and disease. *Mol. Cell. Neurosci.* 9, 103–108 (1997).

161. Bray, S. J. Notch signalling: a simple pathway becomes complex. *Nat. Rev. Mol. Cell Biol.* 7, 678–689 (2006).

162. Fiúza, U.-M. & Arias, A. M. Cell and molecular biology of Notch. *J. Endocrinol.* 194, 459–474 (2007).

163. Zeng, Y., Graner, M. W., Thompson, S., Marron, M. & Katsanis, E. Induction of BCR-ABL-specific immunity following vaccination with chaperone-rich cell lysates derived from BCR-ABL+ tumor cells. *Blood* 105, 2016–2022 (2005).

164. Weng, A. P. *et al.* Activating mutations of NOTCH1 in human T cell acute lymphoblastic leukemia. *Science* 306, 269–271 (2004).

165. Kao, H. Y. *et al.* A histone deacetylase corepressor complex regulates the Notch signal transduction pathway. *Genes Dev.* 12, 2269–2277 (1998).

166. Villa, N. *et al.* Vascular expression of Notch pathway receptors and ligands is restricted to arterial vessels. *Mech. Dev.* 108, 161–164 (2001).

167. Suchting, S. *et al.* The Notch ligand Delta-like 4 negatively regulates endothelial tip cell formation and vessel branching. *Proc. Natl. Acad. Sci. U. S. A.* 104, 3225–3230 (2007).

168. Lobov, I. B. *et al.* Delta-like ligand 4 (Dll4) is induced by VEGF as a negative regulator of angiogenic sprouting. *Proc. Natl. Acad. Sci. U. S. A.* 104, 3219–3224 (2007).

169. Holderfield, M. T. *et al.* HESR1/CHF2 suppresses VEGFR2 transcription independent of binding to E-boxes. *Biochem. Biophys. Res. Commun.* 346, 637–648 (2006).

170. Dufraine, J., Funahashi, Y. & Kitajewski, J. Notch signaling regulates tumor angiogenesis by diverse mechanisms. *Oncogene* 27, 5132–5137 (2008).

171. Enenstein, J. & Kramer, R. H. Confocal microscopic analysis of integrin expression on the microvasculature and its sprouts in the neonatal foreskin. *J Invest Dermatol* 103, 381–6 (1994).
172. Senger, D. R. *et al.* Angiogenesis promoted by vascular endothelial growth factor: regulation through alpha1beta1 and alpha2beta1 integrins. *Proc Natl Acad Sci U A* 94, 13612–7 (1997).
173. Gamble, J. *et al.* B1 integrin activation inhibits in vitro tube formation: effects on cell migration, vacuole coalescence and lumen formation. *Endothelium* 7, 23–34 (1999).
174. Davis, G. E., Black, S. M. & Bayless, K. J. Capillary morphogenesis during human endothelial cell invasion of three-dimensional collagen matrices. *Vitro Cell Dev Biol Anim* 36, 513–9 (2000).
175. Sweeney, S. M. *et al.* Angiogenesis in collagen I requires alpha2beta1 ligation of a GFP*GER sequence and possibly p38 MAPK activation and focal adhesion disassembly. *J Biol Chem* 278, 30516–24 (2003).
176. Zhang, Z. *et al.* alpha2beta1 integrin expression in the tumor microenvironment enhances tumor angiogenesis in a tumor cell-specific manner. *Blood* 111, 1980–8 (2008).
177. Kang, L. *et al.* Diet-induced muscle insulin resistance is associated with extracellular matrix remodeling and interaction with integrin alpha2beta1 in mice. *Diabetes* 60, 416–426 (2011).
178. Cailleteau, L. *et al.* alpha2beta1 integrin controls association of Rac with the membrane and triggers quiescence of endothelial cells. *J Cell Sci* 123, 2491–501 (2010).

179. Woodall, B. P. *et al.* Integrin alpha2beta1 is the required receptor for endorepellin angiostatic activity. *J Biol Chem* 283, 2335–43 (2008).
180. San Antonio, J. D. *et al.* A key role for the integrin alpha2beta1 in experimental and developmental angiogenesis. *Am. J. Pathol.* 175, 1338–1347 (2009).
181. Estrach, S. *et al.* Laminin-binding integrins induce Dll4 expression and Notch signaling in endothelial cells. *Circ Res* 109, 172–82 (2011).
182. Alon, U. Biological networks: the tinkerer as an engineer. *Science* 301, 1866–1867 (2003).
183. Kim, D., Kwon, Y.-K. & Cho, K.-H. Coupled positive and negative feedback circuits form an essential building block of cellular signaling pathways. *BioEssays News Rev. Mol. Cell. Dev. Biol.* 29, 85–90 (2007).
184. Bentley, K., Gerhardt, H. & Bates, P. A. Agent-based simulation of notch-mediated tip cell selection in angiogenic sprout initialisation. *J. Theor. Biol.* 250, 25–36 (2008).
185. Klekotka, P. A., Santoro, S. A., Wang, H. & Zutter, M. M. Specific residues within the alpha 2 integrin subunit cytoplasmic domain regulate migration and cell cycle progression via distinct MAPK pathways. *J Biol Chem* 276, 32353–61 (2001).
186. Klekotka, P. A., Santoro, S. A. & Zutter, M. M. alpha 2 integrin subunit cytoplasmic domain-dependent cellular migration requires p38 MAPK. *J Biol Chem* 276, 9503–11 (2001).
187. Ivaska, J. *et al.* Integrin alpha 2 beta 1 promotes activation of protein phosphatase 2A and dephosphorylation of Akt and glycogen synthase kinase 3 beta. *Mol Cell Biol* 22, 1352–9 (2002).

188. Deakin, A. S. Model for initial vascular patterns in melanoma transplants. *Growth* 40, 191–201 (1976).
189. Balding, D. & McElwain, D. L. A mathematical model of tumour-induced capillary growth. *J. Theor. Biol.* 114, 53–73 (1985).
190. Muthukkaruppan, V. R., Kubai, L. & Auerbach, R. Tumor-induced neovascularization in the mouse eye. *J. Natl. Cancer Inst.* 69, 699–708 (1982).
191. Byrne, H. M. & Chaplain, M. A. Mathematical models for tumour angiogenesis: numerical simulations and nonlinear wave solutions. *Bull. Math. Biol.* 57, 461–486 (1995).
192. Orme, M. E. & Chaplain, M. A. Two-dimensional models of tumour angiogenesis and anti-angiogenesis strategies. *IMA J. Math. Appl. Med. Biol.* 14, 189–205 (1997).
193. Anderson, A. R. & Chaplain, M. A. Continuous and discrete mathematical models of tumor-induced angiogenesis. *Bull. Math. Biol.* 60, 857–899 (1998).
194. Stokes, C. L. & Lauffenburger, D. A. Analysis of the roles of microvessel endothelial cell random motility and chemotaxis in angiogenesis. *J. Theor. Biol.* 152, 377–403 (1991).
195. Stevens, A. & Othmer, H. G. Aggregation, Blowup, and Collapse: The ABC's of Taxis in Reinforced Random Walks. *SIAM J. Appl. Math.* 57, 1044–1081 (1997).
196. Turner, D. L. & Cepko, C. L. A common progenitor for neurons and glia persists in rat retina late in development. *Nature* 328, 131–136 (1987).
197. Reichenbach, A. *et al.* Distribution of Bergmann glial somata and processes: implications for function. *J. Für Hirnforsch.* 36, 509–517 (1995).

198. Guérin, C. J., Anderson, D. H. & Fisher, S. K. Changes in intermediate filament immunolabeling occur in response to retinal detachment and reattachment in primates. *Invest. Ophthalmol. Vis. Sci.* 31, 1474–1482 (1990).
199. Lewis, G. P., Matsumoto, B. & Fisher, S. K. Changes in the organization and expression of cytoskeletal proteins during retinal degeneration induced by retinal detachment. *Invest. Ophthalmol. Vis. Sci.* 36, 2404–2416 (1995).
200. Liberto, C. M., Albrecht, P. J., Herx, L. M., Yong, V. W. & Levison, S. W. Pro-regenerative properties of cytokine-activated astrocytes. *J. Neurochem.* 89, 1092–1100 (2004).
201. Watkins, W. M. *et al.* Hypoxia-induced expression of VEGF splice variants and protein in four retinal cell types. *Exp. Eye Res.* 116, 240–246 (2013).
202. Forsythe, J. A. *et al.* Activation of vascular endothelial growth factor gene transcription by hypoxia-inducible factor 1. *Mol. Cell. Biol.* 16, 4604–4613 (1996).
203. Stone, J. *et al.* Roles of vascular endothelial growth factor and astrocyte degeneration in the genesis of retinopathy of prematurity. *Invest. Ophthalmol. Vis. Sci.* 37, 290–299 (1996).
204. Ashton, N. Pathological basis of retrolental fibroplasia. *Br. J. Ophthalmol.* 38, 385–396 (1954).
205. Lutty, G. A. *et al.* Proceedings of the Third International Symposium on Retinopathy of Prematurity: an update on ROP from the lab to the nursery (November 2003, Anaheim, California). *Mol. Vis.* 12, 532–580 (2006).
206. Roth, A. M. Retinal vascular development in premature infants. *Am. J. Ophthalmol.* 84, 636–640 (1977).

207. Chen, J. & Smith, L. E. H. Retinopathy of prematurity. *Angiogenesis* 10, 133–140 (2007).
208. Gao, G. *et al.* Difference in ischemic regulation of vascular endothelial growth factor and pigment epithelium--derived factor in brown norway and sprague dawley rats contributing to different susceptibilities to retinal neovascularization. *Diabetes* 51, 1218–1225 (2002).
209. Pierce, E. A., Foley, E. D. & Smith, L. E. Regulation of vascular endothelial growth factor by oxygen in a model of retinopathy of prematurity. *Arch. Ophthalmol.* 114, 1219–1228 (1996).
210. Alon, T. *et al.* Vascular endothelial growth factor acts as a survival factor for newly formed retinal vessels and has implications for retinopathy of prematurity. *Nat. Med.* 1, 1024–1028 (1995).
211. Ozaki, H. *et al.* Hypoxia inducible factor-1alpha is increased in ischemic retina: temporal and spatial correlation with VEGF expression. *Invest. Ophthalmol. Vis. Sci.* 40, 182–189 (1999).
212. Geisen, P. *et al.* Neutralizing antibody to VEGF reduces intravitreous neovascularization and may not interfere with ongoing intraretinal vascularization in a rat model of retinopathy of prematurity. *Mol. Vis.* 14, 345–357 (2008).
213. Aiello, L. P. *et al.* Suppression of retinal neovascularization in vivo by inhibition of vascular endothelial growth factor (VEGF) using soluble VEGF-receptor chimeric proteins. *Proc. Natl. Acad. Sci. U. S. A.* 92, 10457–10461 (1995).
214. Robinson, G. S. *et al.* Oligodeoxynucleotides inhibit retinal neovascularization in a murine model of proliferative retinopathy. *Proc. Natl. Acad. Sci. U. S. A.* 93, 4851–4856 (1996).

215. Bainbridge, J. W. B. *et al.* Inhibition of retinal neovascularisation by gene transfer of soluble VEGF receptor sFlt-1. *Gene Ther.* 9, 320–326 (2002).
216. Ozaki, H. *et al.* Blockade of vascular endothelial cell growth factor receptor signaling is sufficient to completely prevent retinal neovascularization. *Am. J. Pathol.* 156, 697–707 (2000).
217. Mintz-Hittner, H. A. Intravitreal pegaptanib as adjunctive treatment for stage 3+ ROP shown to be effective in a prospective, randomized, controlled multicenter clinical trial. *Eur. J. Ophthalmol.* 22, 685–686 (2012).
218. Curtis, T. M., Gardiner, T. A. & Stitt, A. W. Microvascular lesions of diabetic retinopathy: clues towards understanding pathogenesis? *Eye Lond. Engl.* 23, 1496–1508 (2009).
219. Klein, R., Klein, B. E., Moss, S. E., Davis, M. D. & DeMets, D. L. The Wisconsin epidemiologic study of diabetic retinopathy. III. Prevalence and risk of diabetic retinopathy when age at diagnosis is 30 or more years. *Arch. Ophthalmol.* 102, 527–532 (1984).
220. Aiello, L. P. *et al.* Vascular endothelial growth factor in ocular fluid of patients with diabetic retinopathy and other retinal disorders. *N. Engl. J. Med.* 331, 1480–1487 (1994).
221. Malecaze, F. *et al.* Detection of vascular endothelial growth factor messenger RNA and vascular endothelial growth factor-like activity in proliferative diabetic retinopathy. *Arch. Ophthalmol.* 112, 1476–1482 (1994).
222. Fong, G.-H. & Takeda, K. Role and regulation of prolyl hydroxylase domain proteins. *Cell Death Differ.* 15, 635–641 (2008).

223. Keely, S. *et al.* Selective induction of integrin beta1 by hypoxia-inducible factor: implications for wound healing. *FASEB J. Off. Publ. Fed. Am. Soc. Exp. Biol.* 23, 1338–1346 (2009).
224. Gonzalez-Flores, A. *et al.* Interaction between PARP-1 and HIF-2α in the hypoxic response. *Oncogene* 33, 891–898 (2014).
225. Hirota, K. & Semenza, G. L. Rac1 activity is required for the activation of hypoxia-inducible factor 1. *J. Biol. Chem.* 276, 21166–21172 (2001).
226. Emerling, B. M. *et al.* Mitochondrial reactive oxygen species activation of p38 mitogen-activated protein kinase is required for hypoxia signaling. *Mol. Cell. Biol.* 25, 4853–4862 (2005).
227. Mylonis, I. *et al.* Identification of MAPK phosphorylation sites and their role in the localization and activity of hypoxia-inducible factor-1alpha. *J. Biol. Chem.* 281, 33095–33106 (2006).
228. Smith, L. E. *et al.* Oxygen-induced retinopathy in the mouse. *Invest. Ophthalmol. Vis. Sci.* 35, 101–111 (1994).
229. Connor, K. M. *et al.* Quantification of oxygen-induced retinopathy in the mouse: a model of vessel loss, vessel regrowth and pathological angiogenesis. *Nat. Protoc.* 4, 1565–1573 (2009).
230. Mechoulam, H. & Pierce, E. A. Expression and activation of STAT3 in ischemia-induced retinopathy. *Invest. Ophthalmol. Vis. Sci.* 46, 4409–4416 (2005).
231. Recchia, F. M., Xu, L., Penn, J. S., Boone, B. & Dexheimer, P. J. Identification of genes and pathways involved in retinal neovascularization by microarray analysis of two animal models of retinal angiogenesis. *Invest. Ophthalmol. Vis. Sci.* 51, 1098–1105 (2010).

232. Fukushima, Y. *et al.* Sema3E-PlexinD1 signaling selectively suppresses disoriented angiogenesis in ischemic retinopathy in mice. *J. Clin. Invest.* 121, 1974–1985 (2011).
233. Barnett, J. M., McCollum, G. W. & Penn, J. S. Role of cytosolic phospholipase A(2) in retinal neovascularization. *Invest. Ophthalmol. Vis. Sci.* 51, 1136–1142 (2010).
234. Rahmani, B. *et al.* The cause-specific prevalence of visual impairment in an urban population. The Baltimore Eye Survey. *Ophthalmology* 103, 1721–1726 (1996).
235. Steinkuller, P. G. *et al.* Childhood blindness. *J. AAPOS Off. Publ. Am. Assoc. Pediatr. Ophthalmol. Strabismus Am. Assoc. Pediatr. Ophthalmol. Strabismus* 3, 26–32 (1999).
236. Bressler, N. M. & Bressler, S. B. Preventative ophthalmology. Age-related macular degeneration. *Ophthalmology* 102, 1206–1211 (1995).
237. Wang, G. L., Jiang, B. H., Rue, E. A. & Semenza, G. L. Hypoxia-inducible factor 1 is a basic-helix-loop-helix-PAS heterodimer regulated by cellular O2 tension. *Proc. Natl. Acad. Sci. U. S. A.* 92, 5510–5514 (1995).
238. Mowat, F. M. *et al.* HIF-1alpha and HIF-2alpha are differentially activated in distinct cell populations in retinal ischaemia. *PloS One* 5, e11103 (2010).
239. Morita, M. *et al.* HLF/HIF-2alpha is a key factor in retinopathy of prematurity in association with erythropoietin. *EMBO J.* 22, 1134–1146 (2003).
240. Chen, S. *et al.* Regulation of vascular endothelial growth factor expression by extra domain B segment of fibronectin in endothelial cells. *Invest. Ophthalmol. Vis. Sci.* 53, 8333–8343 (2012).
241. Weidemann, A. *et al.* Astrocyte hypoxic response is essential for pathological but not developmental angiogenesis of the retina. *Glia* 58, 1177–1185 (2010).

242. Aiello, L. P., Northrup, J. M., Keyt, B. A., Takagi, H. & Iwamoto, M. A. Hypoxic regulation of vascular endothelial growth factor in retinal cells. *Arch. Ophthalmol. Chic. Ill 1960* 113, 1538–1544 (1995).
243. Aiello, L. P. *et al.* Suppression of retinal neovascularization in vivo by inhibition of vascular endothelial growth factor (VEGF) using soluble VEGF-receptor chimeric proteins. *Proc. Natl. Acad. Sci. U. S. A.* 92, 10457–10461 (1995).
244. Pierce, E. A., Avery, R. L., Foley, E. D., Aiello, L. P. & Smith, L. E. Vascular endothelial growth factor/vascular permeability factor expression in a mouse model of retinal neovascularization. *Proc. Natl. Acad. Sci. U. S. A.* 92, 905–909 (1995).
245. Robbins, S. G., Rajaratnam, V. S. & Penn, J. S. Evidence for upregulation and redistribution of vascular endothelial growth factor (VEGF) receptors flt-1 and flk-1 in the oxygen-injured rat retina. *Growth Factors Chur Switz.* 16, 1–9 (1998).
246. Robbins, S. G., Conaway, J. R., Ford, B. L., Roberto, K. A. & Penn, J. S. Detection of vascular endothelial growth factor (VEGF) protein in vascular and non-vascular cells of the normal and oxygen-injured rat retina. *Growth Factors Chur Switz.* 14, 229–241 (1997).
247. Ishida, S. *et al.* VEGF164-mediated inflammation is required for pathological, but not physiological, ischemia-induced retinal neovascularization. *J. Exp. Med.* 198, 483–489 (2003).
248. Hynes, R. O. A reevaluation of integrins as regulators of angiogenesis. *Nat. Med.* 8, 918–921 (2002).
249. Petrovic, M. G., Hawlina, M., Peterlin, B. & Petrovic, D. BglII gene polymorphism of the alpha2beta1 integrin gene is a risk factor for diabetic retinopathy in Caucasians with type 2 diabetes. *J. Hum. Genet.* 48, 457–460 (2003).

250. Abhary, S., Hewitt, A. W., Burdon, K. P. & Craig, J. E. A systematic meta-analysis of genetic association studies for diabetic retinopathy. *Diabetes* 58, 2137–2147 (2009).

251. Casey, R. & Li, W. W. Factors controlling ocular angiogenesis. *Am. J. Ophthalmol.* 124, 521–529 (1997).

252. Werdich, X. Q., McCollum, G. W., Rajaratnam, V. S. & Penn, J. S. Variable oxygen and retinal VEGF levels: correlation with incidence and severity of pathology in a rat model of oxygen-induced retinopathy. *Exp. Eye Res.* 79, 623–630 (2004).

253. Hicks, D. & Courtois, Y. The growth and behaviour of rat retinal Müller cells in vitro. 1. An improved method for isolation and culture. *Exp. Eye Res.* 51, 119–129 (1990).

254. Bai, Y. *et al.* Müller cell-derived VEGF is a significant contributor to retinal neovascularization. *J. Pathol.* 219, 446–454 (2009).

255. Yanni, S. E., McCollum, G. W. & Penn, J. S. Genetic deletion of COX-2 diminishes VEGF production in mouse retinal Müller cells. *Exp. Eye Res.* 91, 34–41 (2010).

256. Moshfegh, K. *et al.* Association of two silent polymorphisms of platelet glycoprotein Ia/IIa receptor with risk of myocardial infarction: a case-control study. *Lancet Lond. Engl.* 353, 351–354 (1999).

257. Bensellam, M. *et al.* Glucose-induced O_2 consumption activates hypoxia inducible factors 1 and 2 in rat insulin-secreting pancreatic beta-cells. *PloS One* 7, e29807 (2012).

258. Klettner, A., Westhues, D., Lassen, J., Bartsch, S. & Roider, J. Regulation of constitutive vascular endothelial growth factor secretion in retinal pigment epithelium/choroid organ cultures: p38, nuclear factor κB, and the vascular

endothelial growth factor receptor-2/phosphatidylinositol 3 kinase pathway. *Mol. Vis.* 19, 281–291 (2013).

259. Hellström, M., Phng, L.-K. & Gerhardt, H. VEGF and Notch signaling: the yin and yang of angiogenic sprouting. *Cell Adhes. Migr.* 1, 133–136 (2007).
260. Kim, J., Oh, W.-J., Gaiano, N., Yoshida, Y. & Gu, C. Semaphorin 3E-Plexin-D1 signaling regulates VEGF function in developmental angiogenesis via a feedback mechanism. *Genes Dev.* 25, 1399–1411 (2011).
261. Anderson, A. R. & Chaplain, M. A. Continuous and discrete mathematical models of tumor-induced angiogenesis. *Bull. Math. Biol.* 60, 857–899 (1998).
262. Watson, M. G., McDougall, S. R., Chaplain, M. a. J., Devlin, A. H. & Mitchell, C. A. Dynamics of angiogenesis during murine retinal development: a coupled in vivo and in silico study. *J. R. Soc. Interface R. Soc.* 9, 2351–2364 (2012).
263. Bentley, K., Gerhardt, H. & Bates, P. A. Agent-based simulation of notch-mediated tip cell selection in angiogenic sprout initialisation. *J. Theor. Biol.* 250, 25–36 (2008).
264. Collier, J. R., Monk, N. A., Maini, P. K. & Lewis, J. H. Pattern formation by lateral inhibition with feedback: a mathematical model of delta-notch intercellular signalling. *J. Theor. Biol.* 183, 429–446 (1996).
265. Madamanchi, A. *et al.* Mitigation of oxygen-induced retinopathy in α2β1 integrin-deficient mice. *Invest. Ophthalmol. Vis. Sci.* 55, 4338–4347 (2014).
266. Nguyen, L. K. Regulation of oscillation dynamics in biochemical systems with dual negative feedback loops. *J. R. Soc. Interface R. Soc.* 9, 1998–2010 (2012).
267. Brooks, P. C. *et al.* Integrin alpha v beta 3 antagonists promote tumor regression by inducing apoptosis of angiogenic blood vessels. *Cell* 79, 1157–1164 (1994).

268. Brooks, P. C. *et al.* Localization of matrix metalloproteinase MMP-2 to the surface of invasive cells by interaction with integrin alpha v beta 3. *Cell* 85, 683–693 (1996).
269. Brooks, P. C., Clark, R. A. & Cheresh, D. A. Requirement of vascular integrin alpha v beta 3 for angiogenesis. *Science* 264, 569–571 (1994).
270. Eliceiri, B. P. & Cheresh, D. A. The role of alphav integrins during angiogenesis: insights into potential mechanisms of action and clinical development. *J. Clin. Invest.* 103, 1227–1230 (1999).
271. Senger, D. R. *et al.* The alpha(1)beta(1) and alpha(2)beta(1) integrins provide critical support for vascular endothelial growth factor signaling, endothelial cell migration, and tumor angiogenesis. *Am. J. Pathol.* 160, 195–204 (2002).
272. Senger, D. R. *et al.* Angiogenesis promoted by vascular endothelial growth factor: regulation through alpha1beta1 and alpha2beta1 integrins. *Proc. Natl. Acad. Sci. U. S. A.* 94, 13612–13617 (1997).
273. Chen, J., Diacovo, T. G., Grenache, D. G., Santoro, S. A. & Zutter, M. M. The alpha(2) integrin subunit-deficient mouse: a multifaceted phenotype including defects of branching morphogenesis and hemostasis. *Am. J. Pathol.* 161, 337–344 (2002).
274. Zweers, M. C. *et al.* Integrin alpha2beta1 is required for regulation of murine wound angiogenesis but is dispensable for reepithelialization. *J. Invest. Dermatol.* 127, 467–478 (2007).
275. Zhang, Z. *et al.* alpha2beta1 integrin expression in the tumor microenvironment enhances tumor angiogenesis in a tumor cell-specific manner. *Blood* 111, 1980–1988 (2008).

276. Cailleteau, L. *et al.* alpha2beta1 integrin controls association of Rac with the membrane and triggers quiescence of endothelial cells. *J. Cell Sci.* 123, 2491–2501 (2010).
277. San Antonio, J. D. *et al.* A key role for the integrin alpha2beta1 in experimental and developmental angiogenesis. *Am. J. Pathol.* 175, 1338–1347 (2009).
278. Phng, L.-K. & Gerhardt, H. Angiogenesis: a team effort coordinated by notch. *Dev. Cell* 16, 196–208 (2009).
279. Stenzel, D. *et al.* Endothelial basement membrane limits tip cell formation by inducing Dll4/Notch signalling in vivo. *EMBO Rep.* 12, 1135–1143 (2011).
280. Estrach, S. *et al.* Laminin-binding integrins induce Dll4 expression and Notch signaling in endothelial cells. *Circ. Res.* 109, 172–182 (2011).
281. Jakobsson, L. *et al.* Endothelial cells dynamically compete for the tip cell position during angiogenic sprouting. *Nat. Cell Biol.* 12, 943–953 (2010).
282. Gerhardt, H. *et al.* VEGF guides angiogenic sprouting utilizing endothelial tip cell filopodia. *J. Cell Biol.* 161, 1163–1177 (2003).
283. Dubrac, A. *et al.* Targeting NCK-Mediated Endothelial Cell Front-Rear Polarity Inhibits Neo-Vascularization. *Circulation* (2015). doi:10.1161/CIRCULATIONAHA.115.017537
284. Lobov, I. B. *et al.* Delta-like ligand 4 (Dll4) is induced by VEGF as a negative regulator of angiogenic sprouting. *Proc. Natl. Acad. Sci. U. S. A.* 104, 3219–3224 (2007).
285. Benedito, R. *et al.* The notch ligands Dll4 and Jagged1 have opposing effects on angiogenesis. *Cell* 137, 1124–1135 (2009).

286. del Toro, R. *et al.* Identification and functional analysis of endothelial tip cell-enriched genes. *Blood* 116, 4025–4033 (2010).
287. Kesisis, G., Broxterman, H. & Giaccone, G. Angiogenesis inhibitors. Drug selectivity and target specificity. *Curr. Pharm. Des.* 13, 2795–2809 (2007).
288. Kusuhara, S. *et al.* Arhgef15 promotes retinal angiogenesis by mediating VEGF-induced Cdc42 activation and potentiating RhoJ inactivation in endothelial cells. *PloS One* 7, e45858 (2012).
289. Mac Gabhann, F., Ji, J. W. & Popel, A. S. Computational model of vascular endothelial growth factor spatial distribution in muscle and pro-angiogenic cell therapy. *PLoS Comput. Biol.* 2, e127 (2006).